Studies on soil compaction combining classic soil mechanical methods and X-ray computed tomography

Dissertation

zur Erlangung des
Doktorgrades der Naturwissenschaften (Dr. rer. nat.)

der

Naturwissenschaftlichen Fakultät III
Agrar- und Ernährungswissenschaften,
Geowissenschaften und Informatik

der Martin-Luther-Universität Halle-Wittenberg

vorgelegt von
Frau Pöhlitz, Julia
Geb. am 10.02.1992 in Weißenfels

Erstgutachter: Prof. Dr. Hans-Jörg Vogel

Zweitgutachter: Prof. Dr. Stephan Peth

Verteidigung: 15.04.2019

Acknowledgements

Table of contents

Summary

The use of heavy agricultural equipment often produces significant changes in soil physical properties through compaction. Soil compaction is one of the environmental factors in agriculture that adversely affect soil functions and crop growth. In recent years there has been an increased application of conservation-oriented tillage techniques where instead of being turned the soil is only loosened or not tilled at all. Nevertheless, tillage always impacts on soil physical properties and processes. Some soil physical properties can easily be measured using classic laboratory methods. However, explicit information about soil structural changes cannot be obtained with classic methods. This requires non-destructive measurements such as X-ray computed tomography (CT), a non-invasive 3D image analysis technique which allows to analyze the soil pore system in some detail.

This study, divided into three separate trials, combines parameters obtained with computed tomography (mean macropore diameter, macroporosity, pore connectivity, anisotropy) and classic laboratory methods (dry bulk and aggregate density, saturated hydraulic conductivity, mechanical precompression stress) to analyze soil compaction, exemplified on samples from different tillage treatments (strip tillage, mulch tillage, no tillage, tillage with a disc harrow, rotary tiller, cultivator and plough), different moisture tensions (6 and 1000 kPa) and different textures (sandy loam, loam, silt loam, silty clay loam) in the topsoil. In addition, biological (earthworm activity) and crop factors (grain and straw yield) are used to describe the effects of compaction on soils with different textures. Based on all the listed parameters, critical stress values and critical stress ranges are derived which make it possible to assess site-specific effects of compaction on soil functions, and the maximum allowable load to prevent such negative effects, respectively.

In particular the trials showed that:

- Strip tillage combines the advantages of no tillage and a deeper soil conservation-oriented primary tillage, because, on a small scale, it creates two distinct soil structures which are beneficial in terms of optimal plant growth as well as mechanical resistance to driving over the soil.

- The matric potential can have a decisive impact on the mechanical stability of a soil, in particular in case of conventional soil tillage with a plough. Ploughing has only a temporary positive effect that persists as long as macroporosity and mean macropore diameter remain high.

- The critical stress ranges display differences between sites that occur due differences in the pore space, but the medians of the critical stress ranges are similar and concur with the values of the mechanical precompression stresses. This trial did not find a

dependence on texture of the critical stress value for various parameters, or of the critical stress range defined by these critical stress values for a soil. This means that studies which recommend maximum values for mechanical loads to prevent harmful soil compaction solely on the basis of texture should be treated with caution.

- Soil mechanical and morphometric parameters supplement each other in terms of what they reveal about the mechanical properties of a soil and its structure. With CT the soil structure is made visible, which provides a more definite picture of the effects of compaction. The CT parameters are therefore highly suitable for providing additional information about the compaction process.

- The classic soil mechanical parameters are closely related to the CT ones. However, the relationships are affected by the tillage method and soil texture, with the former having the more pronounced effect. Due to these two factors there are, for example, several different values for macroporosity for the same dry bulk density and vice versa. This implies that neither classic soil physical parameters alone, nor CT parameters alone provide a complete picture of soil compaction.

- The CT parameters are all related to each other. The precise relationships are again dependent on the tillage method and on soil texture. Tillage usually has the bigger effect here, too.

List of figures

List of tables

Abbreviations

Δz	discrete units of thickness
$\Sigma \mu_i$	sum of the attenuation by different components
σ	total stress
σ_1	first principal stress
σ_2	second principal stress
σ_3	third principal stress
σ_n	mean normal stress
$\sigma_{P\,AD}$	mechanical precompression stress of aggregates
$\sigma_{P\,BDxi}$	mechanical precompression stress based on dry bulk density
$\sigma_{P\,MP}$	mechanical precompression stress based on macroporosity
τ	octahedral shear stress
μ	attenuation coefficient
μ_i	attenuation coefficient for component i
AD	aggregate density
BD	dry bulk density
BD_0	initial dry bulk density
BD_{xi}	resulting dry bulk density
C	cultivator
CCD	charge-coupled device
CT	computed tomography
D	thickness of the object
DTS	displacement
E	east
FC	field capacity
h_0	initial height of the soil sample
H. vulgare	*Hordeum vulgare*
I	intensity of the X-radiation after passing through the object
I_0	initial intensity of the X-radiation received by the object
K_s	saturated hydraulic conductivity
L. terrestris	*Lumbricus terrestris*
m_d	dry mass of the soil
m_s	mass of the soil
MT	mulch tillage
n	number of samples
N	north
N_{min}	mineralizable nitrogen

NT	no tillage
pH	negative decadic logarithm of the hydrogen ion concentration
p	porosity
P	plough
PD	particle density
pF	decadic logarithm of water tension expressed in cm
r^2	coefficient of determination
ROI	region of interest
s	settlement
SST	stress state transducer
STBS	strip tillage between seed rows
STWS	strip tillage within the seed row
V_{sm}	volume of the soil mass
V_{ss}	volume of soil solids
Vol.-%	volume percent
VR	void ratio

1. Introduction

One of humanity's most important mediums worthy of protection is the soil. Soil is the irreplaceable basis of life which has a habitat function for humans, animals, plants and soil organisms. All occurrences of life in the soil are affected by interactions between its solid, liquid and gaseous phases, but also by transport and translocation processes and are thus directly or indirectly related to soil texture and porosity. Soil is therefore a variable medium and can be irreversibly damaged. For that reason it is a top priority to use soil in a sustainable manner, since it ensures the food basis for humans through the cultivation of crops. This is in line with the following definition of tillage by Estler and Knittel (1996): "The tasks of tillage are timeless and subordinate to just one goal, namely to increase the productivity of a site in the short term and maintain it in the long term, without negatively affecting the environment" (free translation from German). So, soil tillage aims to help to achieve optimal crop establishment, i.e. to optimize gas exchange and the water balance, and at the same time to preserve ecological soil functions, like habitat functions and regulatory functions for water and nutrients. This was pointed out by many other authors (e.g. Gantzer and Anderson, 2002; KTBL, 1993). Therefore, every tillage step not only needs to meet the demands of the following crop, but also to be adapted to the entire crop rotation, taking into account the location and its climatic conditions.

A soil is used by plants as a growth medium which supplies water, oxygen and nutrients. On agricultural soils an attempt is therefore made with various tillage systems to create a soil structure that allows optimal plant and root growth, optimal biological activity to release nutrients, and facilitates the supply of water and oxygen (Carter, 1986). The most common categorization of tillage systems in Germany which corresponds to modern situations is (i) conventional tillage with a plough, (ii) conservation tillage, i.e. merely tilling the soil with a cultivator, and (iii) direct seeding which omits tillage altogether (Wiermann, 1998). In recent decades an increasing number of practitioners have abandoned traditional tillage methods which turn the soil using a plough (conventional) in favour of conservation-oriented soil tillage (e.g. Licht and Al-Kaisi, 2005; Nowatzki et al., 2009). The latter does not involve turning the soil with a plough, but instead only loosening it or leaving it completely untilled. This allows dead plant material to remain close to or on the surface of the soil, which offers both ecological and economic benefits, such as the conservation of water, the prevention of soil erosion, and less time spent on seedbed preparation (Carter, 2004; FAO, 1993, Strudley et al. 2008). There are a variety of conservation tillage systems which can be roughly divided into no tillage, mulch tillage, strip tillage, ridge tillage and minimum tillage (FAO, 1993). Strip tillage is special in that the soil is divided into a sowing zone and a soil management zone. The sowing zone is 5-15 cm wide and worked mechanically down to a depth of 25 cm to optimize soil and microclimatic conditions for crop germination and growth, while the soil

management zone is left untilled (Lal, 1983). Strip tillage therefore combines the advantages of no tillage and those of deeper, non-turning primary tillage. It also allows farmers to combine individual working steps which reduces the number of times the field is driven over (Nowatzki et al., 2009). The American Soil Conservation Service (1983) describes conservation-oriented tillage (as opposed to conventional tillage) as any tillage method that leaves at least 30% of the soil surface covered with plant residues from preceding crops and catch crops. This means that it views direct seeding as a form of conservation-oriented tillage, too. Regardless of these classifications, any form of tillage affects the soil structure which was popularly defined by Dexter (1988) as "the spatial heterogeneity of the different components or properties of a soil". However, not just tillage operations, but also the driving required during seeding, fertilization, crop protection and harvest (e.g. Dürr et al., 1995; Hamza and Anderson, 2005) affects the physical, mechanical and biological properties of the soil (Carter, 2004). If the machinery is not adapted to the site and local conditions (Rücknagel et al., 2012a; Koch et al., 2008), e.g. by not adjusting the air pressure in the tires, or if the soil water content during agronomic operations is unfavorable (Pagliai et al., 2000; Rücknagel et al., 2012a), there will be a risk of soil damage due to compaction. The Soil Science Society of America (1996) defines soil compaction as "the process by which the soil grains are rearranged to decrease void space and bring them into closer contact with one another, thereby increasing the dry bulk density".

In an agricultural system one can speak of harmful soil compaction, if the soil properties are changed to such an extent that this significantly affects the growth and development of crops as well as soil life (Semmel and Horn, 1995). Harmful soil compaction causes serious environmental and agricultural problems, e.g. soil erosion and flooding due to increased runoff, water quality problems due to the deposition of eroded material in water bodies, and yield reductions due to the loss of fertile topsoil and the restriction of root growth. More directly, compaction has a negative impact on soil aeration and the water balance (FAO, 1993; Pagliai and Jones, 2002; Voorhees, 1986). Economic implications are reflected in the need for higher tractive power, rising fuel consumption, and increased expenditure on fertilizers and crop protection agents (e.g. Dürr et al., 1995; Krümmelbein et al., 2008; Semmel and Horn, 1995). The extent of the ecological and economic impairments depends on exogenous (load intensity and duration, number and type of loads, driving speed, contact surface pressure) and endogenous soil factors (structural arrangement and stability, degree of cross-linkage of roots, hyphae and humic substances, particle size distribution and particle shape, clay mineral type and adsorbed cations, organic matter and fertilization, shear resistance, angles of internal friction, cohesion, water potential, degree of soil aggregation) (Dürr et al., 1995; Horn, 1981; Koolen and Kuipers, 1983; Kühner, 1997; Semmel and Horn,

1995; Wiermann, 1998). In addition to site-related factors, weather conditions when performing soil tillage operations also play an important role.

Studies of soil mechanical parameters are increasingly concerned with structural differences due to individual soil tillage systems, especially under consideration of modern soil conservation tillage systems (strip tillage, zone tillage, slot tillage etc.). When comparing different tillage methods the greatest differences in the aforementioned parameters are seen in the structure of the topsoil. Physical soil properties such as dry bulk density, aggregate stability or pore size distribution are directly influenced by mechanical disturbances during tillage (FAO, 1993), and by driving over the ground (Carter, 2004). Soil compaction is an undesireable change in soil structure (Ishaq et al., 2001a) which influences not only pore functions such as air and water movement (Lipiec and Hatano, 2003), but also biological activity (Imhoff et al., 2004; Lipiec and Simota, 1994; Pagliai and Jones, 2002; Saffih-Hdadi et al., 2009). One or more of these factors can become critical. To what extent this happens depends on climatic conditions, soil type and crop species (Rashid and Sheikh, 1977).

With respect to soil matric potential there is a sensitive response, due to its effect on the mechanical stability of a soil (Rücknagel et al., 2012b). This is well known and adequately researched. The water content, and hence soil moisture tension, is not only subject to seasonal fluctuations, but also affected by soil tillage and crop type (Khan et al., 1999; Mackie-Dawson et al., 1989). Thus, the mechanical stability of a soil varies considerably over the course of the year, too. This means that even with a suitable tillage system and suitable tillage tools the local operating conditions at the site remain as one of the factors which can massively influence harmful soil compaction. Many previous studies have extensively dealt with the effect of different tillage systems on soil compaction (e.g. Dal Ferro et al., 2014; Jarvis et al., 2017), with the interactions between mechanical precompression stress, dry bulk density and water content (e.g. Alexandrou and Earl, 1998), and with models and predictions of mechanical precompression stress at different water contents (e.g. Rücknagel et al., 2012b; Saffih-Hdadi et al., 2009).

Numerous studies conducted under the same weather conditions have shown that, in addition to tillage, the reaction of a crop to compaction is strongly influenced by soil type and differences in soil texture (Lehfeldt, 1988; Tursic, 1982). Hence, attempts have been made by different authors to base the resulting restrictions on loads on soil texture and display them in tables or maps showing different maximum wheel loads depending on soil texture (Diserens, 2009; Schjonning et al., 2015).

Biological properties as well as physical or mechanical properties are important components of the soil ecosystem (Carter, 1986). Indices of both soil structure and biological conditions are important for understanding the behaviour of soil functions (Carter, 1986) and,

thus, the ability to avoid soil damage. Earthworms are important biological factors in soil ecosystems. They are sensitive to tillage techniques and can therefore be used as bio-indicators of soil conditions (Lemtiri et al., 2014). For plants a common reaction to compaction is decreasing root penetration (Lipiec and Simota, 1994) due to excessive mechanical resistance and insufficient aeration. The study of root system parameters such as root mass and root length (e.g. Czyz et al., 2001; Ishaq et al., 2001b) is very elaborate. For this reason, and from a practical agricultural point of view, above ground plant parameters such as yield, biomass, grain weight or number of shoots are often used to assess the effects of compaction (Rashid and Sheikh, 1977; Saqib et al., 2004) which are mostly related to constraints in the extent and functioning of the root system in compacted soils.

Some of the aforementioned soil physical and biological properties can easily be measured using classic laboratory methods. Traditionally the most widely used method to assess the effects of compaction on soil physical properties are soil compression tests. They make it possible to assess the compaction process and identify volumetric soil deformation for different initial soil structures. This yields indirect information about functional properties of the internal structure, such as the stress - strain relationship and the aggregate density/dry bulk density ratio (Rücknagel et al., 2007). Typically there is a lack of direct information about changes to geometric properties and morphologies of the void system. Explicit information about soil structure changes cannot be obtained with classic methods. With non-destructive 3D imaging methods such as X-ray computed tomography (CT) additional information on the geometry of the pore space can be gained to describe the shape, arrangement and continuity of pores, while the disturbance of soil samples used in the analysis of compaction is minimized (Lipiec and Hatano, 1993; Pöhlitz et al., 2018). CT has been increasingly used in recent decades for the visualization and subsequent quantification of structural changes to obtain more information about the soil non-destructively (e.g. Keller et al., 2013; Pöhlitz et al., 2018; Rabot et al. 2018; Schlüter et al., 2011, 2016). Computed tomography not only detects the spatial distribution of pore geometries and maps their positions precisely, but also enables a quantitative image analysis.

Imaging methods such as CT focus on the possibilities of visualization and calculation. In the studies here imaging and classic methods are brought together to obtain a more extensive array of parameters than in previous work, leading to the following central research issues:

(i) Comparison of classic soil mechanical methods (stress-strain test) with modern methods (CT) and combining them for greater informational benefit.

(ii) Application of information from these two methodological complexes to ascertain the limits of soil compaction on soil functions for a variety of cultivation systems and locations.

The studies involve three different trials. In each trial the classic soil mechanical parameters are related to the morphometric parameters determined by CT to assess what additional information the latter can provide about the mechanical properties of soils and their structures. The interactions between high soil stresses and changes in soil structure, and the mechanical stability under different management systems were investigated in detail under three different aspects as outlined below:

Trial 1: Computed tomography and soil physical measurements of compaction behaviour under strip tillage, mulch tillage and no tillage

Only a few studies have dealt with the analysis of structural differences between individual conservation tillage systems and compaction effects under those tillage systems with the aid of CT scans in conjunction with classic methods (e.g. Dal Ferro et al., 2014; Jarvis et al., 2017; Luo et al., 2010). None of these studies considered the strip tillage method. In addition, no links have been established between classic soil mechanical methods and those involving computed tomography.

This trial focuses on the dual soil structure present under strip tillage compared to mulch tillage and no tillage. Specifically, it aims to answer the following questions: (i) Does the strip tillage method create small-scale structural differences within and between the seed rows? (ii) Under strip tillage, how do dry bulk density and aggregate density change compared to mulch tillage and no tillage as stress increases? (iii) To what extent can morphometric parameters based on CT describe the difference in soil compaction under strip tillage compared to mulch tillage and no tillage? (iv) Are there correlations between the parameters determined using classic methods and those determined with CT? (v) What implications do the results have for agricultural land use?

Overall, this trial focuses on the role of the different soil tillage methods in the compaction process.

Trial 2: Effects of soil moisture during soil compaction due to soil tillage as assessed by classic and CT methods

Previous studies have either dealt with the interactions between mechanical precompression stress, water content and dry bulk density (e.g. Alexandrou and Earl, 1998) and subsequently developed models and predictions of mechanical precompression stress

for different water contents (e.g. Rücknagel et al., 2012b; Saffih-Hdadi et al., 2009), or tried to demonstrate the compaction effects of individual soil tillage systems (e.g. Dal Ferro et al., 2014; Jarvis et al., 2017). None of the previous studies involved determining stress-related changes to pore space geometries depending on water content and different tillage systems by means of a combined application of classic soil mechanical and CT methods, except for Pöhlitz et al. (2018).

In this trial the effects of increasing stress on soil samples from two tillage treatments (cultivator and plough) and at two moisture tensions (6 and 1000 kPa) are explored. The following questions are considered in detail: (i) As stress increases, how do the soil physical properties change in the plough compared to the cultivator treatment, depending on soil moisture tension? (ii) To what extent does matric potential as a destabilising or stabilising factor influence the compaction effects? (iii) To what extent can morphometric parameters explain the compaction effects for 'cultivator' compared to 'plough' based on CT at different matric potentials? (iv) Are there any correlations between the classic parameters and those determined using CT?

Trial 3: Estimation of critical stress ranges to preserve soil functions at differently textured sites using computed tomography, soil physical, biological and agronomic measurements

The questions arise, whether different soil functions react differently to soil compaction, or if they become limiting at the same applied stress, and whether there are texture dependent differences as shown by various authors quoted above. With regard to compaction, attempts have only been made in the literature to date to define critical values for single soil functions or properties. For example, O'Connell (1975) shows regression equations that can be used to calculate limiting dry bulk density values based on 10% air filled porosity at field capacity using soil organic matter, particle density, and silt and clay content. Kaufmann et al. (2010) list optimal and limiting values for dry bulk density derived from parabolic relationships between dry bulk density and crop yield which show a pronounced maximum depending on soil conditions, crop species and climate. Although dry bulk density is often closely correlated with root and plant growth, there are also studies that do not show such a correlation (Kaufmann et al., 2010).

In this trial critical stress values are defined as the values at which the effects of compaction result in a limitation of soil functions. Soil functions are influenced to a different degree by soil compaction, so one has to assume that there is not a single stress value for a soil, but a range of critical stress values, hereafter called critical stress range. The focus of the present trial is to quantify critical stress values and critical stress ranges of soil functions

for differently textured sites. To see how big the influence of texture really is a number of parameters which are important for different soil functions are tested. Classic soil mechanical parameters, CT parameters, biological and plant parameters are linked. It is investigated, if there are differences in the critical stress values for the different soil functions, and if these differ for different textures. This should provide extended insights into the compaction process and structural characteristics of different soil textures, and contribute to the management of soils so that soil physical, morphological, biological and plant parameters are not adversely affected by soil compaction.

In all thee trials field samples were taken and subjected to classic soil physical and CT measurements. While the primary goal in the three trials is different, they have in common that a combination of classic and CT measurements is employed.

I am well aware that some aspects of the trials here were already researched extensively. However, the trials were deliberately set up in the manner described later to be able to make clear statements about what can be gained, if computed tomography is used in conjunction with classic methods to describe soil compaction under different conditions.

Before turning to a detailed description of the material and methods employed here, a brief review of some classic soil mechanical methods and CT is given.

2. Brief review of some classic soil mechanical methods and X-ray computed tomography (CT)

2.1. Stress and deformation behavior

To be able to take timely action against unwanted structural changes in agricultural soils before harmful soil compaction becomes a serious problem the structural characteristics of the soil as they are changed by applied compressive loads need to be identified as accurately as possible. The procedures used for this must reflect typical field conditions so that the information gained can be directly applied to agricultural practice (Semmel and Horn, 1995). Mechanical loads are forces on the soil (Wiermann, 1998). If those forces are related to an area, this results in a pressure (DVWK, 1997). Since a compressive load causes stresses inside a soil mass, the term 'stress' is also used for this pressure to describe the situation within the soil arrangement itself (Wiermann, 1998).

The 'total stress' (σ) is the sum of all stresses acting on a point (Kühner, 1997). The three main variables for the spatial propagation of stresses are the three principal stresses σ_1, σ_2 and σ_3 (Semmel and Horn, 1995). The largest stress which is oriented in the direction of maximum force is called the first principal stress (σ_1). Under a static load in naturally layered soils it is vertically aligned. The second (σ_2) and third principal stress (σ_3) act at right angles to the first and are usually considered to be equal, but lower than σ_1, i.e. $\sigma_2 = \sigma_3 < \sigma_1$. The stress distribution in structured soils is therefore anisotropic (Hartge and Horn, 1991; Kezdi, 1969). Other important variables which are derived from the three principal stresses are the mean normal stress σ_n (average of the three principal stresses), and the octahedral shear stress τ (remaining strain energy in the state of stress) (Hartge and Horn, 1991; Semmel and Horn, 1995; Wiermann, 1998).

Each point within a soil volume subjected to a load not only has a certain state of stress, but also a certain state of deformation - the strain. Analogous to stress theory, strain theory describes the state of deformation (Kühner, 1997). The components of a deformation are 'normal strain' and 'shear strain'. The assumptions for the description of the state of deformation correspond to those of stress theory (Kühner, 1997).

The propagation of stress and strain is a time-dependent process (Dürr et al., 1995; Fazekas and Horn, 2005). Strain is the downward movement or settlement. At the very moment of load application air is squeezed out of the soil pores. The ensuing reduction in pore space is called primary settlement. Next, pore water is squeezed out, leading to so-called secondary settlement. If the applied load greatly exceeds the mechanical precompression stress, then plastic flow occurs. This means a soil completely looses its original structure and the deformation which has taken place is no longer reversible.

The relationship between stress and deformation depends on soil stability and is therefore specific to a given soil. In a stable soil high stresses only cause relatively small deformations, while in unstable soils low stresses cause relatively high deformations (Kühner, 1997).

2.2.   Measures of compaction in the field

To investigate soil compaction in the field a soil is studied which has already experienced different levels of compaction in different areas of the site. Alternatively, a soil can be compacted in a driving experiment where a machine is driven over it several times with a different load or tire pressure.

To actually measure compaction undisturbed soil cores are collected and analyzed in the laboratory. Another method is to install in the soil (before its compaction) a device called stress state transducer (SST) which measures soil deformation directly on site, namely at the point of compaction. This technique evolved over the years to yield ever better results.

The first soil pressure measurements were performed in the 1930s in order to assess building sites (Rütemann, 1996). The sensors developed since that time differ in how they record pressure and deformation behaviour (Rütemann, 1996), but still work on the same physical principals. The mechanical pressure gauges placed in the soil by Bolling in the mid-1980s only allowed the measurement of the maximum ground pressures (Rütemann, 1996).

At around the same time scientists in Germany, England and America (Nichols et al., 1987) used stress state transducers (SSTs) as we know them today to measure ground pressure. These allow direct measurements of ground pressures which can be used to calculate the principal and shear stresses as well as their directional vectors (Horn et al, 1996; Rütemann, 1996). Disadvantages include the installation of the device which results in the disturbance of the surrounding material, as well as the highly laborious data analysis (Rütemann, 1996). In a next step Kühner (1997) connected an SST to a mobile measuring device, a so-called displacement transducer system (DTS), to determine the vertical and horizontal displacement of the SST. This recorded the movement of the soil particles and enabled a more accurate description of the soil compaction process, e.g. as caused by wheel tires (Wiermann et al., 1999).

2.3.   Measures of compaction in the laboratory

According to Hartge and Horn (1991) soil deformation induced by mechanical loads generally follows Hooke's law and is therefore, up to some load, elastic and reversible. The soil returns to its original state once the load is removed - the recompression range. If the

mechanical load continues to increase, Hooke's law no longer applies to the deformation and the behaviour of the soil is semi-elastic, i.e. the deformation can only be partially reversed. This means the deformation is partially plastic, and particle displacement occurs until the grain contact points have been increased to the extent necessary for the establishment of a new equilibrium of forces (DVWK, 1997) - the virgin compression range. The stress at the point where the recompression range reaches the virgin compression range is referred to as the mechanical precompression stress. It indicates the soil's current intrinsic stability and thus represents the highest possible load at which the soil will not change its current properties (DVWK, 1995; Lebert, 1989).

Mechanical precompression stress can be determined by means of the frequently used (Dürr et al., 1995; Fazekas and Horn, 2005; Kühner, 1997; Peth and Horn, 2011) semi-quantitative graphical method of Casagrande (1936) illustrated in Figure 2.3-1. In this method the point of greatest curvature of the load - settlement curve is determined first (A) (Fig. 2.3-1). Through this point a line I parallel to the abscissa (B) and the tangent II (C) are drawn. The angle bisector between line I and line II is then constructed (D). The virgin compression line, i.e. the inclined line which intersects the abscissa, is now extrapolated backwards from the intersection as a straight line III (E) until it intersects with the angle bisector. This intersection point defines the value of the mechanical precompression stress which can be read off the abscissa at IV (F).
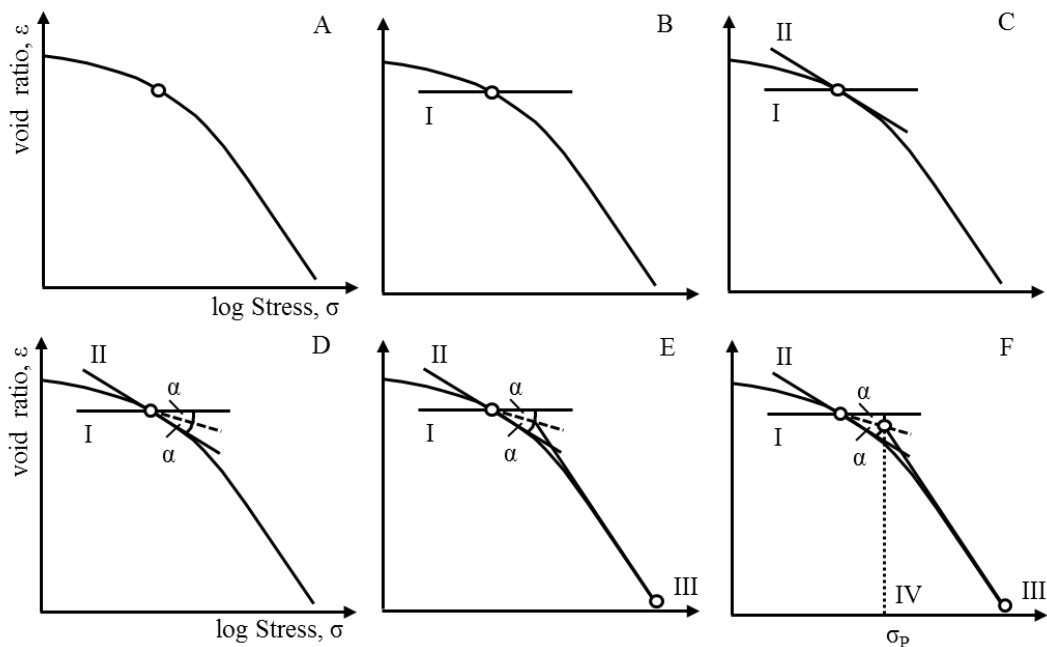
Figure 2.3-1: Identification of the mechanical precompression stress according to Casagrande (1936). For further details see text.

The load - settlement behaviour of a soil is usually expressed by relating the log of the stress (load) to the void ratio (VR) or the dry bulk density (BD) (settlement = strain) (Mosaddeghi et al., 2003). VR is commonly used in civil engineering, BD in agricultural applications.

The void ratio VR describes the volume fraction of pores (porosity, p) in relation to the volume fraction of solid matter (Dürr et al., 1995; DVWK, 1997). Porosity is computed using dry bulk density (BD) and particle density (PD). The following equations show how BD, PD, p and VR are related (DVWK, 1997):

$$BD = m_d / V_{st} \qquad\qquad (2.1)$$

$$PD = m_s / V_{ss} \qquad\qquad (2.2)$$

$$p \quad = 1 - BD/PD \qquad\qquad (2.3)$$

$$VR = P / (1-p) \qquad\qquad (2.4)$$

where m_s is the mass of the soil, V_{ss} the total volume of soil solids, m_d the dry soil mass, and V_{st} the total soil volume.

Measuring the stress - strain relationship (strain is represented in this study here by BD) generally involves studying undisturbed soil samples in a triaxial or uniaxial oedometer under drained conditions for a specified time (DVWK, 1995; Wiermann, 1998). The triaxial test is very time consuming. Hence, for general strength analysis agricultural soil mechanics primarily employs uniaxial compaction tests which hinder lateral expansion (i.e. samples in rigid rings). It is often criticized that the determination of mechanical precompression stress under static load conditions does not quite correspond to field conditions, because soils are repeatedly subjected to a series of brief and intermittent instances of load application, relief and reapplication, or to a high number of loads over time (Krümmelbein et al., 2008). However, the effects of many brief mechanical loads on a soil add up so that repeatedly driving over the ground over the course of a year produces a total settlement which has similar consequences for the soil as a prolonged load event, which in turn can be equated with a long-term load in the oedometer (DVWK, 1997; Krümmelbein et al., 2008). Hence, this test for the determination of mechanical strength is valid.

It should be noted that soil compaction not only changes the size and number of pores, but also their shape and continuity (Dürr et al., 1995). Even if soil type and dry bulk density are the same, other properties such as aggregation or water content are not necessarily identical. If the aim is a comprehensive characterization of the structural conditions of relevance for crop cultivation, these cannot be determined exclusively using soil compression tests and mechanical precompression stress. They show only a change in height reduction or an increase in density, but, for example, not the arrangement of individual particles. For

this purpose 'microscopic' methods such as non-destructive measurements with CT must be used. The latter shall be discussed in section 2.5.

Until today soil structural changes have been described only by changes in pore size distribution derived indirectly from water retention curves. In this way local shifts and (micro-) structural changes are statistically averaged for a given volume, assuming that the stress - strain relationship progresses homogeneously within the soil sample between loads. However, this completely neglects the spatial heterogeneity of the various components which form soil structure (Gantzer and Anderson, 2002), and the complex modifications of internal morphologies arising from locally changing pressure conditions (Peth et al., 2010). These are prerequisites for making realistic statements about the use-related genesis and functioning of a soil's structure (Werner, 1993).

2.4.   Mathematically derived measures of compaction

A method which involves reasonable effort and provides reproducible "in situ" measurements of the current strain is lacking (Vorderbrügge and Brunotte, 2011). Therefore, laboratory soil physical parameters are used to investigate soil compaction and soil property changes in the field (Raghavan and Ohu, 1985). The results, for example, of the mechanical precompression stress according to the graphical method of Casagrande (1936), or the degree of compactness introduced by Håkansson (1988) can be used as guidelines for carrying out agricultural activities at specific times (Shafig et al. 1994).

There is some subjectivity in the graphical method of Casagrande (1936) which can be reduced, if it is carried out by several independent people. Nevertheless, it is difficult to determine the maximum curvature, which is a prerequisite to get the mechanical precompression stress. There are other graphical methods for determining the mechanical precompression stress (Burmister, 1951; Dias Junior and Pierce, 1995; Jose et al., 1989; Lebert and Horn, 1991; Schmertmann, 1955; Sällfors, 1975), as well as models and pedotransfer functions which mathematically approximate the load capacity of a soil (Berli et al., 2003; DVWK, 1995, 1997; Lebert, 1989; Rücknagel et al., 2007, 2012a). In the latter case, however, a disadvantage lies in the multitude of parameters to be estimated, since soils are heterogeneous systems which do not lend themselves to calculations. In addition, pedotransfer functions are difficult to reproduce, cannot withstand statistical validation, and there is no demonstrable correspondence between estimates and measurements (Vorderbrügge and Brunotte, 2011).

The degree of compactness which is defined as the ratio (in %) between the dry bulk density of the soil and the dry bulk density of the same soil in a compacted reference state is often used to facilitate comparisons of compaction effects between sites, and to eliminate the

influence of soil texture. However, this is only applicable to sites which are disturbed by tillage every year. In layers not ploughed annually the volume and properties (continuity, tortuosity, etc.) of the macropore system may be more important for the functioning of the soil than its density. In such layers the degree of compactness is too rough a parameter to characterize the soil properties (Håkansson, 1990).

In addition to the above, there are a variety of other soil and plant properties which can be used to describe the effect of soil compaction on tilth (Carter, 2006). For this purpose the measured value of a soil property can be classified as "optimal" or "limiting" for a particular land use. Staying below the limit ensures that soil processes and functions are not impaired (Carter, 2006). For many soil properties a quantitative range of values (e.g. low, optimal, high) can be given based on empirically derived relationships between the property and soil processes or an aspect of a soil function (e.g. plant growth). Selected properties, e.g. soil hydraulic conductivity (Marshall and Holmes, 1978), macroporosity and aeration (Thomasson, 1978), dry bulk density (Håkansson and Lipiec, 2000), strength or penetration resistance (Glinski and Lipiec, 1990), or the least limiting water range (Kay and Angers, 1999) can provide a quantitative index of soil quality (Carter, 2006). These parameters have been applied to describe a variety of limiting situations in the field, e.g. for plant root development and growth (Carter, 2006). With respect to aeration an air filled porosity at field capacity of 10% is often considered as necessary for an optimal air supply in a soil (Carter, 1988; Greenland, 1981; Lipiec and Hatano, 2003; O'Connell, 1975). The disadvantage of the "10% rule" is the great simplification, since only the topsoil is taken into account, and seasonal fluctuations as well as changes in crops are ignored (Greenland, 1981). Kaufmann et al. (2010) suggest that optimal or limiting values of dry bulk density should be defined, because there is a parabolic relationship between dry bulk density and crop yield with a pronounced maximum depending on soil conditions, crop species and climate. In general, critical values for soil properties are location and soil specific (Carter, 2006).

Previous studies have rarely identified limits or thresholds for various soil functions to characterize the state of compacted soils and their suitability for plant growth (e.g. Daddow and Warrington, 1983; Greenland, 1981; Werner and Paul, 1999). Håkansson and Lipiec (2000) pointed out the need to find a single parameter for the characterization of the state of compaction of a soil which gives directly compatible values to compare soils among each other. The question remains whether this is possible, because soils are highly variable.

2.5.   X-ray computed tomography

At the microscopic level changes in soil structure can be investigated using image analysis methods (Wiermann, 1998). One method of directly measuring the structure of an

undisturbed (by sampling) soil core is the use of an CT scanner to determine the spatial arrangement of soil particles (Anderson et al., 1988; Gantzer and Anderson, 2002). CT measures the soil structure of a sample non-destructively and provides a three-dimensional, high-resolution visualization and characterization of pores and the soil matrix. Since the data are digital, this method is easy to use for quantitative analyses (Ketcham and Carlson, 2001).

The purpose of computed tomography is to capture multiple sets of views of an object over a range of angular orientations (Ketcham and Carlson, 2001) by exposing the object to radiation and determining the attenuation with the help of a charge-coupled device (CCD) detector. This leads to additional representations of different structures.

The technical principle of computed tomography lies in the varying attenuation of beams as they traverse a matrix (e.g. Pires et al., 2010; Taina et al., 2008). Computed tomography is based on the Beer-Lambert law:

$$I = I_0 \exp(-\mu D) \tag{2.5}$$

where I = intensity of the radiation after passing through the object, I_0 = initial intensity of the radiation received by the object, μ = attenuation coefficient of the object, and D = thickness of the object.

According to this law only part of the emitted X-radiation passes through the object, and the relative attenuation of the X-ray beams is exponentially related to the product of an attenuation coefficient and the thickness of the object. Theoretically, for a homogeneous object there needs to be only one X-ray beam to describe the object. This is represented in a simplification with one pixel in Figure 2.5-1. In a soil μ depends on the density of the material (the higher the density, the more energy is absorbed and vice versa), the effective atomic number, and the energy of the incoming X-ray beam (Taina et al., 2008).
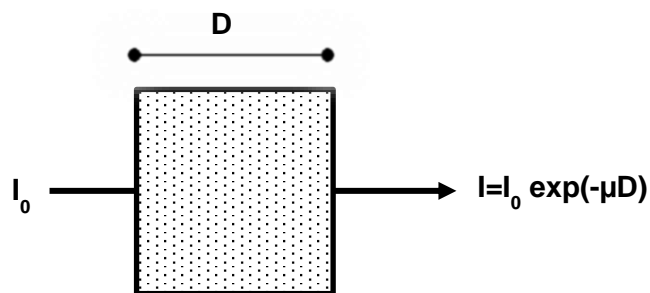
Figure 2.5-1: Schematic representation of the attenuation of an X-ray beam of initial intensity I_0 through a material of thickness D with a constant attenuation coefficient μ.

Since objects can be heterogeneous, the X-ray beams pass through areas of varying attenuation, which is related to density. The attenuation of the X-ray beams is then made up

of the sum of the attenuation by the different components of the object, weighted by their thickness:

$$I = I_0 \exp[-\Sigma(\mu_i \cdot \Delta z_i)] \tag{2.6}$$

where μ_i = attenuation coefficient of component i of the object, and Δz_i = thickness of the component. This is exemplified in Figure 2.5-2 with four pixels. By passing beams at two different angles through these pixels one gets four equations with four unknowns. This means one can solve for the attenuation coefficient in each pixel.
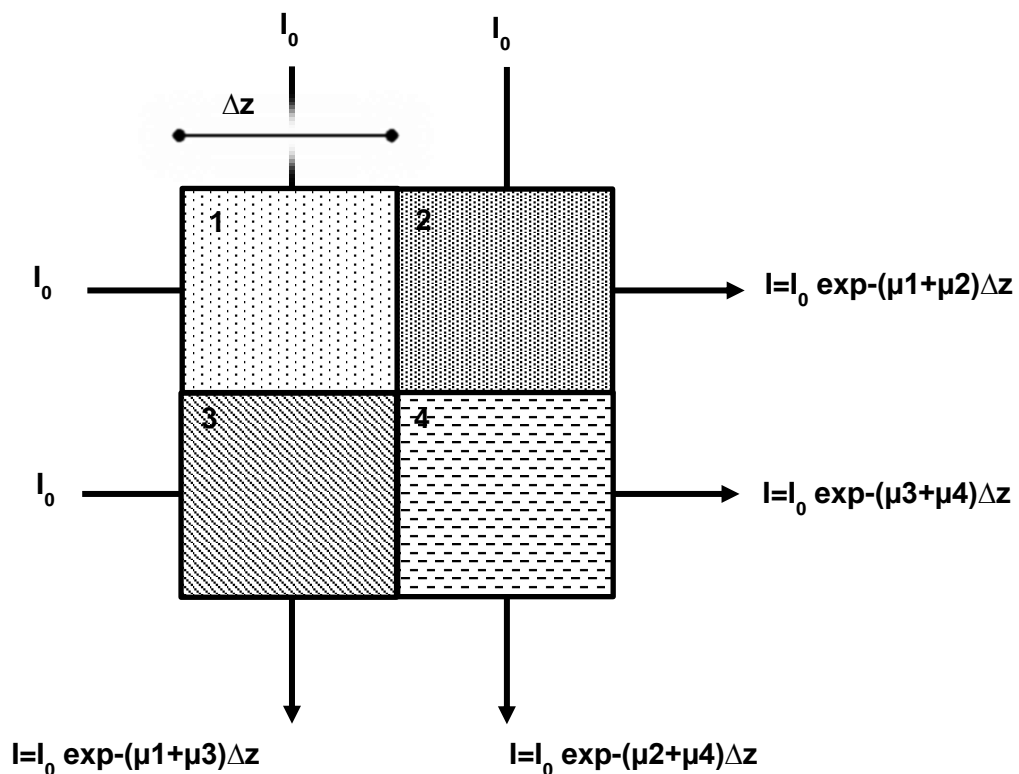
Figure 2.5-2: Schematic representation of the attenuation of an X-ray beam of initial intensity I_0 through a material of total thickness D and variable attenuation coefficients (µ1 to µ4) for four discrete components of thickness Δz.

In a soil there is usually a large number of possible densities. This fact is displayed in a simplified manner in Figure 2.5-3. There are 64 pixels of which 8 are irradiated from the left side and 8 from the top by the beams shown. This yields 16 equations, but to solve for the attenuation coefficient in each pixel one needs 64 equations. Hence, 48 further equations are required.

I_0

$I_0 \rightarrow$

$I=I_0 \ exp\text{-}(\Sigma\mu_i)\Delta z$

....

$I=I_0 \ exp\text{-}(\text{-}\Sigma\mu_i)\Delta z$ ....
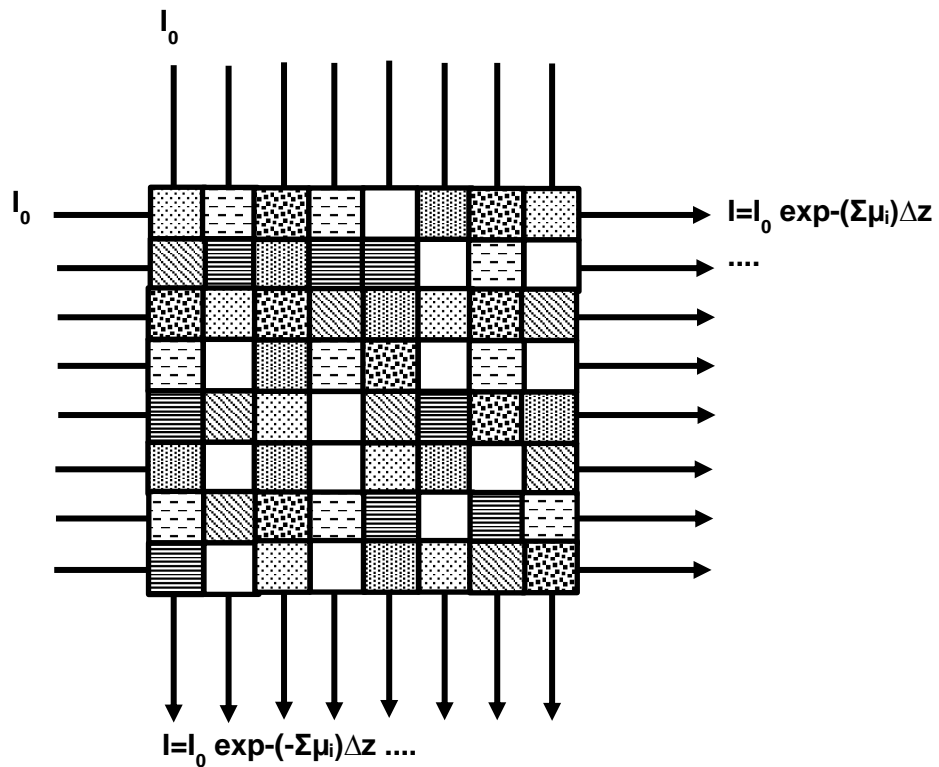
Figure 2.5-3: Schematic representation of the attenuation of an X-ray beam of initial intensity I_0 through a material of thickness D and variable attenuation coefficients (μ_i) for 64 discrete units of thickness Δz.

To obtain them X-ray beams are send through the object at additional angles. The above explanations are simplified to illustrate the need for various beam angles to get enough equations. In the CT machine used for the samples in this study the beams are not parallel, but cone beams (Fig. 2.5-4) and the sample is three-dimensional as opposed to the 2D examples described in Figure 2.5-2 and 2.5-3. So, the situation is a bit more complicated than just described, but the same in principle.

360°
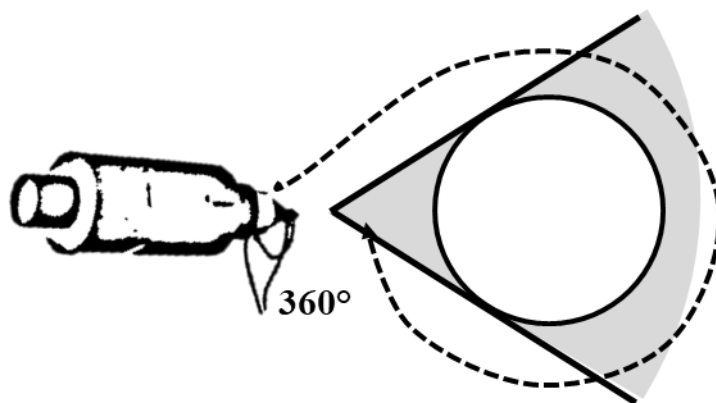
Figure 2.5-4: Schematic representation of a cone X-ray beam in a 360° rotation.

The purpose of a scan is to determine the attenuation coefficient μ for every voxel in the matrix. As already described, a soil sample can have different attenuation coefficients at different positions. The measured attenuation coefficients are in turn used to determine the average density of every voxel in the scanned matrix (Brown et al., 1987). To visualize the various densities they are converted into a grey scale where the pixel with the highest density (typically a mineral grain or small rock fragment) is assigned the colour white, and the pixel with the lowest (typically a void in the pore space) is assigned the colour black. All other densities, e.g. that of the soil matrix, roots or other organic matter, and of the water filled pore space are represented by various shades of grey. The method used for this scaling is called filtered back projection.

A detailed explanation of how tomography works can be found in Anderson et al. (1988), Brown et al. (1987), Ketcham and Carlson (2001), Pires et al. (2010), Taina et al. (2008) and Wildenschild et al. (2002).

3. Material and Methods

3.1. Trial sites and sampling design

3.1.1. Trial 1

Soil sampling was performed at the strip tillage experiment set up by the International Crop Production Centre in Bernburg-Strenzfeld (Germany, federal state of Saxony-Anhalt, 11°41′E, 51°50′N; 80 m above sea level) in 2012. The average annual temperature at the site is 9.7°C, the average annual precipitation 511 mm, and the average annual evapotranspiration 650 mm. The soil type is a chernozem (FAO, 1998). The texture of the topsoil (0-30 cm) is comprised of 60 g kg^{-1} sand, 740 g kg^{-1} silt and 200 g kg^{-1} clay, thus constituting a silt loam (Soil Survey Staff, 1997). The total organic carbon content in the topsoil is 1.65 g kg^{-1}, the pH is 6.8.

The field experiment is organized as a completely randomised block design, including four blocks each with the treatments strip tillage, mulch tillage and no tillage. Each individual trial plot measures 18 x 50 m. The row spacing in the strip tillage treatment is 50 cm. The tilled strips measure 15-20 cm across and are ploughed to a depth of 20-25 cm. Under strip tillage there is no soil tillage between seed rows. Because of this differentiation in the strip tillage treatment, spatially separate samples were taken from within (strip tillage WS) and between seed rows (strip tillage BS). These were considered as independent treatments for the rest of the experimental procedure and during evaluation. In the mulch tillage treatment the soil was tilled with a cultivator to a depth of 15-20 cm, while the no tillage treatment was, as the name says, not tilled at all.

For the measurement of dry bulk density and saturated soil hydraulic conductivity, two classic soil physical parameters, undisturbed soil samples (volume = 250 cm^3, height = 6 cm) were taken in the years 2014 and 2015 in three replications per tillage treatment and field block from a soil depth of 2-8 cm (n = 3 x 4 x 4 = 48 samples), and 12-18 cm (n = 48). In addition, in 2012, before the tillage treatments were initiated, soil cores (n = 48) were taken in three replications from the same four blocks and two depths (3 x 4 x 2 = 24 samples) to determine the initial physical conditions. The soil conditions at sampling were the same in all three sampling years (water content close to field capacity) and always took place under a winter wheat crop.

Two types of soil compression test were conducted in this trial, which required two different sampling regimes. In both, undisturbed soil samples (220 cm^3, height = 2.8 cm) were taken at soil depth 12-18 cm from each tillage treatment per field block and later subjected to 8 different load steps (5, 10, 25, 50, 100, 200, 350 and 550 kPa). In the first type of compression test a load was applied to a sample which was broken up afterwards to

determine the aggregate density (AD) after compression (section 3.3.). Because of the destruction, a different soil sample was required for each load step. Hence, at total of 5 x 4 x 8 = 160 samples was required. In the following this type of load application is called 'single load application'. In the second type of compression test all eight aforementioned loads were successively applied to the same sample. After each load step a CT scan of the sample was carried out (section 3.4.). Since each sample was loaded and scanned eight times, only of 5 x 4 = 20 samples were required. In the following this type of load application is called 'sequential load application' (Bradford and Gupta, 1986).

3.1.2. Trial 2

The site is located near Buttelstedt (Germany, federal state of Thuringia, 11°20′O, 51°4′N; 200 m above sea level) where a tillage trial was established in 2008. The average annual temperature is 8.4°C, the average annual precipitation amounts to 541 mm and the average annual evapotranspiration to 641 mm. The soil type is a chernozem (FAO, 1998), the texture of the topsoil (0-30 cm) is silty clay loam (Soil Survey Staff, 1997) with 293 g kg^{-1} clay, 662 g kg^{-1} silt and 45 g kg^{-1} sand. The total organic carbon content in the topsoil amounts to 1.9 g kg^{-1}, the pH is 7.0.

Samples were taken from one plot each under the tillage treatments 'cultivator' and 'plough' (cultivation depth 5 cm, ploughing depth 25 cm) on winter wheat stubble before summer barley was sown in March 2016. Throughout the trial primary tillage was always performed in the previous autumn, some six months before sampling. There was no traffic on the plots during this time and they were fallow, except for stubble.

For the determinations of dry bulk density and saturatred hydraulic conductivity undisturbed soil samples (volume 250 cm^3, height = 6 cm) were taken from a soil depth of 16-22 cm in three replications at five places per tillage treatment, resulting in a total of 3 x 5 x 2 = 30 samples.

For the soil compression tests undisturbed soil samples (volume 220 cm^3, height = 2.8 cm) were taken from a depth of 16-19 cm in each tillage treatment. As in trial 1 the soil compression tests required two sampling regimes. The samples were collected at five places for each tillage treatment in two replications for two soil moisture tensions, this time for nine load steps (10, 25, 50, 100, 200, 350, 550, 1250 and 2500 kPa). This amounts to a total of 9 x 5 x 2 x 2 = 180 samples for single load application, but only 5 x 2 x 2 = 20 samples for sequential load application.

3.1.3. Trial 3

In autumn 2016 soil samples were taken from the topsoil (0-20 cm) of four cropped sites (Quellendorf, Buttelstedt, Rothenberga, Kranichborn) which were specifically selected to represent a wide range of soil textures. The clay content varies between locations from 70 g kg^{-1} to 280 g kg^{-1}. The sand contents are between 40 g kg^{-1} and 530 g kg^{-1}. An overview and description of the locations is given in Table 1.

For the initial characterization of the soils (Tab. 1) undisturbed and disturbed soil samples were taken. The former were analyzed for saturated hydraulic conductivity and dry bulk density, the latter were air-dried, passed through a 2 mm sieve and analyzed for particle size distribution, total organic carbon content, pH and nutrient content. The undisturbed samples (volume = 250 cm^3, height = 6 cm) were taken in three repetitions at 5 places per site (3 x 5 x 4 = 60).

For both soil mechanical and CT examinations undisturbed soil samples (volume = 220 cm^3, height = 2.8 cm) were taken at 4 places per site (4 x 4 = 16). For the compression tests with eight load steps (5, 10, 25, 50, 100, 200, 350 and 550 kPa) sequential load application was used.

For the column experiments (section 3.5) a total of approximately 750 kg of disturbed soil from 0-20 cm depth was taken from each site (750 x 4 = 3000 kg). This soil mass was distributed among 240 columns.

Table 3.1-1: Description of the sites sampled sites for trial 3.

Site	T (°C)	N (mm)	Taxonomy[a]	Texture (g kg^{-1}) Clay	Texture (g kg^{-1}) Sand	Texture class[b]	TOC (g kg^{-1})	pH	Nutrients (mg per 100 g) P	Nutrients (mg per 100 g) K	Nutrients (mg per 100 g) Mg	N_{min} (kg N ha^{-1})	BD (g cm^{-3})	K_s (cm d^{-1})
Quellendorf	8.7	526	Chernozem	130	450	loam	14	7.4	6.8	22.1	10.4	11	1.29	158
Buttelstedt	8.4	541	Chernozem	280	40	silty clay loam	21	6.9	3.5	51.3	24.1	15	1.14	157
Rothenberga	8.5	500	Haplic Luvisol	130	60	silt loam	13	6.7	5.9	19.0	6.0	17	1.10	137
Kranichborn	8.5	500	Mollic Fluvisol	70	530	sandy loam	51	7.4	12.4	13.9	12.1	30	0.82	157

T = average annual temperature; N = average annual precipitation

TOC = total organic carbon; P = phosphorus; K = potassium; Mg = magnesium; N_{min} = mineralizable nitrogen; BD = dry bulk density; K_s = saturated hydraulic conductivity

all parameters except BD and K_s were determined by Eurofins Agraranalytik Deutschland GmbH, Jena, Germany

[a] FAO (1998)

[b] USDA classification scheme (Gee and Bauder, 1986)

3.2.   Soil compression tests

The soil samples (volume = 220 cm^3, height = 2.8 cm) were first slowly saturated by capillary rise before being drained for at least seven days in a sandbox with a hanging water column to a matric potential of -6 kPa (Klute, 1986) and then weighed.

In trial 2 two different tensions had to be achieved. Hence, half of the soil mechanical (n = 90) and half of the CT (n = 10) samples from the cultivator and plough treatments were drained as just described to a matric potential of -6 kPa, corresponding to pF1.8. The gravimetric water content was identified by weight loss (Gardner, 1986). These samples are labelled as $C_{pF1.8}$ ('cultivator' drained to -6 kPa matric potential) and $P_{pF1.8}$ ('plough' drained to -6 kPa). The other half of the soil mechanical (n = 90) and computed tomography (n = 10) samples from the cultivator and plough treatments were drained for seven days to a matric potential of -1000 kPa using the pressure plate method (Klute, 1986). Their gravimetric water content was again identified by weight loss (Gardner, 1986). They are labelled as $C_{pF4.0}$ ('cultivator' drained to -1000 kPa) and $P_{pF4.0}$ ('plough' drained to -1000 kPa).

Fully automated oedometers and the associated software (WINBOD32, Wille Geotechnik, APS Antriebs-, Prüf- und Steuertechnik GmbH, Göttingen-Rosdorf, Germany) were used to determine the stress - strain relationships under drained conditions. Load application was uniaxial. Each load step was applied with a load time of 120 min and a subsequent relaxation time of 15 min with a 2 kPa load. According to previous studies on similar soils a longer load time does not cause significant further settlement (Rücknagel et al., 2007). The oedometer dial indicator records settlement with an accuracy of 0.01 mm.

It should be noted that the present study only involves uniaxial compaction. In practice, when driving over a field with agricultural machinery the soil is also subjected to dynamic loads which are propagated three-dimensionally. Nevertheless, the results of the present study can be applied to the field scale, because the greatest principal stress acts in the direction of the maximum force applied which is vertical in naturally layered soils (Horn and Peth, 2011).

After the compression tests the soil samples were dried at 105°C for 48 h and then weighed (Blake and Hartge, 1986). The thus obtained dry mass was then divided by the initial sample volume to compute the dry bulk density prior to the compression tests (BD_0). Using the settlement (s), the initial height of the soil sample (h_0), and BD_0 the resulting BD after each load application (BD_{xi}) was calculated as follows:

$$BD_{xi} = BD_0 \cdot \frac{h_0}{h_0 - s} \qquad\qquad\qquad\qquad (3.1)$$

A semi-logarithmic stress - BD_{xi} curve was then created. The mechanical precompression stress was determined based on these curves using the graphical method of Casagrande

(1936). To minimize subjectivity (Rücknagel et al., 2010) it was applied by several experimenters.

3.3.   General soil physical investigations

The saturated hydraulic conductivity (K_s, cm d^{-1}) of the soil samples (volume = 250 cm³, height = 6 cm) was measured by means of a stationary system (Klute and Dirksen, 1986) with a flow duration of 4 h. The dry bulk density (BD, g cm^{-3}) of the same samples was subsequently determined by drying them at 105°C for 48 h and then weighing them (Blake and Hartge, 1986).

For the determination of aggregate density (AD) the soil samples were carefully broken up by hand after the load application. Following that, aggregates with a size of 8-10 mm were sieved out. A subsample thereof was then dried at 105°C for 48 h to determine the aggregate dry mass. Another subsample was prepared to determine the aggregate volume. In three parallel repetitions these aggregates were submerged into 100% rapeseed oil at room temperature until no more air leakage was detected before draining the oil residue onto absorbent paper. Next, the aggregates' volume was determined using "immersion weighing" (Koenigs, 1981). The volume and dry mass of the aggregates served to calculate AD. For the calculations the aggregate volume was reduced by 3.5 vol.-% to account for a minimal oil film coating the aggregates. This correction value for the amount of oil on the aggregates was obtained from test measurements using differential weighing. AD was only determined in trial 1 and 2.

In aggregated agricultural soils the ratio of aggregate density to dry bulk density (AD/BD_{xi}) can serve as an indicator of density heterogeneity (Rücknagel et al. 2007). A low AD/BD_{xi} ratio (< 1.05 to 1.10) suggests damaging soil compaction, whereas a high AD/BD_{xi} ratio (1.15 to > 1.20) is indicative of a loose soil structure (Rücknagel et al. 2013).

In trial 2 only, semi-logarithmic load - AD diagrams were created and curves fitted according to the method of least squares. Mechanical precompression stress was determined based on these curves using the graphical method of Casagrande (1936) to assess, if it is possible to determine the mechanical precompression stress of aggregates.

3.4.   Computed tomography and image processing

Soil samples from the stress - strain tests were scanned with an energy of 150 kV and a beam current of 550 µA using an industrial X-ray scanner (X-Tek XTH225, Nikon Metrology). One scan comprised 2480 projections with an exposure time of 1.41 s (2 frames per projection). A CCD detector panel with 2000×1750 diodes recorded the projections. Beam

hardening was reduced with a 0.1 mm copper filter. The CT scans were reconstructed with a spatial resolution of 60 µm and an 8-bit greyscale resolution using the X-Tek CT Pro software package. This is the maximum resolution which allows to scan the entire sample (10 cm in diameter) and to get representative CT images. The results therefore pertain to pore sizes larger than 60 µm. Image processing was performed with the Java software ImageJ 1.50e (Rasband, 1997-2015). To reduce scatter and noise the CT scans were filtered using the "Non-local Means Denoising" plugin in Fiji (Fiji Is Just ImageJ) (Buades et al., 2005).

To make full use of the detector panel three samples of 3 cm height were stacked on top of each other. For demarcation plastic plates were placed between the samples. This also ensured that the samples did not dry out.

In order to exclude artefacts at the edges of the sample and reduce the data volume a cylindrical region of interest (ROI) with a diameter of 90 mm was used in the middle of the reconstructed CT scan. The vertical extent of the ROI was adjusted to the reduction in sample height after each load step. This was based on the positions of small and identifiable features, e.g. stones, at the upper and lower ends of the sample. Regardless of compaction status it was thus always possible to locate the original soil volume again after each consecutive load application.

Automatic segmentation was then applied to the scan of the ROI to separate the image into pores and soil matrix. This was carried out using the thresholding method by Otsu (1979). Segmentation is a prerequisite for the determination of mean macropore diameter, macroporosity, pore connectivity and anisotropy. In trial 3 only macroporosity and pore connectivity were determined.

The ImageJ plugin "BoneJ − Thickness" (Doube et al., 2010) was used to determine the pore size distribution by means of the maximum inscribed sphere method. The mean macropore diameter was then calculated as the weighted mean of the measured macropore diameters with the frequency of a given diameter range as the weighting factor.

Macroporosity (here pore diameter > 60 µm) was quantified as the ratio of the number of pore voxels to the total number of voxels within the ROI (Dewry et al., 2008).

The ImageJ analysis "Particle Analyzer" (Ferreira and Rasband, 2010-2012) was employed to calculate pore connectivity which represents the connection probability between two arbitrarily chosen pore voxels, i.e. the chance to belong to same pore cluster. This dimension free number is also denoted as the Γ indicator (Renard and Allard, 2013; Schlüter et al., 2014) and has a value between 0 and 1.

The ImageJ plugin "BoneJ - Anisotropy" (Doube et al., 2010) was used to determine the degree of anisotropy which is a measure of how highly oriented substructures are within a

volume, with 0 reflecting the minimum (completely isotropic) and 1 the maximum (completely anisotropic).

3.5.   Soil biological and agronomic measurements

Soil biological and agronomic measurements were only carried out in trial 3.

Column preparation

The soil biological and agronomic analyses were performed only in trial 3. For the column experiments with earthworms (*Lumbricus terrestris*) and also for the column experiments with spring barley (*Hordeum vulgare*) six bulk densities were produced in five repetitions for each site (6 x 5 x 4 = 120 columns). For both column experiments the columns were positioned in a randomized order. The two column experiments took place independently of each other.

Opaque polyvinyl chloride (PVC) pipes were used for the column experiments (19 cm inside diameter, 283.52 cm^2 surface area, 30 cm height). For each site it was tested in advance how far the soil was compactable. From this the remaining five bulk densities were calculated in steps of 0.07 g cm^{-3}. Thus, for the four sites dry bulk density ranges of 1.42-1.77 g cm^{-3} (Quellendorf), 1.28-1.63 g cm^{-3} (Buttelstedt), 1.21-1.56 g cm^{-3} (Rothenberga) and 0.72-1.07 g cm^{-3} (Kranichborn) were produced.

As an explanation for the different dry bulk density ranges consider the following: The particle size distribution which theoretically allows the most compact packing consists of 67% sand, 24% silt and 9% clay, because the particles thusly graded in size fit best into a tight packing. This particle size distribution corresponds to a sandy loam (Larson and Allmaras, 1971). In the present study, however, the sandy loam at the Kranichborn site had the lowest dry bulk density as a result of the rather high organic matter content. Since the Quellendorf site has the next most graded mixture of sand, silt and clay of the four sites, but relatively little organic matter, it has the highest BD here. In contrast, the Buttelstedt and Rothenberga sites have a more equal particle size distribution and therefore a less dense packing.

The soil was manually compacted at a water content near field capacity using metal plates. To get the first layer a pre-weighed amount of soil was filled into a column and beaten until its volume was reduced to the required extent. The second layer was then filled onto the compacted first layer in the column and treated in the same manner, and so on, until all the pre-weighed soil was filled into the column. In the columns representing a given site the same soil mass was used for all six bulk densities. This resulted in decreasing filling heights with increasing dry bulk density. The soil mass was chosen to yield a maximum filling height of 25 cm at the lowest dry bulk density.

Using the same soil mass means the amount of nutrients in each column representing the same field site are the same. If one would have used the same soil volume rather than the same soil mass, then there would have been fewer nutrients at low BD values than at higher ones, which may have affected growth.

On the inside of the columns a strong tape was attached after the second (10 cm), third (15 cm) and fourth (20 cm) layer counting from the top. It reached about 2.5 cm into the column. This was done to prevent earthworms from crawling and plant roots from growing preferentially along the inside column wall.

Biological measurements (Earthworm activity)

The earthworm genus *Lumbricus terrestris L.* was used for these column experiments. In each column six earthworms were placed on the soil surface. To prevent soil drying while permitting gas exchange (O_2) at the same time 30 g of wheat and oat straw about 5 cm in length was mixed together and placed on each surface. The upper end of the columns was covered with gauze and the lower one with a fleece to prevent an escape of the earthworms. The experimental conditions were constantly dark at 20°C. The total burrowing period of *L. terrestris* was 18 days, from 29.01.2017 to 16.02.2017.

After the experiment the straw was carefully removed and collected by hand, together with the earthworm casts on the soil, to make the earthworm burrows visible on the surface. The number of biopores was counted at the top (0 cm), after the second (10 cm), third (15 cm), fourth (20 cm) and bottom layer (25 cm) of the columns and added up. Furthermore, mortality was determined as a percentage of the original number of earthworms.

Agronomic measurements

For the agronomic column experiments summer barley (*Hordeum vulgare L.*) of the variety Avalon was used. In each column 15 plants were sown, covered with a roughly 3 cm thick soil layer, and thinned to ten plants after emergence. For nitrogen a target value of 90 kg N ha^{-1} was aimed at. To achieve it N_{min} was determined (Tab. 1) and subtracted from the target value to obtain the amount of nitrogen to be applied to the surface of the columns in the form of calcium ammonium nitrate.

The bottom of each column was covered with a fleece to prevent roots from growing beyond it. The columns were weighed regularly every few days to monitor water loss by evapotranspiration. This loss was then replaced by watering so that lack of water did not restrict plant growth.

The experiments were carried out in a greenhouse with the climatic conditions regulated according to the BBCH stages of cereals (Witzenberger et al., 1989) as follows: (i) germination, leaf development and tillering: constant 15°C with a 12 h photoperiod; (ii) stem elongation and booting: 20°C during the day and 15°C at night with a 14 h photoperiod; (iii) inflorescence emergence, heading, flowering, anthesis, development of fruit, ripening and senescence: 25°C during the day and 20°C at night with a 15 h photoperiod. The total growing period of the crop was 130 days, from 09.03.2017 to 17.07.2017.

At the senescence stage the plants were harvested 1 cm above the soil. Straw and grain were dried separately at 105°C to a constant weight which was then converted into a yield ($g\,m^{-2}$).

3.6. Derivation of critical stress values and critical stress ranges

This point also applies only to trial 3.

The mechanical precompression stress is widely viewed as the most important measure to assess harmful soil compaction. Hence, it is used in trial 3 as a benchmark to compare other critical stress values to, i.e. it is viewed as a critical stress value, too. Its value for the soils under investigation here is derived from the stress - BD_{xi} curves (section 3.2.).

According to Werner and Paul (1999) an air capacity of ≥ 8 vol.-% at pF1.8 (pores > 50 µm) is necessary to maintain the ecological functionality of cohesive soils. Air capacity, when measured at this matric potential, can be considered equivalent to macroporosity (Drewry et al., 2008). Here, macroporosity was determined with CT quantitative image analysis at a resolution of 60 µm. Following Werner and Paul (1999) a macroporosity ≥ 8 % was considered to be the minimum required. So, as soon as a macroporosity of 8 % was reached, the corresponding stress value was read off the abscissa of the stress - macroporosity diagram and considered to be the critical stress value.

There are no critical values given in the literature regarding pore connectivity, i.e. for the collapse of a well-connected pore network into many isolated pores. The first significant change in connectivity with increasing load application is therefore considered to be the critical stress value.

In the case of the effect of dry bulk density on yield the literature (Czyz et al., 2001, Czyz, 2004) often reports an optimal dry bulk density for maximum yields. This relationship is frequently described with a second or third degree polynomial, depending on the statistical quality. As will be shown later, such polynomials can also be employed to describe the relationship between dry bulk density and the number of biopores. They have the general form:

$$y = a \cdot BD^2 + b \cdot BD + c \qquad\qquad\qquad (3.2a)$$

or

$$y = a \cdot BD^3 + b \cdot BD^2 + c \cdot BD + d \qquad\qquad\qquad (3.2b)$$

where y can be number of biopores, grain or straw yield, and a, b, c and d are coefficients to be determined by regression. The maximum of these curves, i.e the maximum number of biopores, or the maximum yield at an optimal dry bulk density (BD_{opt}) is found at:

$$\frac{dy}{dBD} = 0 \qquad\qquad\qquad (3.3)$$

Applying equation 3 to equation 2a and b yields:

$$BD_{opt\,y} = -\frac{b}{2a} \qquad\qquad\qquad (3.4a)$$

$$BD_{opt\,y} = \frac{-2b \pm \sqrt{4b^2 - 12ac}}{6a} \qquad\qquad\qquad (3.4b)$$

BD_{opt} is then used to derive the critical stress value with the help of the stress - BD_{xi} diagram as follows: BD_{opt} is targeted on the ordinate. Then the BD_{opt} value is tracked in the direction of higher stress values until the stress - BD_{xi} curve is hit and the critical stress value can be read off the abscissa.

Not only were the critical stress values derived, but also the range of the possible variation of those values, in the following referred to as 'bars' and shown in the respective figures. For the mechanical precompression stress the bars correspond to the real standard deviation of the values obtained with the graphical method of Casagrande (1936) by several experimenters. For the critical stress values of the CT parameters the bars correspond to the load steps which lie before and after the stress values in the stress - macroporosity or stress - pore connectivity diagram. For the critical stress values of the number of biopores and agronomic parameters only BD levels were included in the bars which were overlapping clearly.

3.7. Statistical analyses

The statistical analyses were carried out with the statistics program 'R Studio' (version 0.99.893, R Foundation for Statistical Computing).

For the variance analyses all parameters were tested for normal distribution (Shapiro-Wilk test) and variance homogeneity (Levene's test). The arithmetic mean values for BD, BD_{xi}, AD, macroporosity, pore connectivity and anisotropy were calculated separately for each tillage variant, pF or texture treatment from the site repetitions. The means of the log-normally distributed saturated hydraulic conductivity and precompression stress values were

calculated based on the logarithmized values. The mortality of *L. terretris* was calculated per site.

In trial 1 a two-way analysis of variance was conducted for the soil physical parameters BD and K_s with soil tillage and year as the independent factors. A one-way analysis of variance was conducted for the soil mechanical and for the morphometric parameters between load steps for the respective tillage treatment, and between the individual tillage treatments within a particular load step. Using Tukey's honestly significant difference test differences among group mean values were identified and considered to be significant at a significance level of $p \leq 0.05$.

In trial 2 the statistical analysis was carried out separately for 'cultivator' and 'plough' and is presented in figures and in tables. The figures show the results of the one-way analysis of variance between the different matric potentials. The tables give the results of the one-way analysis of variance performed across the load steps (10-2500 kPa). Tukey's honestly significant difference test served to determine differences from group mean values ($p \leq 0.05$).

In trial 3 a one-way analysis of variance was performed for all parameters along the eight load steps of the compression tests, and along the six bulk densities from the column experiments for each location. The Tukey honestly significant difference test was applied to determine differences in group means and was considered significant at a significance level of $p \leq 0.05$.

In addition, in trial 1 and 2 correlations were performed between BD_{xi}, AD and the AD/BD_{xi} ratio on the one hand, and mean macropore diameter, macroporosity, pore connectivity and anisotropy on the other hand. In trial 2 the CT parameters were correlated with each other as well.

For most correlations in this study no equation is presented, because no physically meaningful mathematical description was obvious.

4. Results

4.1. CT and soil physical measurements of compaction behaviour under strip tillage, mulch tillage and no tillage

4.1.1. Soil physical conditions

Dry bulk density

Before the strip tillage trial was set up in 2012, BD at soil depths 2-8 cm and 12-18 cm was 1.15 g cm^{-3} and 1.36 g cm^{-3}, respectively, in all plots, regardless of the later tillage treatment (Tab. 4.1-1). In 2014 and 2015 neither depth displayed any significant differences in BD between mulch tillage and strip tillage WS on the one hand, and strip tillage BS and no tillage on the other. By contrast, at both depths and in both years BD was significantly lower for mulch tillage and strip tillage WS compared to strip tillage BS and no tillage.

Table 4.1-1: Dry bulk density (BD) and saturated hydraulic conductivity (K$_s$) at 2-8 and 12-18 cm depth for mulch tillage (MT), strip tillage within the seed row (STWS), strip tillage between seed rows (STBS), and no tillage (NT). Statistically significant differences (p ≤ 0.05) are in lower-case letters (tillage system within year and depth), and upper-case letters (year within tillage system and depth).

Parameter	Depth (cm)	Year	Tillage system			
			MT	STWS	STBS	NT
BD (g cm^{-3})	2-8	2012	1.15 aB	1.15 aB	1.15 aA	1.15 aA
		2014	1.09 aA	1.06 aA	1.29 bB	1.28 bB
		2015	1.11 aAB	1.09 aAB	1.39 bC	1.43 bC
	12-18	2012	1.36 aB	1.36 aB	1.36 aA	1.36 aA
		2014	1.21 aA	1.17 aA	1.41 bAB	1.41 bAB
		2015	1.24 aA	1.22 aA	1.42 bB	1.45 bB
K$_s$ (cm d^{-1})	2-8	2012	111.3 aA	111.3 aA	111.3 aA	111.3 aA
		2014	227.3 aA	255.0 aA	81.7 aA	109.8 aA
		2015	144.9 abA	295.0 bA	39.8 abA	30.4 aA
	12-18	2012	26.7 aA	26.7 aA	26.7 aA	26.7 aA
		2014	145.9 bB	158.2 bB	34.8 aAB	45.2 aA
		2015	147.5 bB	107.6 abB	81.7 abB	22.5 aA

Compared to the beginning of the trial in 2012 there was a significant decline in BD for mulch tillage and strip tillage WS at soil depth 2-8 cm in the year 2014, and at a soil depth of 12-18 cm in the years 2014 and 2015. Strip tillage BS and no tillage displayed a significant increase in BD over time, which was more prominent at soil depth 2-8 cm than at 12-18 cm.

Saturated hydraulic conductivity

In 2012, prior to the initiation of the tillage treatments, the K_s values at soil depths 2-8 cm and 12-18 cm were 111.3 cm d^{-1} and 26.7 cm d^{-1}, respectively, again in all plots, regardless of the later tillage treatment (Tab. 4.1-1). In the years 2014 and 2015 differences in the K_s value were observed between tillage treatments at a soil depth of 2-8 cm. Because of high standard deviations, these differences were only significant in 2015. In this year strip tillage WS had a significantly higher K_s value than no tillage. Mulch tillage and strip tillage BS did not differ significantly from strip tillage WS or from no tillage. In 2014 there were no significant differences between mulch tillage and strip tillage WS on the one hand, and strip tillage BS and no tillage on the other at a soil depth of 12-18 cm. Conversely, mulch tillage and strip tillage WS differed from strip tillage BS and no tillage in that they displayed significantly higher K_s values. In 2015 mulch tillage had a significantly higher K_s value in 12-18 cm depth than no tillage, while strip tillage WS and strip tillage BS did not differ significantly from mulch tillage and no tillage.

In 2014 and 2015 the K_s values in 12-18 cm depth were significantly higher than in 2012 for all tillage variants, with the exception of no tillage and strip tillage BS in 2014.

Relationship between dry bulk density and saturated hydraulic conductivity

It is common soil physical knowledge that an increase in BD results in a decrease in porosity, especially macroporosity. This reduction in the number and size of larger pores then leads to a marked decrease in the saturated hydraulic conductivity of a soil. Hence, as BD increases, K_s decreases and vice versa. Unsurprisingly, this was observed in this study, too, (Fig. 4.1-1). It appears that the points for all depths and tillage treatments fall onto the same line. This would imply that there is a unique relationship between BD and K_s. However, this should be viewed with caution, because the data for MT and STWS all have low BD and high K_s values, while all data for STBS and NT show high BD and low Ks values and there is no overlap between the data for these two groups.
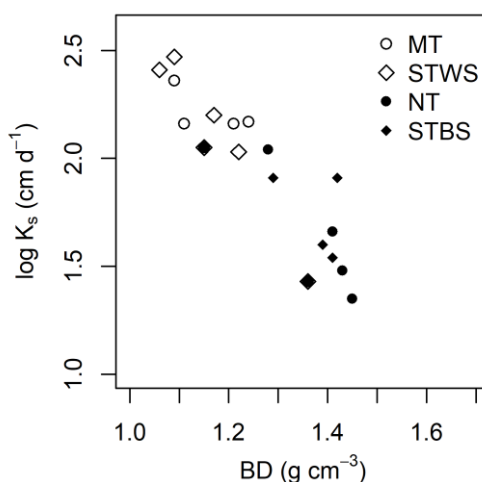
Figure 4.1-1: Correlation between dry bulk density (BD) and the logarithm of hydraulic conductivity (K_s) at 2-8 and 12-18 cm depth in the years 2012, 2014 and 2015 for mulch tillage (MT), strip tillage within the seed row (STWS), strip tillage between seed rows (STBS), and no tillage (NT).

4.1.2. Soil compression tests with single load application

Dry bulk density

In terms of BD_{xi} the load steps 5 and 10 kPa resulted in no significant differences between mulch tillage and strip tillage WS, or between strip tillage BS and no tillage (Tab. 4.1-2). In contrast, mulch tillage and strip tillage WS displayed significantly lower BD_{xi} values than strip tillage BS and no tillage. For the load steps 25 and 50 kPa there was no significant difference between strip tillage BS and no tillage. Both did, however, display significantly higher BD_{xi} compared to mulch tillage. At the 350 kPa load step there was no significant difference between mulch tillage and strip tillage WS. However, both displayed significantly lower BD_{xi} compared to strip tillage BS. In addition, mulch tillage had significantly lower BD_{xi} than no tillage. At the beginning of stress application there was a maximum difference in dry bulk density between the treatments of 0.29 g cm^{-3} which decreased to a maximum of 0.11 g cm^{-3} by the end of stress application. Overall, BD_{xi} increased by approximately 0.40 g cm^{-3} under mulch tillage and strip tillage WS, while the higher initial values meant that BD_{xi} only increased by around 0.25 g cm^{-3} in the strip tillage BS and no tillage treatments.

Table 4.1-2: Dry bulk density (BD_{xi}), aggregate density (AD) and AD/BD_{xi} ratio from single load application to soil cores from 12-18 cm depth for mulch tillage (MT), strip tillage within the seed row (STWS), strip tillage between seed rows (STBS), and no tillage (NT). Statistically significant differences ($p ≤ 0.05$) are indicated by lower case letters (load step within each tillage system), and upper case letters (tillage system within each load step).

Parameter	Tillage system	Load step (kPa)							
		5	10	25	50	100	200	350	550
BD_{xi}	MT	1.14 aA	1.20 abA	1.27 abA	1.31 abcA	1.44 abcA	1.47 acdA	1.49 cdA	1.57 dA
(g cm³)	STWS	1.21 aA	1.23 aA	1.30 abAB	1.38 abcAB	1.46 bcdA	1.49 bcdA	1.53 cdAB	1.61 dA
	STBS	1.43 aB	1.45 aB	1.46 abB	1.53 abB	1.55 bcA	1.59 cdA	1.65 deC	1.68 eA
	NT	1.40 aB	1.47 aB	1.45 abB	1.48 abAB	1.53 bcA	1.59 cdA	1.61 deBC	1.66 eA
AD	MT	1.47 aAB	1.47 aA	1.51 abA	1.50 abA	1.51 abA	1.59 bcA	1.62 cA	1.66 cA
(g cm³)	STWS	1.45 aA	1.50 aA	1.48 aA	1.49 aA	1.56 abA	1.50 aA	1.58 abA	1.66 bA
	STBS	1.58 aC	1.59 aA	1.51 aA	1.59 aA	1.55 aA	1.57 aA	1.58 aA	1.63 aA
	NT	1.57 aBC	1.55 aA	1.53 aA	1.54 aA	1.60 aA	1.59 aA	1.58 aA	1.60 aA
AD/BD_{xi}	MT	1.31 aB	1.30 aB	1.21 abB	1.10 bA	1.08 bA	1.13 abA	1.09 bC	1.07 bA
(-)	STWS	1.20 acA	1.22 aAB	1.14 abcAB	1.08 abcA	1.07 abcA	1.00 bA	1.03 bB	1.04 bcA
	STBS	1.11 aA	1.09 aA	1.03 abA	1.04 abA	1.00 abA	0.99 bA	0.95 bA	0.97 bA
	NT	1.12 bA	1.06 abA	1.06 abA	1.04 abcA	1.04 abcA	1.00 acA	0.98 acAB	0.96 cA

Aggregate density

Significant differences in AD between the tillage treatments were only seen for the 5 kPa load step (Tab. 4.1-2). There were no significant differences in AD between mulch tillage and strip tillage WS, and between strip tillage BS and no tillage. Strip tillage BS displayed significantly higher AD than strip tillage WS and mulch tillage. No tillage displayed significantly higher AD than strip tillage WS. At the beginning of stress application there was a maximum difference in aggregate density between the treatments of 0.13 g cm^{-3}, but during the course of further stress application this difference became ever smaller. At the end of stress application the final AD values were quite similar at around 1.64 g cm^{-3} in all four treatments.

At the end of stress application the final AD values were around 1.65 g cm^{-3} were very similar for all four treatments.

AD increased under mulch tillage and strip tillage WS by around 0.20 g cm^{-3}, while the higher initial values meant that the AD only increased by around 0.05 g cm^{-3} in the strip tillage BS and no tillage treatments.

AD/BD$_{xi}$ ratio

Throughout the entire course of stress application BD$_{xi}$ was significantly lower at most load steps for mulch tillage (5-50, 350, 550 kPa) and strip tillage WS (5-25, 100 kPa) than the corresponding AD, while this only occurred in isolated cases in the strip tillage BS (10, 350 kPa) and no tillage treatments (5, 10, 100 kPa) (Fig. 4.1-2). For all tillage treatments the compaction curves of BD$_{xi}$ and AD converged as stress application increased, resulting in a decline of the AD/BD$_{xi}$ ratios (Tab. 4.1-2). At the 5 kPa load step mulch tillage displayed a significantly higher AD/BD$_{xi}$ ratio than the other three tillage treatments. For the 10 and 25 kPa load steps there were no significant differences between strip tillage BS and no tillage, although they had a significantly lower AD/BD$_{xi}$ ratio than mulch tillage. As further load steps were applied there were no further significant differences between tillage treatments, with the exception of the 350 kPa load step. Here, mulch tillage, strip tillage WS and strip tillage BS differed significantly from each other. Furthermore, no tillage displayed a significantly lower AD/BD$_{xi}$ ratio than mulch tillage. Overall, the AD/BD$_{xi}$ ratios for mulch tillage and strip tillage WS decreased by approximately 0.20 throughout the compaction process, while the AD/BD$_{xi}$ ratios for strip tillage BS and no tillage only decreased by around 0.15.

According to the classification of the AD/BD$_{xi}$ ratios outlined by Rücknagel et al. (2007) the soil structure under strip tillage WS changed from a blocky structure with open positioning and subangular aggregates with semi-open to open positioning to become a

coherent mass with no visible aggregation. The soil in the strip tillage BS treatment initially displayed a blocky structure with semi-open to open positioning and subangular aggregates with semi-open positioning. This also developed into a closed aggregate arrangement.
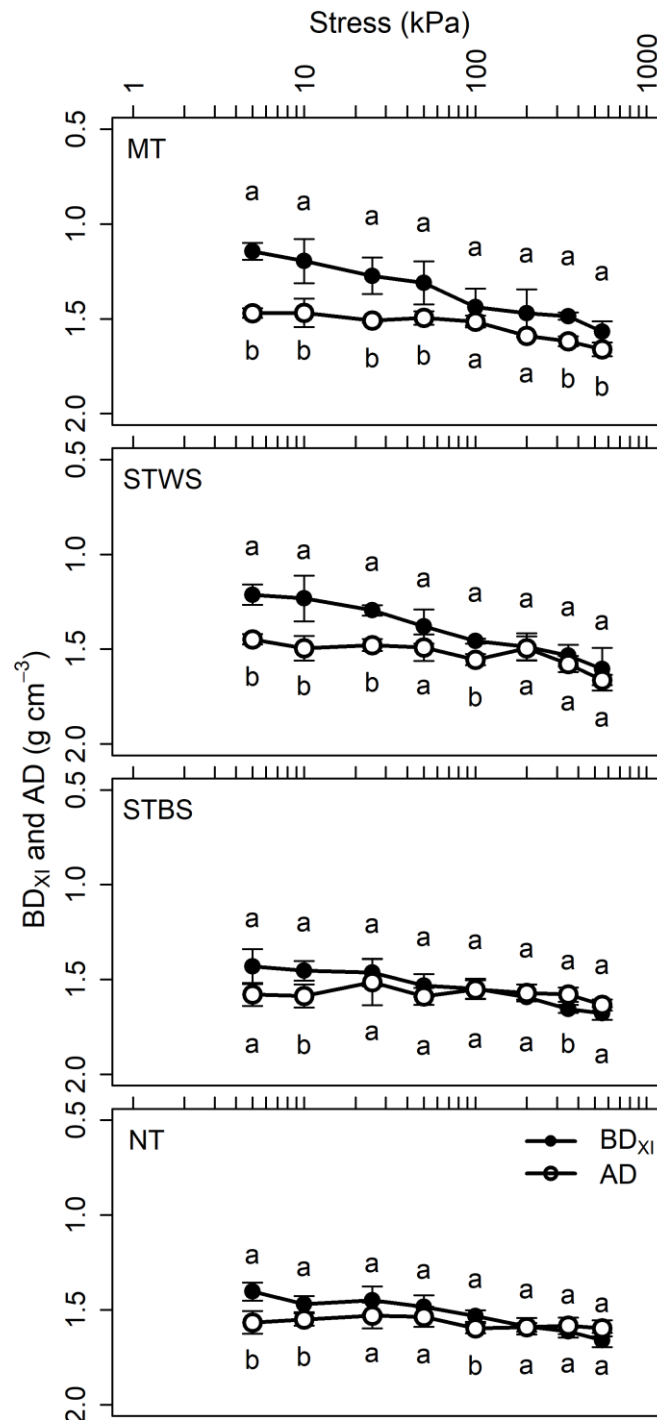
Figure 4.1-2: Dry bulk density (BD_{xi}) and aggregate density (AD) from single load application to soil cores from 12-18 cm depth for mulch tillage (MT), strip tillage within the seed row (STWS), strip tillage between seed rows (STBS), and no tillage (NT). Error bars show the standard deviations, different lower case letters indicate statistically significant differences ($p \leq 0.05$) between BD_{xi} and AD for each load step. The legend is given in the graph for NT.

4.1.3. Soil compression tests with sequential load application

Dry bulk density and mechanical precompression stress

With regard to BD_{xi} the load steps from 5-100 kPa yielded no significant differences between mulch tillage and strip tillage WS, or between strip tillage BS and no tillage (Tab. 4.1-3, Fig. 4.1-3A). On the other hand, within the 5-25 kPa load steps mulch tillage and strip tillage WS displayed significantly lower BD_{xi} values than strip tillage BS and no tillage. At the 50 kPa load step mulch tillage as well as strip tillage WS displayed significantly lower BD_{xi} values than strip tillage BS. In addition, mulch tillage displayed significantly higher BD_{xi} than no tillage. At the 100 kPa load step mulch tillage displayed significantly lower BD_{xi} than strip tillage BS and no tillage. At the beginning of stress application there was a maximum difference in dry bulk density between the tillage treatments of 0.29 g cm^{-3}. At the end of the compaction process there were similar density values of around 1.70 g cm^{-3} for all treatments. As stress increased the BD_{xi} values under mulch tillage and strip tillage WS rose by approximately 0.45 g cm^{-3}, while they only increased by around 0.20 g cm^{-3} under strip tillage BS and no tillage.

The mechanical precompression stress values identified using the stress - BD_{xi} diagrams ($\sigma_{P\ BDxi}$) differed between the tillage systems. Strip tillage WS (log $\sigma_P = 1.58 \triangleq 38$ kPa) displayed significantly lower mechanical precompression stress than strip tillage BS (log $\sigma_P = 2.15 \triangleq 141$ kPa). Mulch tillage (log $\sigma_P = 1.67 \triangleq 46$ kPa) and no tillage (log $\sigma_P = 2.05 \triangleq 112$ kPa) did not differ significantly from each other, or from strip tillage WS or strip tillage BS.

Table 4.1-3: Dry bulk density (BD_{xi}), mean macropore diameter, macroporosity, pore connectivity, anisotropy, and logarithm of the precompression stress (log σ_P) from sequential load application to soil cores from 12-18 cm depth for mulch tillage (MT), strip tillage within the seed row (STWS), strip tillage between seed rows (STBS), and no tillage (NT). Statistically significant differences (p ≤ 0.05) are indicated by lower case letters (load step within each tillage system), and upper case letters (tillage system within each load step).

Parameter	Tillage system	Stress stage (kPa)								log σ_P
		5	10	25	50	100	200	350	550	(kPa)
BD_{xi} (g cm^{-3})	MT	1.23 bA	1.24 abA	1.3 acA	1.35 cA	1.42 dA	1.52 eA	1.61 fA	1.68 gA	1.67 AB
	STWS	1.25 aA	1.28 aA	1.34 abA	1.41 abAB	1.49 bcAB	1.58 cdA	1.66 deA	1.71 eA	1.58 A
	STBS	1.52 aB	1.53 aB	1.55 aB	1.57aC	1.59 aB	1.62 aA	1.64 aA	1.67 aA	2.15 B
	NT	1.45 aB	1.47 aB	1.49 abB	1.52 abBC	1.55 bcB	1.59 cdA	1.65 deA	1.70 eA	2.05 AB
Mean macropore diameter (mm)	MT	0.72 aA	0.72 aA	0.64 aA	0.64 aA	0.56 aA	0.47 aA	0.53 aA	0.55 aA	-
	STWS	0.94 aA	0.92 aA	0.88 aA	0.82 abA	0.65 abA	0.51 bA	0.51 bA	0.53 bA	-
	STBS	0.95 aA	1.12 aA	1.06 aA	1.13 aA	1.10 aA	0.90 aA	0.76 aA	0.64 aA	-
	NT	1.14 aA	1.21 aA	1.19 aA	1.16 aA	1.13 aA	0.83 aA	0.59 aA	0.48 aA	-
Macroporosity (-)	MT	0.12 aB	0.10 aC	0.08 abB	0.04 bcA	0.02 bcA	0.01 cA	0.01 cA	0.00 cA	1.86 A
	STWS	0.10 aB	0.09 aBC	0.06 abAB	0.03 bcA	0.02 bcA	0.01 cA	0.00 cA	0.00 cA	1.69 A
	STBS	0.02 aA	0.02 aA	0.02 aA	0.01 aA	0.01 aA	0.01 aA	0.01 aA	0.00 aA	2.08 AB
	NT	0.04 aA	0.04 aAB	0.03 aA	0.03 aA	0.02 aA	0.01 aA	0.01 aA	0.00 aA	2.39 B
Pore connectivity (-)	MT	0.80 aB	0.74 aC	0.67 aB	0.22 bA	0.08 bA	0.03 bA	0.03 bA	0.05 bA	-
	STWS	0.69 aB	0.60 aBC	0.39 abAB	0.17 bcA	0.07 cA	0.03 cA	0.06 cA	0.07 cA	-
	STBS	0.08 aA	0.09 aA	0.08 aA	0.08 aA	0.09 aA	0.07 aA	0.05 aA	0.06 aA	-
	NT	0.16 aA	0.14 aAB	0.08 aA	0.09 aA	0.06 aA	0.07 aA	0.06 aA	0.04 aA	-
Anisotropy (-)	MT	0.18 aA	0.18 aA	0.16 aA	0.17 aA	0.17 aA	0.25 aA	0.86 bA	0.88 bA	-
	STWS	0.22 aA	0.23 aA	0.25 aA	0.25 aA	0.20 aA	0.22 aA	0.83 bA	0.91 bA	-
	STBS	0.27 aA	0.26 aA	0.26 aA	0.22 aA	0.44 aA	0.45 aA	0.40 aA	0.88 aA	-
	NT	0.28 aA	0.29 aA	0.30 aA	0.24 aA	0.30 aA	0.30 aA	0.54 aA	0.77 aA	-
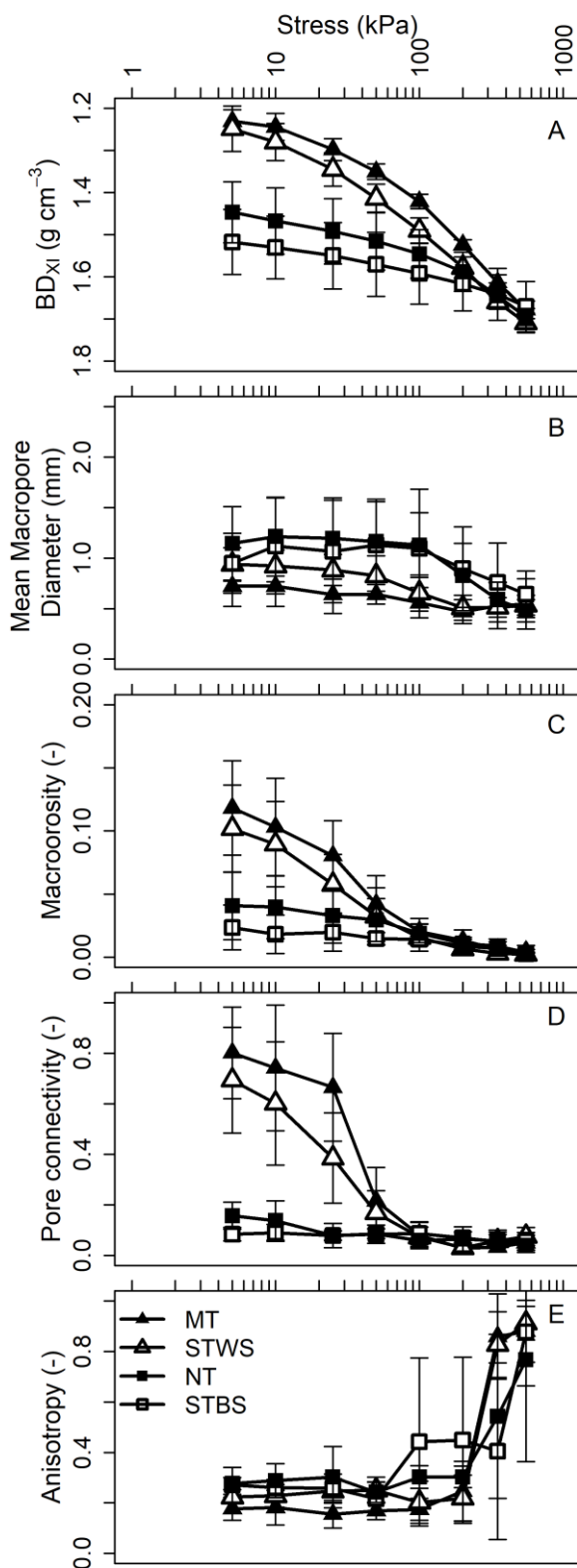
Figure 4.1-3: Dry bulk density (BD$_{xi}$) (A), mean macropore diameter (B), macroporosity (C), pore connectivity (D), and anisotropy (E) of soil cores from 12-18 cm depth from sequential load application for mulch tillage (MT), strip tillage within the seed row (STWS), strip tillage between seed rows (STBS), and no tillage (NT). Error bars show the standard deviations. Unlike in Fig. 4.1-2 statistically significant differences are not stated here, because this would have made the plots somewhat difficult to read. However, they are given in Table 4.1-3. The legend is given in graph E.

Morphometric parameters

Macropore structure characteristics of a representative sample from mulch tillage and no tillage at all eight load steps are depicted in Figure 4.1-4 and 4.1-5, respectively. Note that the following results are only true for pore sizes ≥ 60 μm. Under no tillage the application of higher load steps resulted in only minor visual changes to the macropore space, due to the higher initial density. In contrast, under mulch tillage many macropores, but also aggregates, can be seen at the beginning of stress application. When the applied stress reached 50-100 kPa, the CT scans show that under mulch tillage most macropores were already reduced in size. Overall, increased stress application resulted in a progressive homogenisation of the soil structure in both tillage treatments.
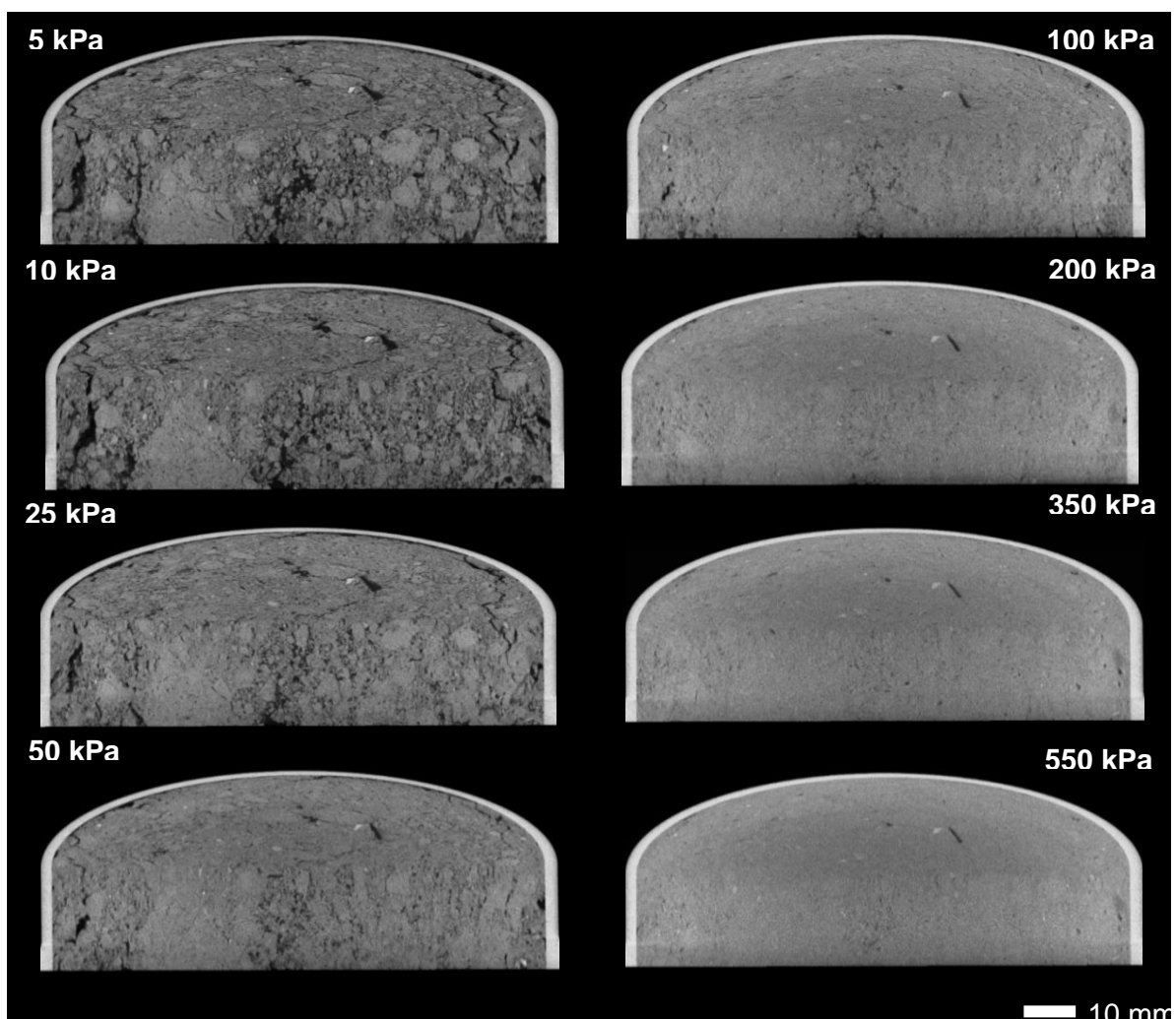
Figure 4.1-4: CT cross section images from sequential load application (5 to 550 kPa) for mulch tillage (MT). The images show half a core viewed from the top at an angle of 45°.
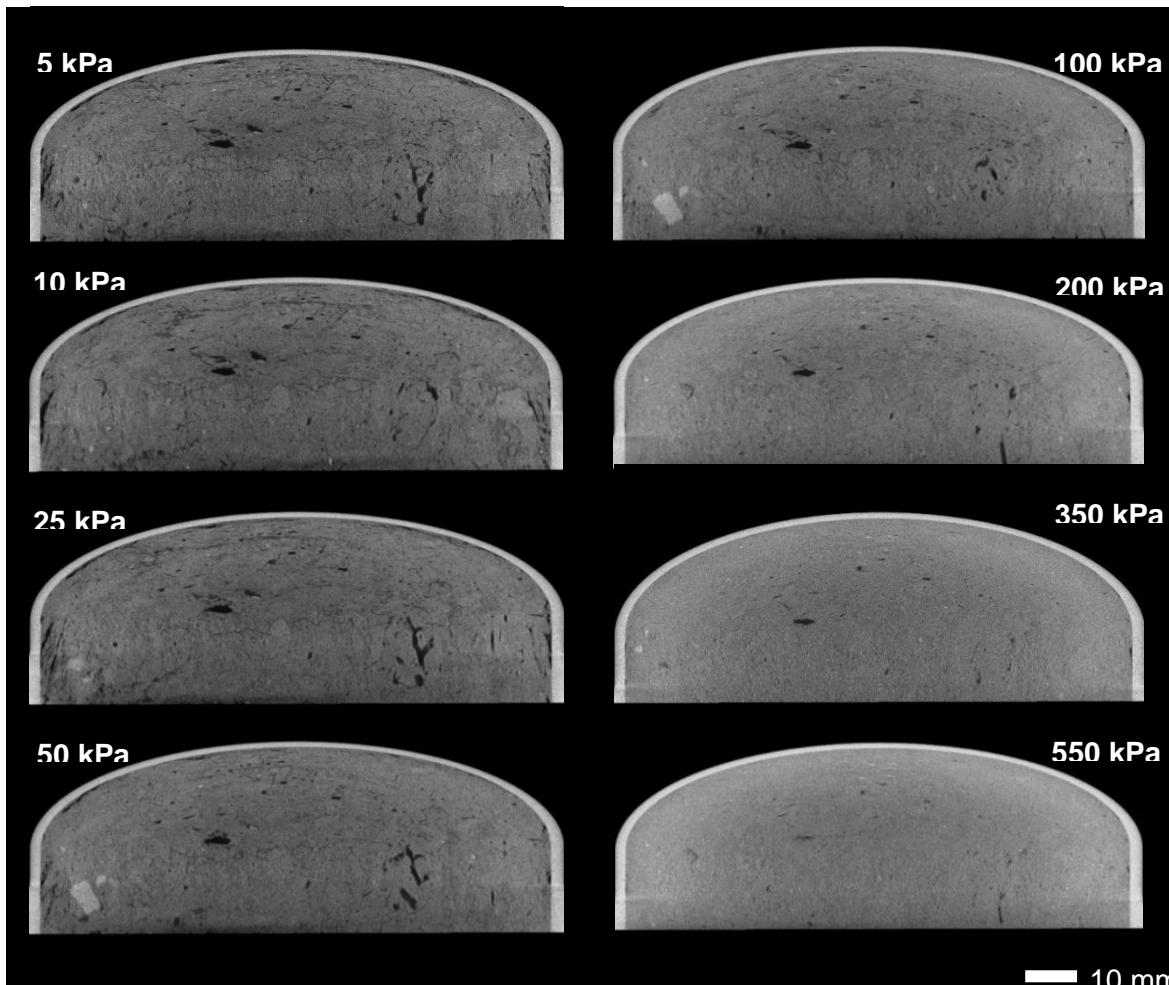
Figure 4.1-5: CT cross section images from sequential load application (5 to 550 kPa) for no tillage (NT). The images show half a core viewed from the top at an angle of 45°.

The reduction in the mean macropore size with increasing stress was only significant under strip tillage WS (Tab. 4.1-3, Fig. 4.1-3B). The differences between the tillage treatments at the individual load steps were not significant. Apparently there is a balance between bigger macropores merely being reduced within the visible range and smaller macropores being compacted beyond the image resolution limit and therefore excluded from averaging. Throughout the course of stress application strip tillage BS and no tillage tended to display higher mean macropore sizes than mulch tillage and strip tillage WS. At the 550 kPa load step all treatments displayed similar average final pore sizes of around 0.55 mm.

The increase in compressive stress resulted in a decline in macroporosity and pore connectivity, irrespective of tillage treatment, although this was only significant under mulch tillage and strip tillage WS (Tab. 4.1-3, Fig. 4.1-3C and D). For the load steps 5-25 kPa there were significant differences in macroporosity and pore connectivity between the tillage treatments. At lower load steps the pairs mulch tillage and strip tillage WS, and no tillage and

strip tillage BS differed significantly from each other with regard to macroporosity and pore connectivity, but hardly at all among each other (Tab. 4.1-3). At the highest load steps almost the entire void volume had been reduced and the tillage treatments displayed similar macroporosity and pore connectivity values.

The mechanical precompression stress values identified using the double logarithmic stress - macroporosity diagrams ($\sigma_{P\ MP}$) differed between the tillage systems (Tab. 4.1-3). There were no significant differences between mulch tillage (log σ_P = 1.86 ≜ 80 kPa) and strip tillage WS (log σ_P = 1.69 ≜ 50 kPa), while both displayed significantly lower mechanical precompression stress values compared to no tillage (log σ_P = 2.39 ≜ 270 kPa). Strip tillage BS (log σ_P = 2.08 ≜ 150 kPa) did not differ significantly from the other tillage treatments.

Increasing the stress application resulted in a change from isotropic to anisotropic conditions, regardless of the tillage treatment. Due to the broad distribution of values, the increase in anisotropy was only significant for mulch tillage and strip tillage WS at the load steps 350 and 550 kPa (Tab. 4.1-3, Fig. 4.1-3E). No significant differences were observed between tillage treatments.

4.1.4. Relationship between morphometric and soil mechanical parameters

Correlations were performed between BD_{xi}, AD and the AD/BD_{xi} ratio on the one hand, and the various CT parameters on the other (Fig. 4.1-6). In eight of them there was a unique relationship, i.e. independent of tillage treatment. In four of them there was such a dependence. For NT and STBS the data for mean macropore diameter and BD_{xi} follow the same course, but for MT and STWS they follow two different courses (Fig. 4.1-6A). The same holds for the correlation between the AD/BD_{xi} ratio and mean macropore diameter (Fig. 4.1-6I). For the relationship between BD_{xi} and macroporosity (Fig. 4.1-6B), as well as between AD and mean macropore diameter (Fig. 4.1-6E) there are two different courses, one for MT and STWS, and one for NT and STBS.

At a given BD_{xi} the mean macropore diameter and the macroporosity are higher for NT and STBS than for the MT and STWS. A given mean macropore diameter corresponds to a higher AD and a lower AD/BD_{xi} ratio in the case of NT and STBS compared to MT and STWS.
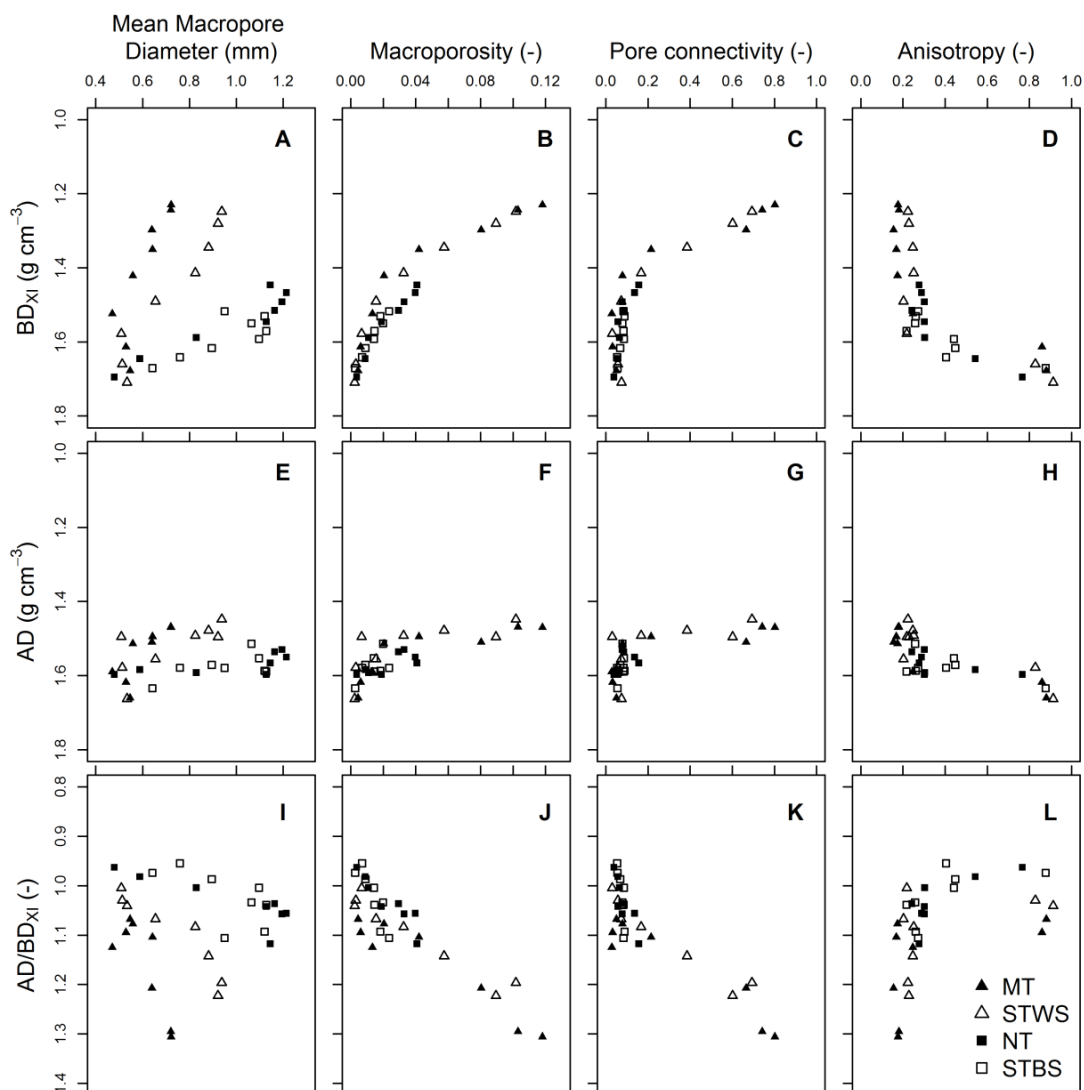
Figure 4.1-6: Correlation between dry bulk density (BD$_{xi}$), aggregate density (AD) and the AD/BD$_{xi}$ ratio on the one hand, and mean macropore diameter, macroporosity, pore connectivity, and anisotropy on the other hand of samples from 12-18 cm depth for mulch tillage (MT), strip tillage within the seed row (STWS), strip tillage between seed rows (STBS), and no tillage (NT). The legend is given in graph L.

4.2. Effects of soil moisture during soil compaction due to soil tillage as assessed by classic and CT methods

4.2.1. Initial soil physical conditions

As one would expect from the research cited in the introduction, the plough treatment initially had a significantly lower BD (1.19 g cm^{-3}) and a significantly higher saturated conductivity (530.3 cm d^{-1}) compared to the cultivator treatment (1.48 g cm^{-3}, 47.9 cm d^{-1}). The gravimetric water content was significantly higher for 'plough' than 'cultivator' at -6 kPa. However, at -1000 kPa matric potential the water content did not differ significantly between 'cultivator' and 'plough' (Tab. 4.2-1).

Table 4.2-1: Gravimetric soil water content (gSWC, g kg^{-1}) and the corresponding soil water content as a percentage of field capacity (SWC, % FC) for single load application and sequential load application for 'cultivator' and 'plough' at -6 kPa and -1000 kPa matric potential. Statistically significant differences (p ≤ 0.05) between tillage systems are indicated by lower case letters.

Tillage system	load application method	Matric potential (kPa)	Soil water tension (pF)	gSWC (g kg^{-1})	SWC (% FC)
Cultivator	single	-6	1.8	255.30 a	100.00
		-1000	4.0	204.50 b	80.10
	sequential	-6	1.8	242.20 a	100.00
		-1000	4.0	184.50 b	76.18
Plough	single	-6	1.8	308.00 c	100.00
		-1000	4.0	191.80 b	62.27
	sequential	-6	1.8	271.00 c	100.00
		-1000	4.0	210.90 b	77.82

4.2.2. Comparison of $C_{pF1.8}$ and $C_{pF4.0}$

Parameters obtained from compression tests

The stress - BD$_{xi}$ curves for both moisture regimes for the single load (Fig. 4.2-1A) and the sequential load application (Fig. 4.2-2A) show a typical compaction behaviour, namely a slow increase in BD at first and then an ever steeper increase in BD with increasing load application. The curves are very similar for the single and sequential load application, irrespective of tillage treatment and matric potential. In the cultivator treatment none of the load steps shows a significant difference in BD$_{xi}$ between the two matric potentials (Fig. 4.2-1A, Tab. 4.2-2). The compaction curves of the sequential load application (Fig. 4.2-2A) show a smoother course, because all load steps were applied to the same sample so that the curve is not composed of individual samples, which increases the variability in the single load application. Therefore, the mechanical precompression stress was determined here from the

curves from the sequential load application. The mechanical precompression stress values for the two pF treatments in the cultivator treatment do not differ significantly from each other (log σ_P = 2.43 for $C_{pF1.8}$, and 2.55 for $C_{pF4.0}$).
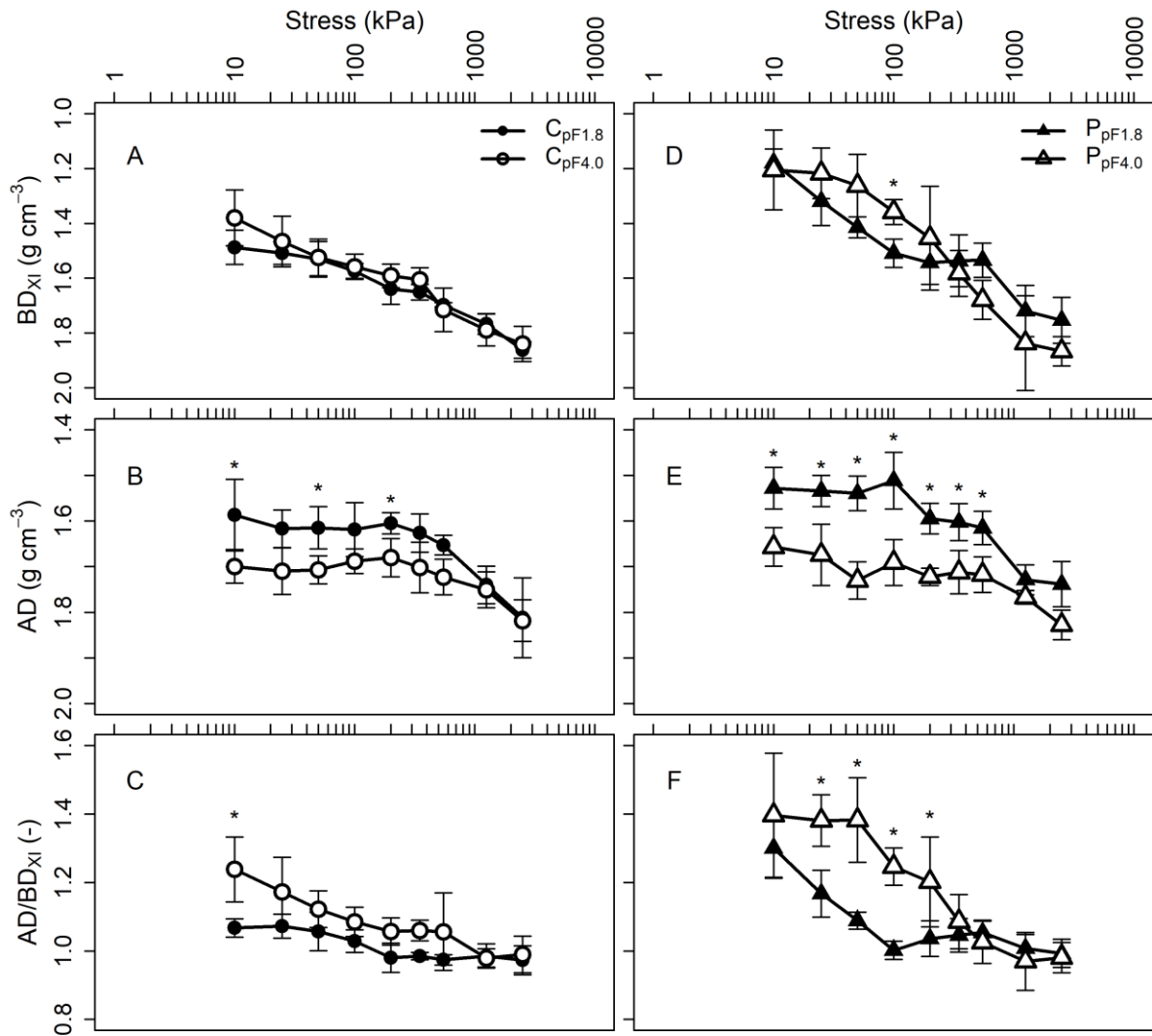
Figure 4.2-1: Dry bulk density (BD_{xi}), aggregate density (AD) and AD/BD_{xi}-ratio from single load application (stress) for 'cultivator' (A-C) at -6 kPa ($C_{pF1.8}$) and -1000 kPa matric potential ($C_{pF4.0}$), and for 'plough' (D-F) at -6 kPa ($P_{pF1.8}$) and -1000 kPa matric potential ($P_{pF4.0}$). Error bars show the standard deviations, stars indicate a statistically significant difference ($p \leq 0.05$) between pF1.8 and pF4.0.
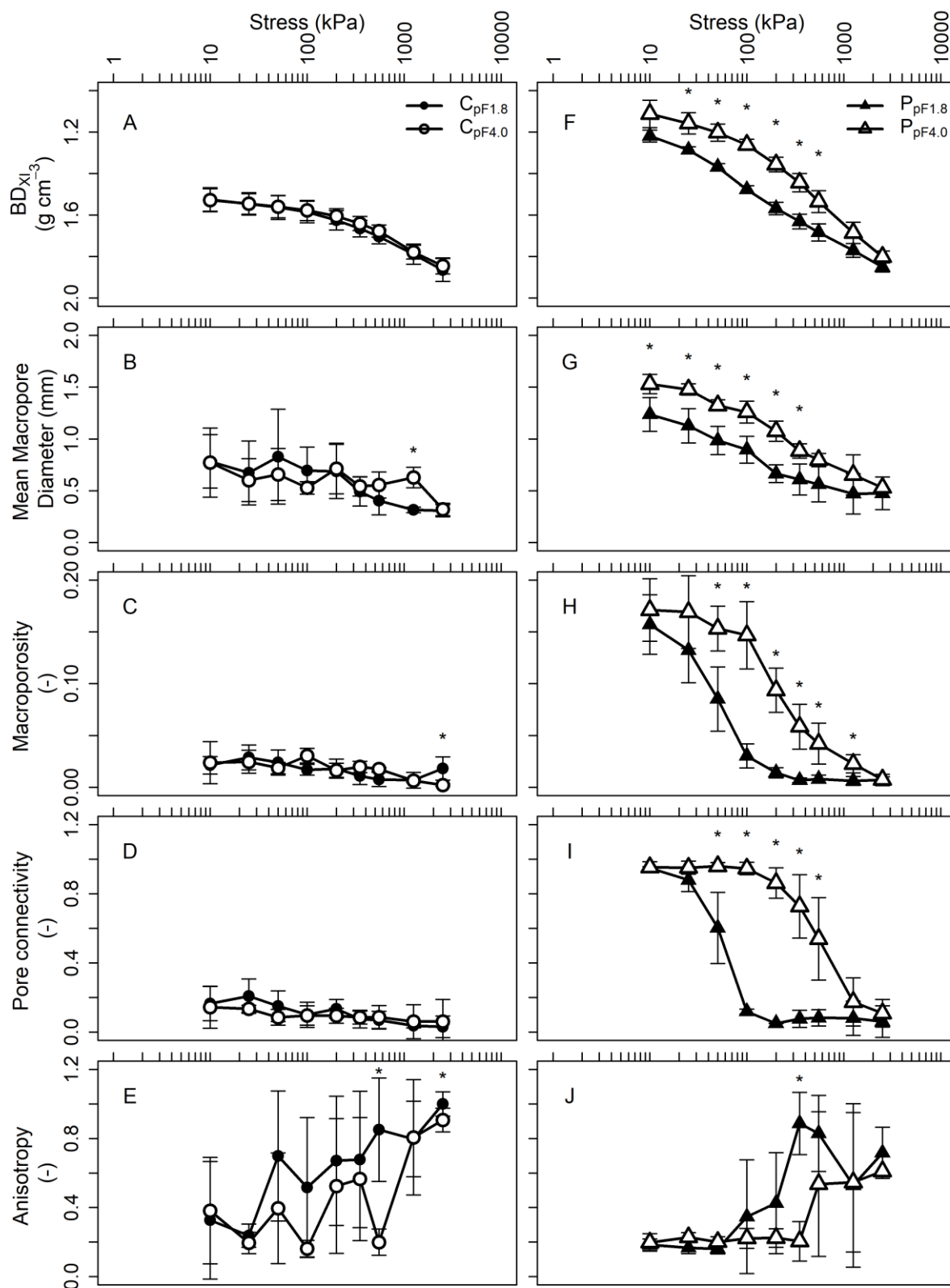
Figure 4.2-2: Dry bulk density (BD_{xi}), mean macropore diameter, macroporosity, pore connectivity and anisotropy from sequential load application (stress) for 'cultivator' (A-E) at -6 kPa ($C_{pF1.8}$) and -1000 kPa matric potential ($C_{pF4.0}$), and for 'plough' (F-J) at -6 kPa ($P_{pF1.8}$) and -1000 kPa matric potential ($P_{pF4.0}$). Error bars show the standard deviations, stars indicate a statistically significant difference ($p \leq 0.05$) between pF1.8 and pF4.0.

Table 4.2-2: Dry bulk density (BD$_{xi}$), aggregate density (AD) and AD/BD$_{xi}$-ratio from single load application, and BD$_{xi}$, mean pore diameter, macroporosity, pore connectivity, anisotropy and logarithmic precompression stress (log σ_P) from sequential load application for 'cultivator' at -6 kPa (C$_{pF1.8}$) and -1000 kPa matric potential (C$_{pF4.0}$). Statistically significant differences (p ≤ 0.05) between load applications are indicated by lower case letters.

Load application	Parameter	Treatment	Load step (kPa)								
			10	25	50	100	200	350	550	1250	2500
single	BD$_{xi}$ (g cm^{-3})	C$_{pF1.8}$	1.49 a	1.51 a	1.53 a	1.57 ab	1.64 bc	1.65 bc	1.70 cd	1.77 de	1.86 e
		C$_{pF4.0}$	1.38 a	1.47 ab	1.52 ab	1.56 ab	1.59 b	1.61 bc	1.72 bc	1.79 cd	1.84 d
	AD (g cm^{-3})	C$_{pF1.8}$	1.59 a	1.62 ab	1.62 ab	1.62 ab	1.60 a	1.63 ab	1.65 ab	1.74 bc	1.81 c
		C$_{pF4.0}$	1.70 a	1.71 a	1.71 a	1.69 a	1.68 a	1.70 a	1.72 ab	1.75 ab	1.82 b
	AD/BD$_{xi}$ (-)	C$_{pF1.8}$	1.07 a	1.07 a	1.06 abc	1.03 abcd	0.98 cd	0.98 bcd	0.97 d	0.99 bcd	0.97 d
		C$_{pF4.0}$	1.24 a	1.17 ab	1.12 abc	1.08 abc	1.06 bc	1.06 bc	1.06 bc	0.98 c	0.99 c
sequential	BD$_{xi}$ (g cm^{-3})	C$_{pF1.8}$	1.53 a	1.55 a	1.56 ab	1.59 ab	1.63 abc	1.67 bc	1.70 cd	1.79 de	1.86 e
		C$_{pF4.0}$	1.53 a	1.55 ab	1.56 ab	1.58 abc	1.61 abc	1.64 bc	1.68 c	1.78 d	1.85 d
	Mean macropore diameter (mm)	C$_{pF1.8}$	0.78 a	0.67 a	0.83 a	0.70 a	0.69 a	0.49 a	0.41 a	0.32 a	0.31 a
		C$_{pF4.0}$	0.77 a	0.60 a	0.66 a	0.53 a	0.71 a	0.54 a	0.56 a	0.63 a	0.32 a
	Macroporosity (-)	C$_{pF1.8}$	0.02 ab	0.03 a	0.02 ab	0.02 ab	0.02 ab	0.01 ab	0.01 ab	0.01 b	0.02 ab
		C$_{pF4.0}$	0.02 ab	0.02 ab	0.02 ab	0.03 a	0.02 ab	0.02 ab	0.02 ab	0.01 ab	0.00 b
	Poreconnectivity (-)	C$_{pF1.8}$	0.16 ab	0.21 a	0.15 ab	0.10 ab	0.13 ab	0.07 ab	0.07 ab	0.04 b	0.03 b
		C$_{pF4.0}$	0.14 a	0.13 a	0.08 a	0.10 a	0.09 a	0.08 a	0.09 a	0.06 a	0.06 a
	Anisotropy (-)	C$_{pF1.8}$	0.33 ab	0.24 a	0.70 ab	0.52 ab	0.67 ab	0.68 ab	0.85 ab	0.80 ab	1.00 b
		C$_{pF4.0}$	0.38 ab	0.20 a	0.40 ab	0.16 a	0.52 ab	0.57 ab	0.20 a	0.81 ab	0.91 b

The compression curves of the aggregates (Fig. 4.2-1B, Tab. 4.2-2) show a somewhat different behavior. There is no change in AD with increasing load until 350 to 550 kPa for both matric potentials. An additional difference compared to the BD_{xi} curves is that the initial densities are higher. At pF4.0 the AD is significantly higher for the load steps 10, 50 and 200 kPa than at pF1.8. This is indicated by the stars above the data points. Visually the curves differ clearly from each other with higher aggregate densities for pF4.0. They have a more or less parallel course until 350 kPa. Thereafter they converge with each further load increase. The mechanical precompression stress identified using the fitted stress - AD diagrams ($\sigma_{P\ AD}$) is the same for both matric potentials (log $\sigma_{P\ AD}$ = 2.95).

In the AD/BD_{xi} curves (Fig. 4.2-1C, Tab. 4.2-2) there are no significant differences between the two matric potentials with regard to the AD/BD_{xi} ratio, except at two loads. According to the classification of the AD/BD_{xi} ratios by Rücknagel et al. (2007) the soil structure in the cultivator treatment at pF1.8 changed from an initial blocky structure with semi-open to open positioning and subangular aggregates with semi-open positioning to a closed aggregate arrangement. At pF4.0 the soil structure developed from a blocky structure with open positioning and subangular aggregates with semi-open to open positioning to become a coherent mass with no visible aggregation.

Parameters obtained from computed tomography

The CT cross sections for 'cultivator' (Fig. 4.2-3A, B) show examples of the macropore structure (here pore sizes ≥ 60 µm) for the entire load range of 10-2500 kPa.

Due to the high initial dry bulk density both cultivator treatments have a compact structure with only a few isolated large biopores visible to begin with. For the same reason compression initially only leads to slight visible changes in the pore space. Still, the biopores are completely 'dissolved' at loads > 350 kPa for pF1.8. In contrast, at pF4.0 they remain pretty stable up to 550 kPa before their diameter is reduced markedly.

The course of the curves of the parameters mean macropore diameter (Fig. 4.2-2B), macroporosity (Fig. 4.2-2C) and pore connectivity (Fig. 4.2-2D) is almost identical for the two matric potentials (Tab. 4.2-2). Especially for the last two parameters the values were already quite low at the beginning of the load application. For this reason neither the matric potential nor the load application has a great effect on these parameters.

The ansiotropy starts with low values for both matric potentials (Fig. 4.2-2E, Tab. 4.2-2). At the end of the load application they have risen to almost 1. The curves show very high standard deviations and fluctuate very much. Hence, there are only occasional significant differences between the two matric potentials.
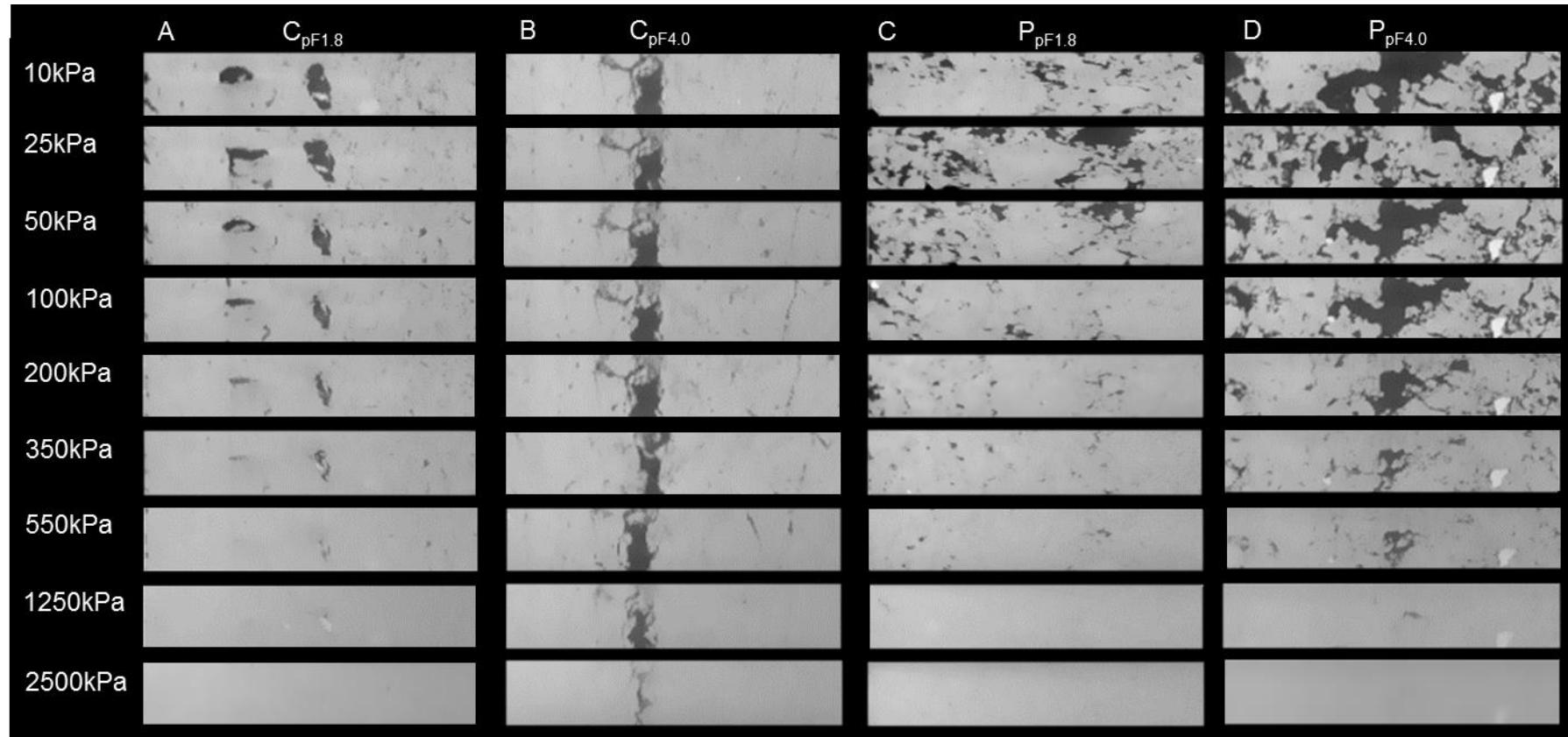
Figure 4.2-3: CT cross sectional images from sequential load application (10 to 2500 kPa) for 'cultivator' at -6 kPa ($C_{pF1.8}$) (A) and -1000 kPa matric potential ($C_{pF4.0}$) (B), and for 'plough' at -6 kPa ($P_{pF1.8}$) (C) and -1000 kPa matric potential ($P_{pF4.0}$) (D).

4.2.3. Comparsion of $P_{pF1.8}$ and $P_{pF4.0}$

Parameters obtained from compression tests

Here, too, the stress curves of both moisture regimes show a classic compaction behaviour. Again, the stress - BD_{xi} curves from the sequential load application (Fig. 4.2-2F) show a smoother course in comparison to the curves from the single load application (Fig. 4.2-1D) for the reason already given. Nevertheless, the curves of both stress - strain tests resemble each other. The stress - BD_{xi} curves at pF4.0 have significantly lower BD values at the middle load steps, particularly for the sequential load application. The mechanical precompression stress values identified using the stress - BD_{xi} diagrams display significantly lower mechanical precompression stress values at pF1.8 (log σ_P = 1.62) than at pF4.0 (log σ_P = 2.08).

In terms of aggregate compaction behaviour (Fig. 4.2-1E, Tab. 4.2-3) the results are similar at first to those obtained for the cultivator treatments. However, now AD does not change up to a load of just 100 kPa. Also, the initial ADs are slightly higher than in 'cultivator'. In the range of 10 to 550 kPa the pF4.0 samples have significantly higher AD values. The mechanical precompression stress identified using the fitted stress - AD diagrams are similar for both moisture regimes, and similar to those in the cultivator treatments.

As one can deduce from the above, the AD/BD_{xi} ratio also results in a significant difference between the two moisture regimes (Fig. 4.2-1F, Tab. 4.2-3). At the beginning of stress application, from 25 to 200 kPa, the pF4.0 data show significantly lower AD/BD_{xi} ratios. According to the classification of the AD/BD_{xi} ratios by Rücknagel et al. (2007) the soil structure for both matric potentials developed from a blocky structure with open positioning and subangular aggregates with semi-open to open positioning to a coherent mass with no visible aggregation.

Parameters obtained from computed tomography

The CT cross sections for the plough treatments (Fig. 4.2-3C, D) show several interaggregate pores before compaction. While at pF1.8 the pore space decreases steadily already at low load steps, large pores remain visible to higher load steps at pF4.0, similar to the cultivator treatments. Overall, the increasing stress application results in a steady homogenisation process of the soil structure at both matric potentials. This process starts with a reduction in macropore diameters and ends when individual aggregates are compressed into a coherent soil mass.

Table 4.2-3: Dry bulk density (BD$_{xi}$), aggregate density (AD) and AD/BD$_{xi}$-ratio from single load application, and BD$_{xi}$, mean pore diameter, macroporosity, pore connectivity, anisotropy and logarithmic precompression stress (log σ$_P$) from sequential load application for 'plough' at -6 kPa (P$_{pF1.8}$) and -1000 kPa matric potential (P$_{pF4.0}$). Statistically significant differences (p ≤ 0.05) between load applications are indicated by lower case letters.

Load application	Parameter	Treatment	Load step (kPa)								
			10	25	50	100	200	350	550	1250	2500
single	BD$_{xi}$ (g cm^{-3})	P$_{pF1.8}$	1.18 a	1.32 ab	1.41 bc	1.51 c	1.54 c	1.54 c	1.53 c	1.72 d	1.75 d
		P$_{pF4.0}$	1.21 a	1.22 a	1.26 a	1.36 ab	1.45 abc	1.58 bcd	1.68 cde	1.84 de	1.87 e
	AD (g cm^{-3})	P$_{pF1.8}$	1.53 ab	1.53 ab	1.54 ab	1.51 a	1.59 ab	1.60 ab	1.62 b	1.73 c	1.74 c
		P$_{pF4.0}$	1.66 a	1.67 ab	1.73 abc	1.69 ab	1.72 ab	1.71 ab	1.72 abc	1.77 bc	1.83 c
	AD/BD$_{xi}$	P$_{pF1.8}$	1.30 a	1.17 b	1.09 bc	1.00 c	1.04 c	1.05 c	1.05 bc	1.01 c	0.99 c
	(-)	P$_{pF4.0}$	1.40 a	1.38 a	1.38 a	1.25 ab	1.20 abc	1.09 bc	1.03 bc	0.97 c	0.98 c
sequential	BD$_{xi}$ (g cm^{-3})	P$_{pF1.8}$	1.22 a	1.29 b	1.37 c	1.48 d	1.57 e	1.63 ef	1.68 f	1.77 g	1.85 h
		P$_{pF4.0}$	1.11 a	1.16 ab	1.20 ab	1.26 bc	1.36 cd	1.44 de	1.53 e	1.69 f	1.80 f
	Mean macropore diamater (mm)	P$_{pF1.8}$	1.24 a	1.13 a	0.99 ab	0.90 abc	0.66 bcd	0.61 bcd	0.56 cd	0.47 d	0.48 d
		P$_{pF4.0}$	1.53 a	1.48 a	1.32 ab	1.26 ab	1.08 bc	0.89 cd	0.80 cd	0.65 d	0.53 d
	Macroporosity	P$_{pF1.8}$	0.16 a	0.13 a	0.09 b	0.03 c	0.01 c	0.01 c	0.01 c	0.01 c	0.01 c
	(-)	P$_{pF4.0}$	0.17 a	0.17 a	0.15 ab	0.15 ab	0.09 bc	0.06 cd	0.04 cd	0.02 d	0.01 d
	Poreconnectivity	P$_{pF1.8}$	0.95 a	0.88 a	0.60 b	0.12 c	0.05 c	0.08 c	0.08 c	0.08 c	0.06 c
	(-)	P$_{pF4.0}$	0.95 a	0.95 a	0.96 a	0.95 a	0.86 ab	0.73 ab	0.54 b	0.17 c	0.11 c
	Anisotropy	P$_{pF1.8}$	0.18 a	0.17 a	0.16 a	0.35 ab	0.43 ab	0.89 b	0.83 b	0.53 ab	0.72 ab
	(-)	P$_{pF4.0}$	0.20 a	0.23 a	0.20 a	0.22 a	0.22 a	0.20 a	0.54 a	0.55 a	0.61 a

The course of the mean macropore diameter curves of both moisture regimes (Fig. 4.2-2G) is very similar in shape to those of the BD_{xi} curves, but slightly more S-shaped.

The stress‑macroporosity (Fig. 4.2-2H) and the stress‑pore connectivity curves (Fig. 4.2-2I) are S-shaped, but the difference between the two moisture regimes is more pronounced (Tab. 4.2-3). For both parameters the initial values are the same for the two moisture regimes. As increasing stress is applied the values at pF1.8 decrease immediately. In contrast, the values at pF4.0 remain constant up to the 100 kPa load step and then decline. So, there are significant differences in the middle range of the stress-strain tests. At the end of the load application the two moisture regimes display the same final value for both parameters.

The anisotropy values (Fig. 4.2-2J, Tab. 4.2-3) for both moisture regimes remain constant at the beginning of the stress application, for pF1.8 up to the 50 kPa, and for pF4.0 up to the 350 kPa load step. Thereafter the values increase. The final values are lower than for 'cultivator'. There are no significant differences between the moisture regimes because the standard deviations are quite high.

4.2.4. Comparison of C and P

Parameters obtained from compression tests

Basically 'plough' has lower initial BD values compared to 'cultivator', regardless of the moisture regime (Fig. 4.2-1A, D, and Fig. 4.2-2A, F) so that the difference in the mechanical precompression stress is also much higher. However, the plough treatment has a significantly lower mechanical precompression stress compared to the cultivator treatment for both the pF1.8 and pF4.0 variant. The density of the aggregates at pF1.8 is lower for 'plough' than for 'cultivator', whereas at pF4.0 the densities are very similar (Fig. 4.2-1B, E).

Parameters obtained from computed tomography

As mentioned earlier, the visible soil structures clearly differ between 'cultivator' and 'plough' (Fig. 4.2-3). At the beginning of stress application both cultivator treatments have a more compact structure with only isolated large biopores. In the plough treatments more pores are visible before compaction. At pF1.8 the pore space decreases more quickly with increasing load steps than at pF4.0. This holds for 'cultivator' and 'plough'.

'Plough' shows a smoother course of the mean macropore diameter curves (Fig. 4.2-2G) compared to 'cultivator' (Fig. 4.2-2B) and has higher initial and final values for both matric potentials. Compared to 'cultivator' there is a distinct difference between the moisture regimes in that 'plough' at pF4.0 has lower values over most of the load step range. For the

parameters macroporosity (Fig. 4.2-2C, H) and pore connectivity (Fig. 4.2-2D, I) this fact is even more obvious.

Uniaxial vertical compression preferentially removes horizontally oriented pores. Hence, there is a shift towards higher anisotropy in both tillage treatments at both matric potentials as the load increases, but the variability among replications is high (Fig. 4.2-2E, J).

4.2.5. Comparison of BD_{xi} obtained from compression tests with parameters obtained from computed tomography

The BD-values from the compression tests were correlated with the parameters obtained from computed tomography (Fig. 4.2-4). In general, increasing dry bulk density leads to decreasing mean macropore diameters, macroporosity and connectivity, while anisotropy increases. In the cultivator treatment the increase in BD_{xi} mainly entails a reduction in mesoporosity, because macroporosity was already low (< 0.05) before compression. In the plough treatment macroporosity was initially higher. An increase in BD_{xi} therefore leads to a macroporosity reduction.

The correlations between BD_{xi} and the CT parameters for 'cultivator' are very similar with respect to the soil matric potential (Fig. 4.2-4A, B, C), except for anisotropy (Fig. 4.2-4D) where for a given BD_{xi} the value is higher for pF1.8.

For 'plough' the correlations between BD_{xi} and mean macropore diameter and macroporosity, respectively, also do not differ with respect to soil matric potential, but they cover a larger range than for 'cultivator'. For pore connectivity the values for both matric potentials agree at the beginning and the end of the BD_{xi} range, but differ at a given BD_{xi} in the intermediate range: They are lower at pF1.8 than at pF4.0. In the case of anisotropy (Fig. 4.2-4H) the values for both matric potentials fall on the same line for $BD_{xi} < 1.5$ g cm^{-3}. At higher BD values there are no data for pF4.0. Hence no statements can be made.

If one superimposes the data for 'cultivator' and 'plough' (Fig. 4.2-5) one can note that all points, irrespective of tillage treatment or matric potential, fall on the same curve for mean macropore diameter and macroporosity. This is partially true for pore connectivity, too, were the 'cultivator' and the 'plough' data for pF1.8 follow the same relationship, while the data for 'plough' at pF4.0 take a different course at midrange BD_{xi}-values. For anisotropy the data seem to diverge for 'cultivator' at BD > 1.5 g cm^{-3} with higher values for pF1.8 than for pF4.0.
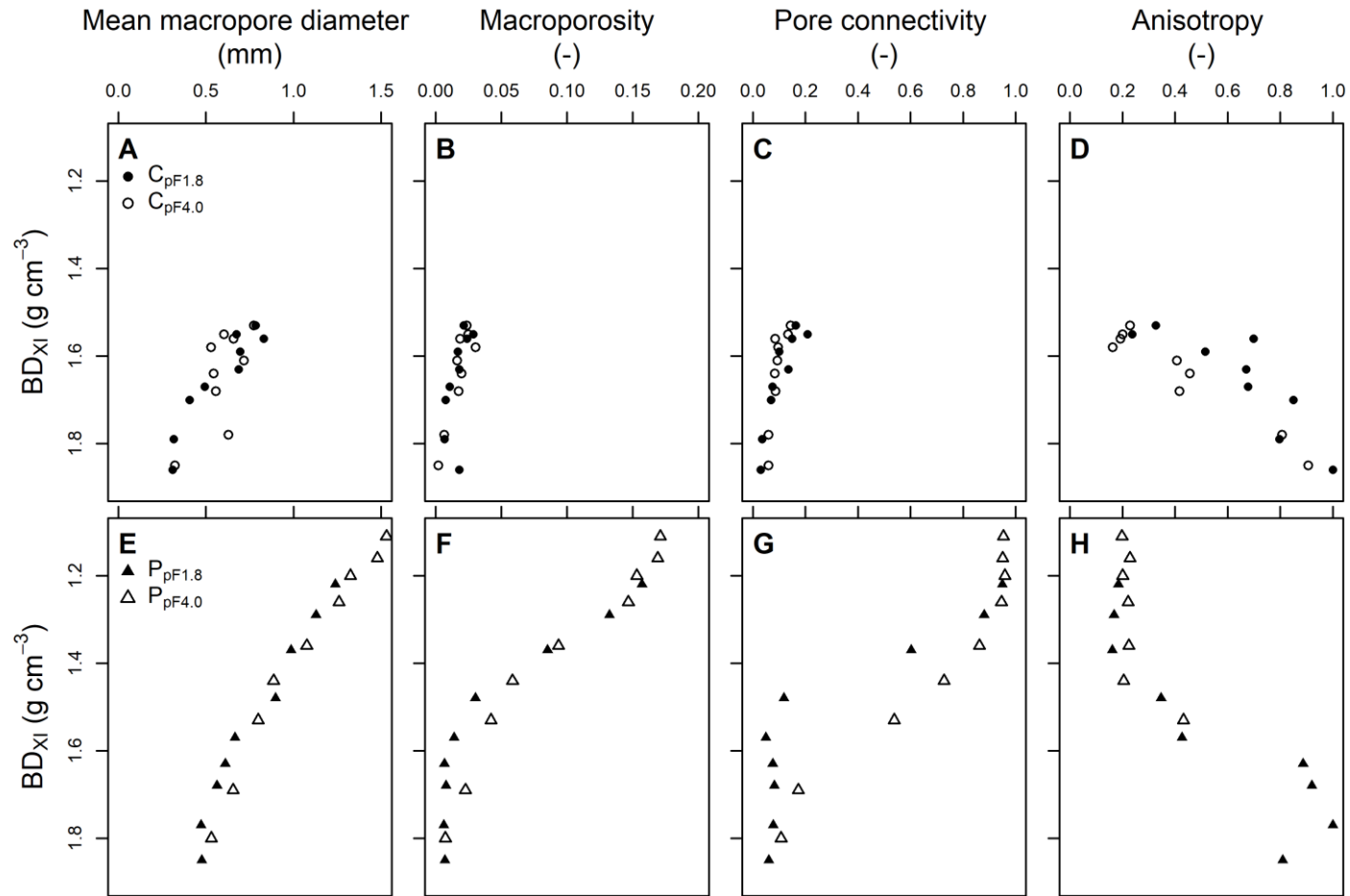
Figure 4.2-4: Correlation between dry bulk density (BD_{xi}) and mean macropore diameter, macroporosity, pore connectivity and anisotropy from sequential load application for 'cultivator' (A-D) at -6 kPa ($C_{pF1.8}$), and for -1000 kPa matric potential ($C_{pF4.0}$) and 'plough' (E-H) at -6 kPa ($P_{pF1.8}$) and -1000 kPa matric potential ($P_{pF4.0}$).
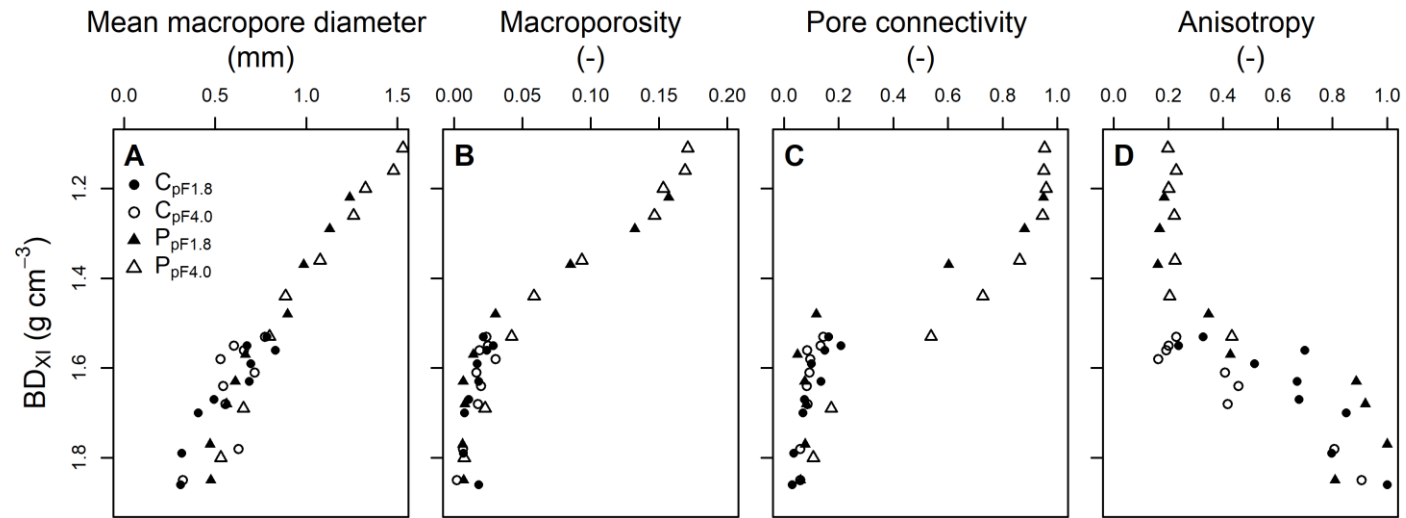
Figure 4.2-5: Superposition of the data from Figure 4.2-4.

This entails that a given BD_{xi} corresponds to just one value of mean macropore diameter and macroporosity and vice versa. However, there can be two different values of pore connectivity and anisotropy, or expressed the other way around, there can be two BD_{xi} for a given pore connectivity or anisotropy. Hence, BD alone is not a sufficient to describe soil compaction in full.

4.2.6. Comparison of parameters obtained from computed tomography with each other

Three of the four relationships are independent of matric potential and tillage treatment, .e. all data points in a given correlation follow the same course (Fig. 4.2-6). In the correlation between macroporosity and pore connenctivity the data for the two matric potentials deviate somewhat from each other, but only in the middle of the range. The cultivator data cover a narrower range than the plough data in all four diagrams.
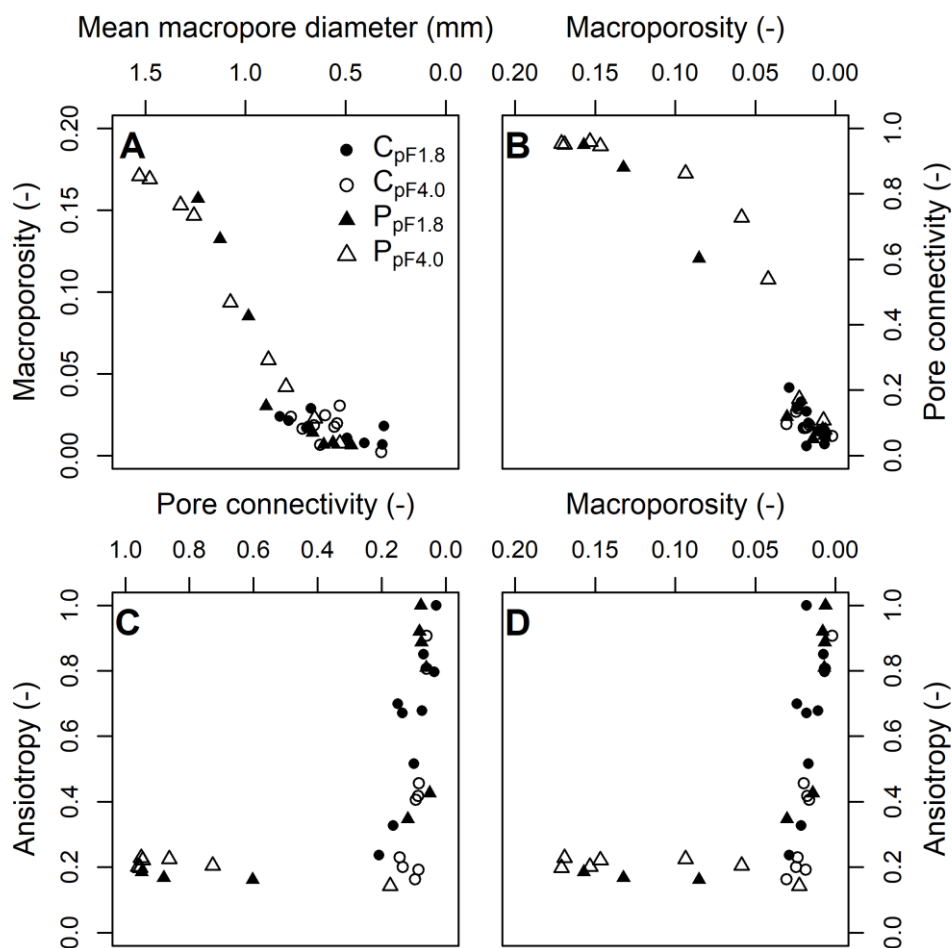
Figure 4.2-6: Cross-correlations between mean macropore diameter, macroporosity, pore connectivity and anisotropy from sequential load application for 'cultivator' at -6 kPa ($C_{pF1.8}$) and -1000 kPa matric potential ($C_{pF4.0}$), and for 'plough' at -6 kPa ($P_{pF1.8}$) and -1000 kPa matric potential ($P_{pF4.0}$). The legend is given in graph A.

Figure 4.2-5A depicts that macroporosity decreases with decreasing mean macropore diameter in a unique correlation. Since this correlation is very close, no further correlations with the mean macropore diameter are shown, macroporosity is used instead. As macroporosity decreases, so does pore connectivity (Fig. 4.2-5B). Pore connectivity (Fig. 4.2-5C) and macroporosity (Fig. 4.2-5D) have to decrease to some point with increasing stress before anisotropy increases. In the investigated soil this point is reached at a pore connectivity of 0.1 and at a macroporosity of 0.025.

4.3. Estimation of critical stress ranges to preserve soil functions at differently textured sites

4.3.1. Soil mechanical parameters and accompanying critical stress values

The stress - BD_{xi} diagrams (Fig. 4.3-1) show classic compaction curves for each of the four sites. For the 5-100 kPa load steps the Quellendorf site (Fig. 4.3-1A) had the significantly highest and the Kranichborn (Fig. 4.3-1D) site the significantly lowest BD_{xi}, while the Buttelstedt (Fig. 4.3-1B) and Rothenberga (Fig. 4.3-1C) sites did not differ significantly in their BD_{xi} (Tab. 4.3-1). At the 200-550 kPa load steps the Kranichborn site differed significantly from the other sites, which did not differ significantly from each other. The BD_{xi} curves for the four sites run more or less parallel, but are shifted up or down with respect to their initial densities. At the beginning of the load application there was a maximum difference in BD_{xi} of 0.61 g cm^{-3} between the sites which did not change until the end of the load application. The values of the mechanical precompression stress ($\sigma_{P\ BDxi}$) determined from the stress - BD_{xi} diagrams do therefore not differ significantly between the sites. They are in the range of log σ_P = 1.65 to 1.85 (45 to 71 kPa).
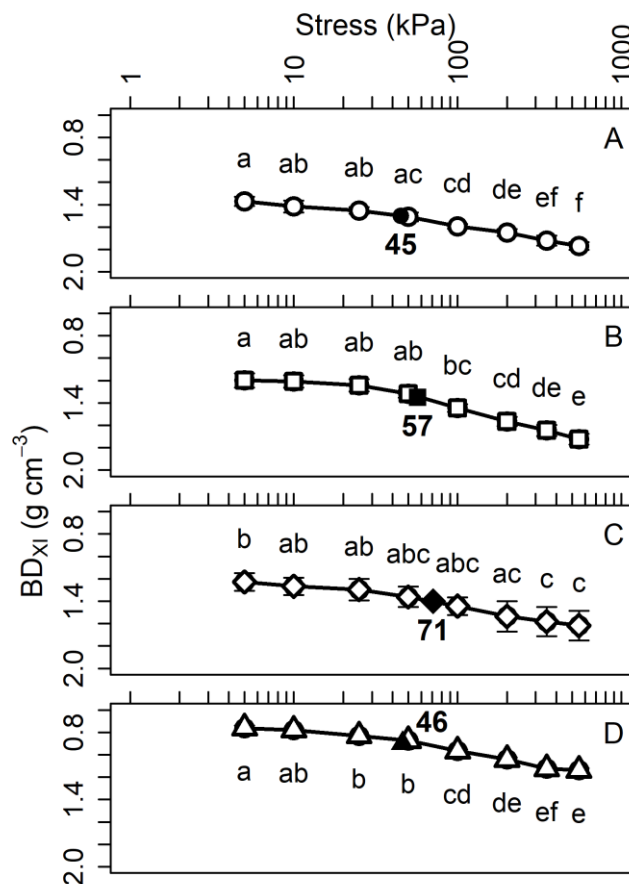
Figure 4.3-1: Dry bulk density (BD_{xi}) from sequential load application (stress) to soil cores from (A) Quellendorf, (B) Buttelstedt, (C) Rothenberga and (D) Kranichborn. Error bars show the standard deviations. Statistically significant differences (p ≤ 0.05) are indicated by lower case letters. Black symbols and numbers indicate the values (kPa) of the mechanical precompression stress.

Table 4.3-1: Dry bulk density (BD_{xi}), macroporosity, pore connectivity, and logarithmic precompression stress (log σ_P) for Quellendorf (QD), Buttelstedt (BS), Rothenberga (RB) and Kranichborn (KB). Statistically significant differences (p ≤ 0.05) are indicated by lower case (load step within each site), and upper case letters (sites within each load step).

Parameter	Texture	Load step (kPa)								log σ_P
		5	10	25	50	100	200	350	550	
BD_{xi}	QD	1.37 aC	1.42 abC	1.45 abC	1.51 acC	1.59 cdC	1.65 deB	1.72 efB	1.77 fB	1.65 a
(g cm^{-3})	BS	1.20 aB	1.21 abB	1.24 abB	1.32 abB	1.45 bcB	1.56 cdB	1.65 deB	1.72 eB	1.76 a
	RB	1.23 bB	1.27 abB	1.30 abB	1.36 abcB	1.44 abcB	1.53 acB	1.58 cB	1.62 cB	1.85 a
	KB	0.76 aA	0.78 abA	0.83 bA	0.87 bA	0.97 cdA	1.04 deA	1.12 efA	1.14 eA	1.66 a
Macroporosity	QD	0.09 aA	0.08 aAB	0.07 aA	0.05 aA	0.01 bA	0.00 bA	0.01 bB	0.01 bA	
(-)	BS	0.23 aB	0.22 abCB	0.21 abC	0.18 aB	0.12 cB	0.06 dB	0.02 dAB	0.02 dA	
	RB	0.12 aA	0.12 aAB	0.10 abAB	0.08 abcA	0.06 abcAB	0.03 bcAB	0.01 cAB	0.00 cA	
	KB	0.23 aB	0.23 aC	0.18 aBC	0.12 abAB	0.05 bcA	0.04 bcAB	0.03 bcAB	0.01 cA	
Pore	QD	0.76 aA	0.81 aA	0.74 aC	0.61 aA	0.34 bA	0.17 bA	0.15 bA	0.13 bA	
Connectivity	BS	0.96 aB	0.96 aB	0.96 aB	0.92 abB	0.82 bA	0.50 cB	0.14 dA	0.10 dA	
(-)	RB	0.81 aAB	0.81 aA	0.75 aAC	0.66 aA	0.51 abA	0.25 bcAB	0.12 cA	0.15 cA	
	KB	0.94 aB	0.95 aAB	0.92 abAB	0.85 abAB	0.48 bcA	0.25 cAB	0.20 cA	0.14 cA	

4.3.2. Morphometric parameters and accompanying critical stress values

The CT images in Figure 4.3-2 show the structural features in samples from the four sites at all eight load steps. At the Quellendorf site (Fig. 4.3-2A) the increased load application leads to only slight visible changes in the pore space. There were few macropores to begin with, due to the high initial BD. At the other sites, in addition to many pores, aggregates can also be seen at the beginning of the load application, especially at the Buttelstedt (Fig. 4.3-2B) and Kranichborn (Fig. 4.3-2D) sites. Overall, the increasing load application leads to a progressive homogenization process of the soil structure at all sites. At Buttelstedt, Rothenberga (Fig. 4.3-2C) and Kranichborn this process begins in the 50-100 kPa range with the compression of the macropores, i.e. a reduction in their diameter. Furthermore, the soil aggregates are pressed together and their structures become disintegrated. The stress range just mentionded covers the values of the mechanical precompression stress for the four soils.

The increase in load results in significant decreases in macroporosity (Fig. 4.3-3) and pore connectivity (Fig. 4.3-4), regardless of the site. Only at the lowest load steps did the sites Quellendorf and Rothenberga on the one hand, and Buttelstedt and Kranichborn on the other differ significantly from each other in terms of macroporosity and pore connectivity (Tab. 4.3-1). The former two mostly have significantly lower macroporosity and pore connectivity values than the latter two.

The stress - macroporosity curves of the four sites (Fig. 4.3-3) show a significant change in their course in the load range of 25-200 kPa. There is a significant decrease in macroporosity at all sites with macropores no longer present at the highest load steps. The macroporosity at Quellendorf can already be regarded as critical at a load of 12 kPa (Fig. 4.3-3A), because at this load the macroporosity is just 8% (see section 3.6.). At Buttelstedt (Fig. 4.3-3B) this macroporosity is reached at much higher load (critical stress value) of 155 kPa. Rothenberga (Fig. 4.3-3C) and Kranichborn (Fig. 4.3-3D) have a critical stress value for macroporosity of 52 and 72 kPa, respectively, which is near the value for the mechanical precompression stress for these two sites.
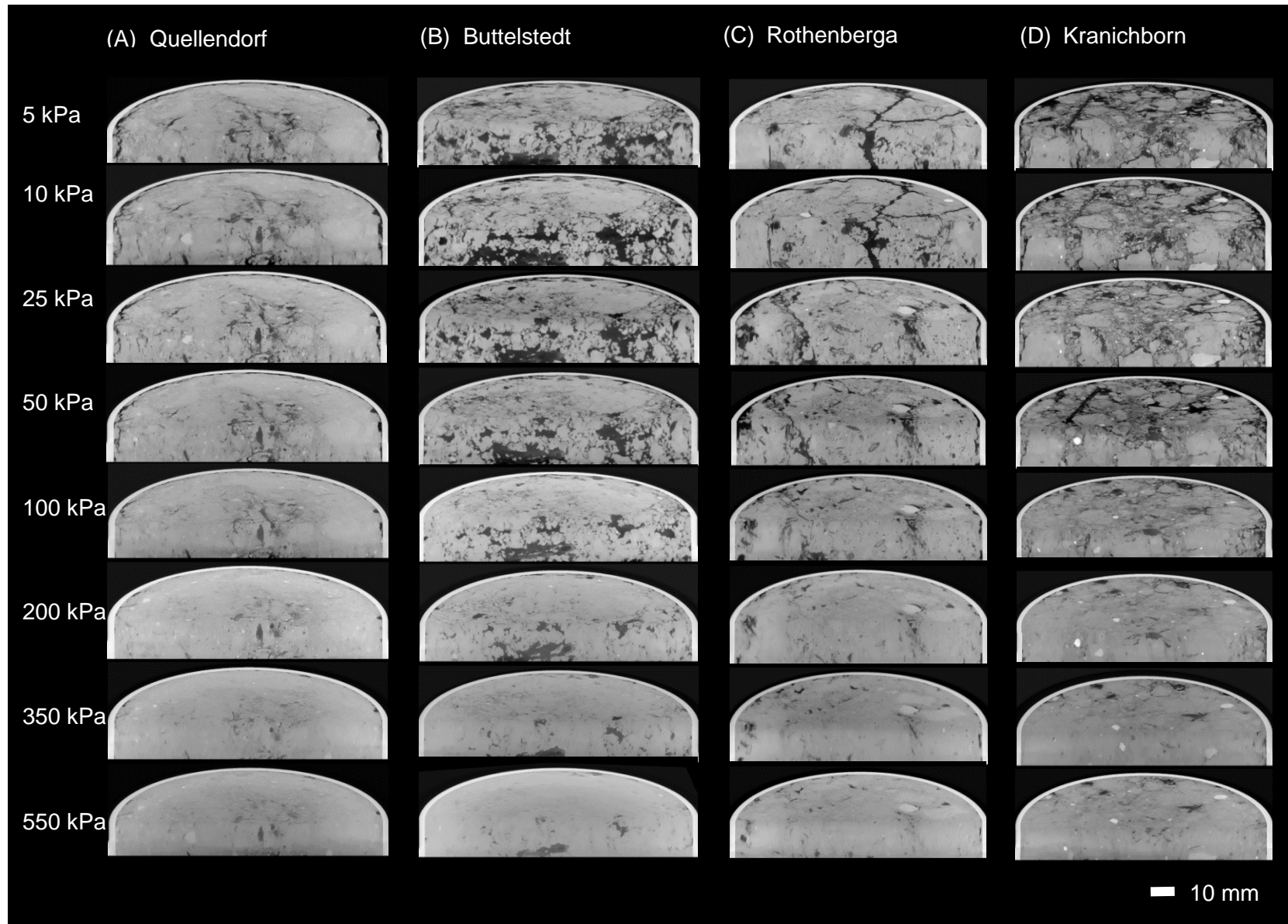
Figure 4.3-2: CT cross section images from sequential load application (5 to 550 kPa) for the sites (A) Quellendorf, (B) Buttelstedt, (C) Rothenberga and (D) Kranichborn. The images show half a core viewed from the top at an angle of 45°.
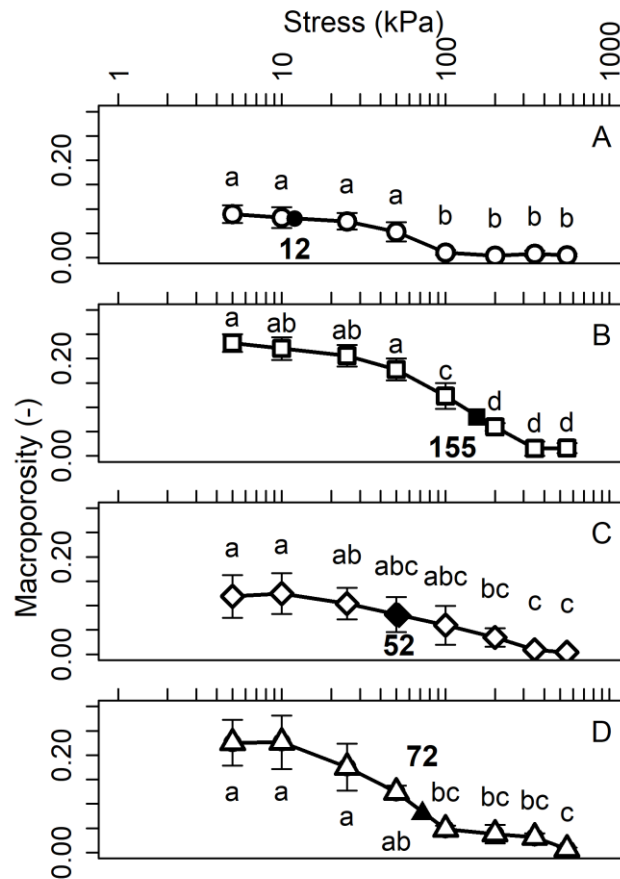
Figure 4.3-3: Macroporosity from sequential load application to soil cores for (A) Quellendorf, (B) Buttelstedt, (C) Rothenberga and (D) Kranichborn. Error bars show the standard deviations. Statistically significant differences (p ≤ 0.05) are indicated by lower case letters. Black symbols and numbers indicate the critical stress values (kPa) which correspond to a macroporosity of 8%.

The course of the stress - pore connectivity curves (Fig. 4.3-4) for all sites is similar to that of the stress - macroporosity curves, with the difference that the pore connectivity remains more constant with increasing load for a longer time before decreasing steeply in the load range of 50-200 kPa. Except for the Rothenberga site (Fig. 4.3-4C) where the critical stress value is 200 kPa, the critical stress value at which pore connectivity collapsed is at the 100 kPa load step for the remaining sites.
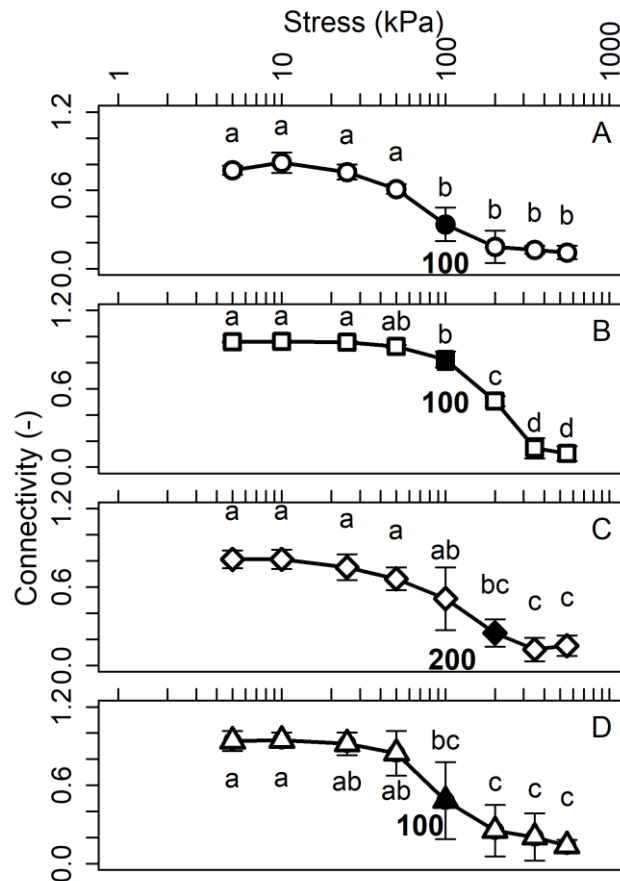
Figure 4.3-4: Pore connectivity from sequential load application to soil cores for (A) Quellendorf, (B) Buttelstedt, (C) Rothenberga and (D) Kranichborn. Error bars show the standard deviations. Statistically significant differences (p ≤ 0.05) are indicated by lower case letters. Black symbols and numbers indicate the critical stress values (kPa) which correspond to the first significant change in pore connectivity.

4.3.3. Soil biological parameters and accompanying critical stress values

L. terrestris dug successfully into the soil in all columns, even at the highest bulk densities, and disappeared from the soil surface. Mortality was too low to mention and did not show a connection to BD. *L. terrestris* formed permanent uninterrupted burrows which showed little branching. Several individuals of *L. terrestris* in a column sometimes used the same burrow system. This means not every earthworm dug a biopore. Since due to the compaction procedure the upper part of a layer was slightly denser than the soil below, *L. terrestris* tended to follow the thin crack between two successive layers so that the burrows in those areas were horizontal. This was especially observed at the maximum burrowing depths of the respective soil texture and density.

At Buttelstedt, Rothenberga and Kranichborn the number of biopores increases with increasing density up to an optimal density value (Fig. 4.3-5B-D). As the density increases further, the number of biopores declines. At the Quellendorf site there are no significant

differences in the number of biopores between the BD stages (Fig. 4.3-5A, Tab. 4.3-2) so that there was no convex curve. For this reason the critical stress value of 170 kPa was set at BD_{xi} = 1.63 g cm^{-3} where the highest number of biopores was determined.
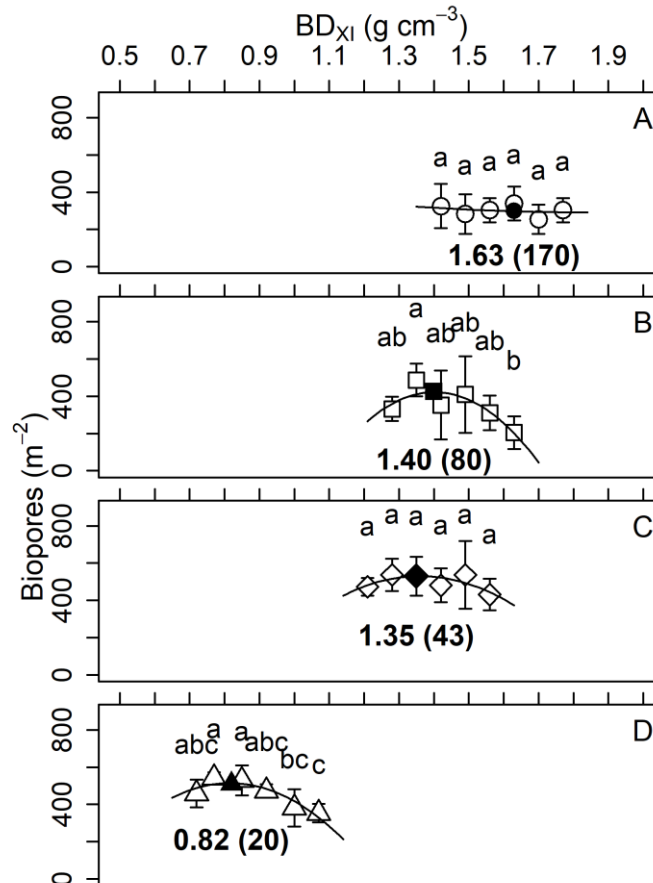
Figure 4.3-5: Number of biopores from *Lumbricus terrestris* as a function of dry bulk density (BD_{xi}) for (A) Quellendorf (1.42-1.77 g cm^{-3}), (B) Buttelstedt (1.28-1.63 g cm^{-3}), (C) Rothenberga (1.21-1.56 g cm^{-3}) and (D) Kranichborn (0.72-1.07 g cm^{-3}). Error bars show the standard deviations. Statistically significant differences ($p \leq 0.05$) are indicated by lower case letters. Black symbols and numbers indicate the maximum number of biopores (in brackets) and the corresponding optimum BD (g cm^{-3}) derived from fitted second order polynomial functions.

Significant differences in the number of biopores occur at the Buttelstedt site (Fig. 4.3-5B). The BD stage 1.35 g cm^{-3} has the significantly highest, and the BD stage 1.63 g cm^{-3} the significantly lowest number of biopores, while the remaining BD stages do not differ significantly from them and from each other. Based on the fitted polynomial an optimum appears at BD_{xi} = 1.40 g cm^{-3}, corresponding to a critical stress value of 80 kPa.

The amplitude of the fitted polynomials, and thus the compression, is lowest at the Quellendorf site where the graph is very flat, whereas the Buttelstedt site has the largest amplitude in the number of biopores and consequently a greater steepness of the polynomial

function, i.e. here the influence of soil compaction on biological activity is clearly noticeable. The sites Rothenberga and Kranichborn fall between these two.

Table 4.3-2: Number of biopores from *Lumbricus terrestris*, grain yield, straw yield, and above ground biomass of *Hordeum vulgare* for different bulk densities (BD) for Quellendorf (QD), Buttelstedt (BS), Rothenberga (RB) and Kranichborn (KB). Statistically significant differences ($p \leq 0.05$) are indicated by lower case letters.

Site	BD ($g\ cm^{-3}$)	Biopores (n)	Grain yield ($g\ m^2$)	Straw yield ($g\ m^2$)	Above ground biomass ($g\ m^2$)
QD	1.42	9.2 a	630 a	927 a	1557 a
QD	1.49	8.0 a	525 ab	949 a	1473 a
QD	1.56	8.6 a	466 abc	944 a	1410 a
QD	1.63	9.6 a	544 abc	792 abc	1337 a
QD	1.70	7.2 a	239 bc	552 bc	792 b
QD	1.77	8.6 a	166 c	430 c	595 b
BS	1.28	9.4 ab	308 a	507 a	815 a
BS	1.35	13.8 a	277 a	478 a	756 a
BS	1.42	10.0 ab	256 a	433 a	688 a
BS	1.49	11.6 ab	72 b	279 b	351 b
BS	1.56	8.8 ab	31 b	261 b	292 b
BS	1.63	5.8 b	13 b	157 b	170 b
RB	1.21	13.4 a	301 a	660 a	961 ab
RB	1.28	15.2 a	333 a	674 a	1006 ab
RB	1.35	15.0 a	288 a	676 a	964 ab
RB	1.42	13.6 a	333 a	682 a	1016 a
RB	1.49	15.2 a	397 a	745 a	1142 a
RB	1.56	12.2 a	182 a	453 b	634 b
KB	0.72	13.0 abc	416 a	653 ab	1069 ab
KB	0.78	15.4 a	520 a	655 ab	1175 ab
KB	0.85	15.0 a	526 a	673 a	1199 ab
KB	0.92	13.4 abc	593 a	699 a	1292 a
KB	1.00	10.8 bc	570 a	708 a	1278 ab
KB	1.07	10.0 c	357 a	508 b	865 b

At Rothenberga (Fig. 4.3-5C) no significant differences in the number of biopores with increasing density can be found, but according to the polynomial regression equation the density value with the maximum number of biopores is 1.35 g cm^{-3}, corresponding to a critical stress value of 43 kPa.

The Kranichborn site (Fig. 4.3-5D) shows only significant differences between the BD stages 0.77 and 0.85 g cm^{-3} on the one hand, and the BD stages 1.00 and 1.07 g cm^{-3} on the

other. At BD_{xi} = 0.82 g cm^{-3} there is a maximum in the biopore number. This BD corresponds to a critical stress value of only 20 kPa.

4.3.4. Agronomic parameters and accompanying critical stress values

Up to a certain density grain yields at Rothenberga and Kranichborn increase (Fig. 4.3-6, Tab. 4.3-2) and then sink again. At Quellendorf and Buttelstedt there are no data points on the left side of the polynomial. The sites Quellendorf (Fig. 4.3-6A) and Buttelstedt (Fig. 4.3-6B) have the largest amplitudes in grain yields. Correspondingly, the graphs of the polynomial functions are steeper than those for Rothenberga (Fig. 4.3-6C) and Kranichborn (Fig. 4.3-6D). At the latter two sites no significant differences in grain yield with increasing density are found.
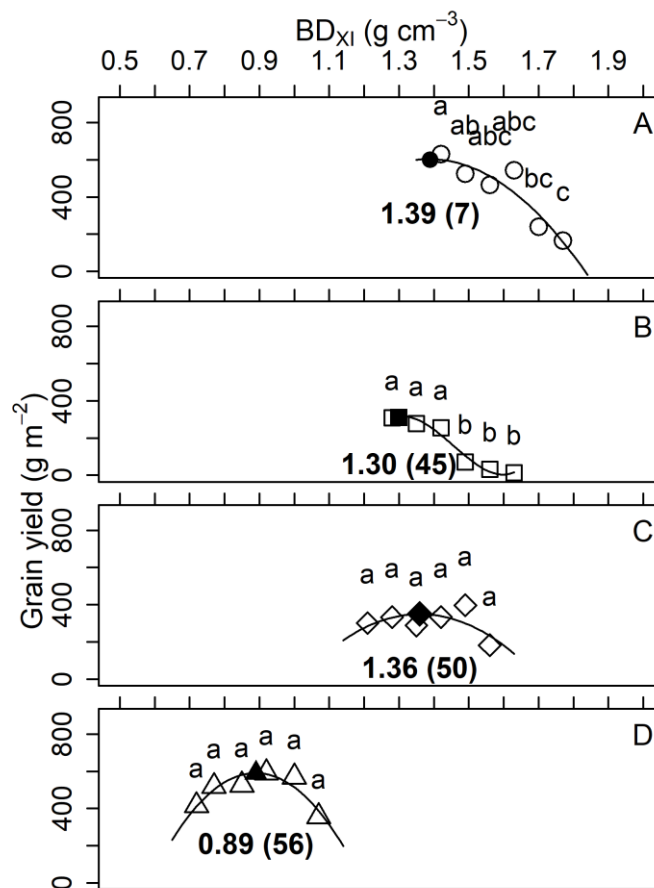
Figure 4.3-6: Grain yield of *Hordeum vulgare* as a function of dry bulk density (BD_{xi}) for (A) Quellendorf (1.42-1.77 g cm^{-3}), (B) Buttelstedt (1.28-1.63 g cm^{-3}), (C) Rothenberga (1.21-1.56 g cm^{-3}) and (D) Kranichborn (0.72-1.07 g cm^{-3}). Statistically significant differences (p ≤ 0.05) are indicated by lower case letters. Black symbols and numbers indicate the maximum yield (g m^{-2}, in brackets) and the corresponding optimum BD (g cm^{-3}) derived from fitted second or third order polynomial functions.

At the Quellendorf site the BD stages 1.42 and 1.49 g cm^{-3} differ significantly from the BD stage 1.77 g cm^{-3}, and the BD stage 1.42 g cm^{-3} from the BD stage 1.70 g cm^{-3}, all other BD stages do not differ significantly in grain yield. At Buttelstedt the first three BD stages have significantly higher grain yields than the last three. The maximum grain yields are achieved at 'optimal' densities of 1.39 g cm^{-3} at Quellendorf, 1.30 g cm^{-3} at Buttelstedt, 1.36 g cm^{-3} at Rothenberga, and 0.89 g cm^{-3} at Kranichborn. The critical stress values derived from these density values are lowest (7 kPa) at the Quellendorf site, highest (56 kPa) at Kranichborn, and in between for Buttelstedt (45 kPa) and Rothenberga (50 kPa). For the last three sites the derived critical stress values for grain yield are in the range of the mechanical precompression stresses (see chapter 4.3.1.).

In principle the results for grain yield are reflected in the results for straw yield, with the difference that more straw was formed than grain, which led to shifts in the optimum density values (Fig. 4.3-7).
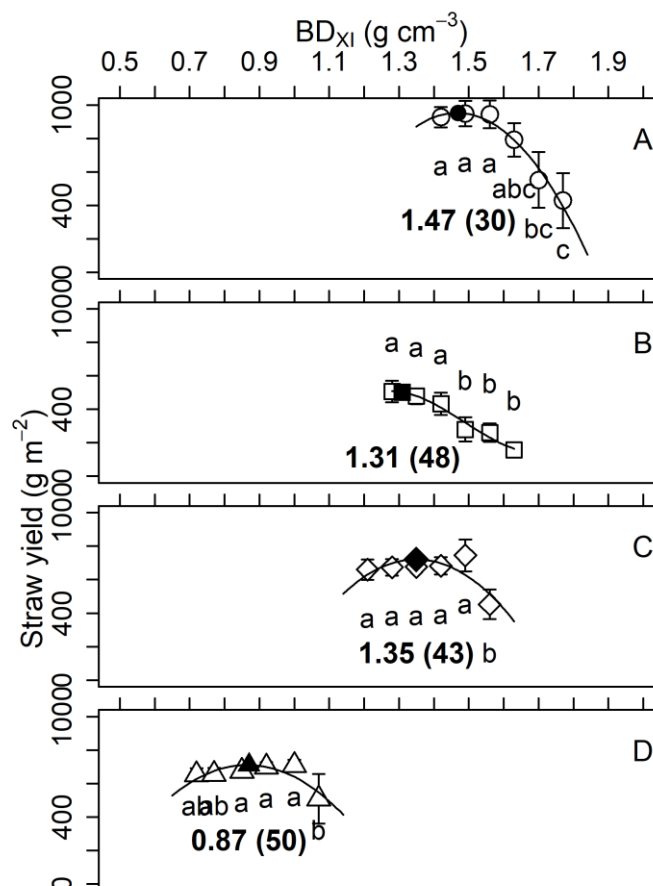
Figure 4.3-7: Straw yield of *Hordeum vulgare* as a function of dry bulk density (BD$_{xi}$) for (A) Quellendorf (1.42-1.77 g cm^{-3}), (B) Buttelstedt (1.28-1.63 g cm^{-3}), (C) Rothenberga (1.21-1.56 g cm^{-3}) and (D) Kranichborn (0.72-1.07 g cm^{-3}). Error bars show the standard deviations. Statistically significant differences (p ≤ 0.05) are indicated by lower case letters. Black symbols and numbers indicate the maximum yield (g m^{-2}, in brackets) and the corresponding optimum BD (g cm^{-3}) derived from fitted second or third order polynomial functions.

The maximum straw yield occurs at a density of 1.47 g cm^{-3} at Quellendorf (Fig. 4.3-7A), 1.31 g cm^{-3} at Buttelstedt (Fig. 4.3-7B), 1.35 g cm^{-3} at Rothenberga (Fig. 4.3-7C), and 0.87 g cm^{-3} at Kranichborn (Fig. 4.3-7D). This corresponds to critical stress values of 30 kPa for Quellendorf, 48 kPa for Buttelstedt, 43 kPa for Rothenberga, and 50 kPa for Kranichborn. Again, for the last three sites the derived critical stress values for straw yield are in the range of the mechanical precompression stresses (see chapter 4.3.1.).

4.3.5. Stress ranges

The critical stress values just given in chapters 4.3.1 to 4.3.4. are summarized in Figure 4.3-8. The minimum and maximum stress values for each site determine the critical stress range, indicated by dotted vertical lines. In the following the middle of the critical stress ranges is called "median".

The ranges the stress values vary across for the six parameters differ between the sites. While the stress range is rather large at the Quellendorf site (7-170 kPa, Fig. 4.3-8A), it is similar and much smaller at Buttelstedt, Rothenberga and Kranichborn. The Buttelstedt site (Fig. 4.3-8B) has the highest median critical stress (101 kPa). The sites Rothenberga (Fig. 4.3-8C) and Kranichborn (Fig. 4.3-8D) have similar medians with 51 and 53 kPa, respectively, the value for Quellendorf is 82 kPa.

At Quellendorf and Kranichborn the critical stress value for macroporosity is below the precompression stress, at Buttelstedt and Rothenberga the reverse is true.

At the Quellendorf and Kranichborn sites which are both sandy textured the mechanical precompression stress sits virtually in the middle of the critical stress range and therefore represents it well. For the Buttelstedt and Rothenberga sites the mechanical precompression stresses are in the lower third of the critical stress range. This is still an acceptable representation of the stress range. The variation bars of the mechanical precompression stress are very small at all four sites.

At the Quellendorf and Rothenberga sites the critical stress value for macroporosity is smaller than the one for pore connectivity. This can also be seen at Kranichborn, but the difference is less. At the Buttelstedt site the situation is reversed. However, since the variation bars overlap, it is possible that here, too, the critical stress value for macroporosity is smaller than the one for pore connectivity.

The critical stress value of the earthworm activity defines the upper limit of the critical stress range at the Quellendorf site, and the lower limit at the Rothenberga and Kranichborn sites. At Buttelstedt it lies in the middle of the critical stress range.
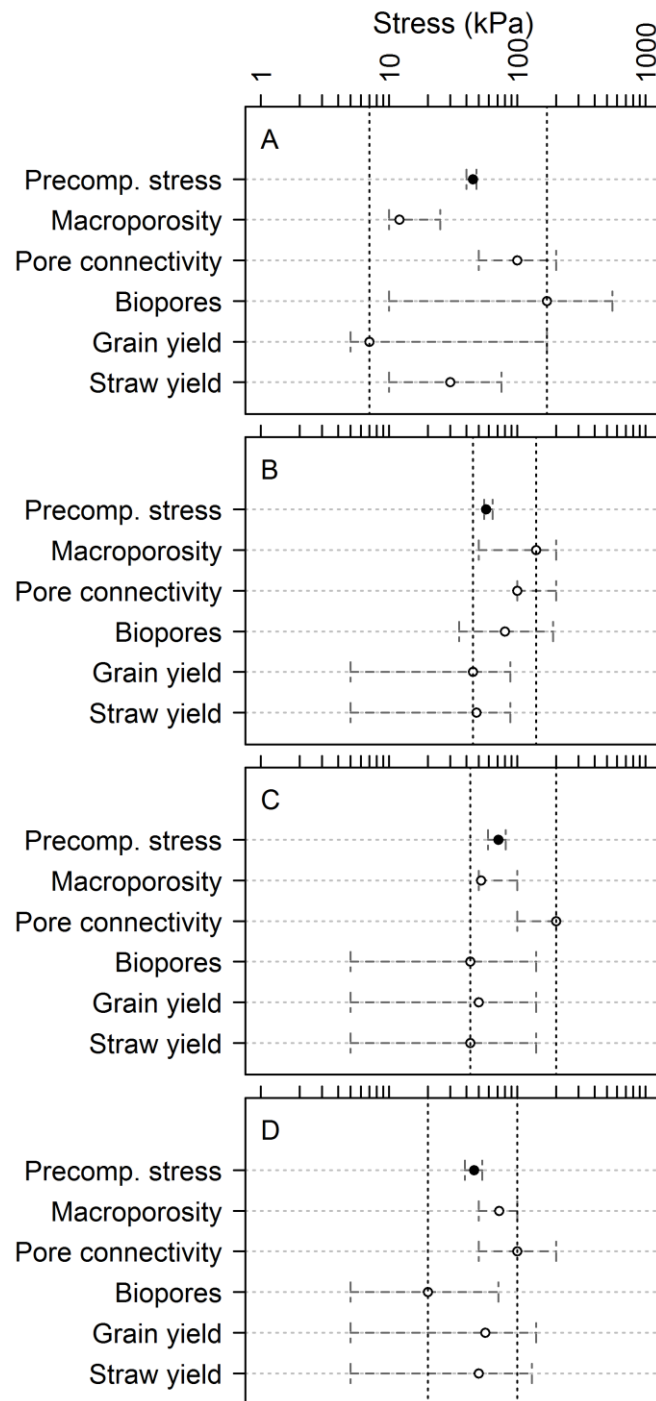
Figure 4.3-8: Critical stress ranges for (A) Quellendorf, (B) Buttelstedt, (C) Rothenberga and (D) Kranichborn based on precompression stress (black circle), critical stress values of macroporosity and pore connectivity, and optimum values for the number of biopores, grain yield and straw yield (empty circles). The dotted vertical lines indicate the lower and upper limit of the critical stress range for a site. The dashed horizontal lines (bars) indicate the spread of the possible critical stress values for a given parameter. For details see text.

The critical stress values for grain and straw yield are similar to each other at all sites, and similar between sites, too, except for Quellendorf, where the critical stress for grain yield

is much lower than at the other sites and differs greatly from the value for straw yield. The latter is similar to the values at the other three sites. At Buttelstedt and Rothenberga both parameters are at the lower end of the range. They are close to the center of the critical stress range at the Kranichborn site. At Quellendorf the critical stress value for grain yield is at the lower end of the range, while the value for straw yield is in the middle.

The bars for biopores as well as grain and straw yield are similar and nearly reach or sometimes even exceed the upper limit of the critical stress range for all sites. They always exceed the lower limit, except at Quellendorf.

5. Discussion

5.1. CT and soil physical measurements of compaction behaviour under strip tillage, mulch tillage and no tillage

5.1.1. Soil physical conditions

There were intact soil structures for all tillage treatments, depths and years, because BD values were always lower than a site-specific root-limiting BD of 1.55 g cm^{-3} (Kaufmann et al., 2010), and K_s values were always higher than the 10 cm d^{-1} minimum stated in Werner and Paul (1999).

Strip tillage WS and mulch tillage displayed very similar soil structural properties. So did strip tillage BS and no tillage, but the groups differed from each other.

Strip tillage WS and mulch tillage displayed significantly lower BD compared to strip tillage BS and no tillage. This is due to the fact that in the former two treatments the soil was loosened by tillage, while in the latter two it was left untilled with natural settlement as well as soil compaction occurring as a result of driving over the ground with agricultural machinery during tillage and harvesting. This result is in line with those of other studies (e.g. Hubbard et al., 1994; Kay and VandenBygaart, 2002). As time passed from 2014 to 2015 BD remained at a similar level at the depths sampled under strip tillage WS and mulch tillage, because the annual soil tillage counteracted the aforementioned processes.

Previous studies have shown contradictory results with respect to the K_s value for various tillage systems. Benjamin (1993), for example, found that untreated variants promoted infiltration as a result of increased macroporosity. In contrast, some studies found that no tillage and other conservation-oriented soil tillage methods displayed lower K_s values compared to conventional soil tillage, due to low macroporosity (e.g. Lindstrom and Onstad, 1984; Rücknagel et al., 2017). Other studies showed that there were no differences with respect to K_s values between untilled and conventionally tilled soils (Tollner et al., 1984; Culley et al., 1987). In this study strip tillage WS and mulch tillage displayed higher K_s values compared to strip tillage BS and no tillage, since the loosening of the soil resulted in an increase in large interaggregate pores which, due to their greater cross section, lead to an increased saturated hydraulic conductivity. This point and the contradictory effects of tillage on K_s will be picked up again in the next chapter.

At 12-18 cm soil depth a significant increase in the K_s value was observed between 2012 and 2015 for mulch tillage, strip tillage WS and strip tillage BS, despite a slight increase in BD under strip tillage BS. This may have been caused by an increased earthworm population. In another study at the same trial site the earthworm population was recorded for the strip tillage WS and strip tillage BS variants in the spring of 2015. Strip tillage WS had a

significantly lower earthworm abundance and biomass (68 individuals m^{-2}, 17.3 g m^{-2};) than strip tillage BS (152 individuals m^{-2}, 36.7 g m^{-2}) (Koblenz et al., 2016). The distance between strip tillage WS and BS is shorter than the extent of the habitat of individual earthworms, which should be considered in the interpretation. The earthworms apparently feel more comfortable in the more compacted strip tillage BS region, which may be due to a higher soil moisture content and more plant residue on the soil, but may feed and move through the less compacted WS region.

Kay and VandenBygaart (2002) found an increase in the number of biopores under no tillage due to an enhanced earthworm population which was able to develop well, because of a high availability of food from dead plant material on the soil surface, and a lack of annual disturbance by tillage. In the present study these positive biological effects were only achieved in the strip tillage BS treatment.

It was possible to show that strip tillage combines, on a small scale, the soil physical properties of mulch tillage, a deeper non-turning form of primary tillage, and those of no tillage.

5.1.2. Soil compression tests

The soil structures which differed from each other over short distances also reacted to mechanical loads in different ways. The loosened rows under strip tillage WS displayed mostly unstable secondary pores (cracks and irregular voids > 60 µm). These were largely destroyed by loads ≤ 100 kPa. The annual soil tillage performed for strip tillage WS destroyed the structure, but thereafter structural formation began anew. This resulted in aggregates which were more porous and, thus, less dense. On the other hand, the lack of soil tillage in the strip tillage BS treatment guaranteed an undisturbed structural framework. The aggregates were not mechanically altered and further strengthened by mechanical loads from driving over the ground. This resulted in higher mechanical precompression stress ($\sigma_{P\ BDxi}$) due to a high number of contact points between the aggregates and primary particles.

While the stress - BD_{xi} curves showed a standard recompression path, virgin compression line and mechanical precompression stress (Lebert and Horn, 1991), the behaviour was not observed in the stress - AD curves. The AD values of the different tillage treatments only increased to a limited extent during the compaction process, making it impossible to determine the mechanical precompression stress values from the stress - AD functions. Apparently, the highest load of 550 kPa was still too low to obtain clear stress - AD curves, and, hence, mechanical precompression stress values for the aggregates at this site. It would therefore make sense to apply higher loads. On the other hand, it could be that it is

simply not possible to determine mechanical precompression stress from the stress - AD curves, since the aggregates do not display a standard compression curve, as suggested in Rücknagel et al. (2017). Overall, it can be stated that soil compression mainly occurred due to compaction of interaggregate pores which are not considered when measuring aggregate density.

At the beginning of stress application there were isotropic initial structures, regardless of tillage treatment, and no significant differences in anisotropy were identified between the tillage treatments during the entire stress application process. Up to the 200 kPa load step strip tillage BS and no tillage tended to display not only higher mean pore diameters, but also slightly higher anisotropies than strip tillage WS and mulch tillage. One reason for this could be the dominance of plant root channels and biopores from macrofauna and their stability in untilled soils (Luo et al., 2010). Drees et al. (1994) also found higher mean pore diameters under no tillage than in conventionally tilled soils. Furthermore, vertically oriented pores are less susceptible to compaction than those aligned horizontally (Hartge and Bohne, 1983). Hence, in the case of uniaxial compaction it can be assumed that horizontal pores are compacted preferentially so that the ensuing predominance of vertical pores results in increased anisotropy. At the highest load steps all tillage treatments displayed a sudden rise in anisotropy. This can be inferred from the CT cross sections, too, because by the end of the stress application only isolated and irregularly distributed biopores were visible.

The morphometric parameters mean macropore size, macroporosity and pore connectivity affect each other. One parameter which depends on pore size is pore connectivity (Jarvis et al., 2017). Generally speaking, the smaller the pores, the higher their connectivity (Vogel and Roth, 1998). Macroporosity also plays a role here. The higher the macroporosity, the higher the likelihood that macropores are connected and form a larger network (Luo et al., 2010). In the present study no tillage displayed just a few large isolated macropores and therefore a low macroporosity and low pore connectivity. At the same time no tillage lacked the multitude of interaggregate pores smaller than the image resolution, which in the mulch tillage treatment reduced the mean pore diameter and, at the same time, ensured a higher macroporosity and pore connectivity. In the untilled treatments the slightly higher mean macropore sizes did not coincide with a higher macroporosity. Pagliai (1988), who also worked with quantitative image analysis, includes a classification of macroporosity for pores > 50 µm. According to this classification mulch tillage and strip tillage WS were moderately porous at the beginning of stress application, and strip tillage BS and no tillage were highly compacted. Furthermore, Pagliai (1988) quotes a macroporosity of 10%, and Reynolds et al. (2009) a macroporosity of 4%, both derived from quantitative image analysis, as the lower limit for an intact soil structure. Here strip tillage BS and no tillage fell below the 4%. Similar results concerning macroporosity with conservation-oriented methods compared

to conventional soil tillage were reported by Bullock et al. (1985) and Gantzer and Anderson (2002). In studies by Dal Ferro et al. (2014) and Jarvis et al. (2017) comparable experimental conditions to those at the Bernburg site also yielded similar values for the morphometric parameters from the quantitative image analysis of CT scans.

In addition to the conventional procedure using stress - BD_{xi} diagrams mechanical precompression stress values were also determined for the four tillage treatments based on the double logarithmic stress - macroporosity diagrams ($\sigma_{P\,MP}$) from the CT investigations. These showed good agreement with the values derived from the stress - BD_{xi} diagrams ($\sigma_{P\,BDxi}$). Despite the general suitability of $\sigma_{P\,MP}$, the double logarithmized representation of the diagrams means it is necessary to examine the extent to which there may be errors in the visual identification of the strongest curvature of the stress - macroporosity curves, which is one of the bases of Casagrande's (1936) graphical method. For all treatments there seems to be a critical stress value of around 100 kPa where macroporosity and pore connectivity reach a minimum which cannot be reduced any further, and where anisotropy increases considerably, but with a rather high variability due to the variable morphology of the remaining few macropores, as evident from the CT cross sections. A similar stress value for soil structure deformation was reported for compaction during centrifugation (Schlüter et al. 2016). This critical stress value is reflected well by the mechanical precompression stress values for the individual tillage treatments.

Strip tillage means that the seed rows are tilled, but the areas in between are not. Hence, the treatment STBS is in essence the same as no tillage (NT), another treatment considered here. Hence, it is not surprising that STBS is similar to NT for most parameters assessed in this study, and that these two treatments show the same course in the correlations presented above. STBS and NT have a higher AD than MT and STWS. Both have a higher mean macropore diameter and a higher macroporosity for a given BD as well. This only seems logical, because AD is higher at a given BD so that the interaggregate space is larger. For the same reason a given mean macropore diameter is associated with a higher AD/BD_{xi} ratio. Hence, it is plausible that MT and STWS have higher values for mean macropore diameter at a given BD than STBS and NT. However, it is not clear why MT differs from STWS in this relationship, while they follow the same course in the rest of the relationships in Figure 4.1-6. It is puzzling that STWS has a lower mean macropore diameter at a given BD than MT, but the same macroporosity and pore connectivity.

At this point it becomes clear again that a strip tillage system is very beneficial for parameters which are important for the tilth of a soil. Among them are the pore space and its connectivity, both of which are important for the conductivity and availability of air and water.

5.2. Effects of soil moisture during soil compaction due to soil tillage as assessed by classic and CT methods

5.2.1. Effects of tillage treatment and matric potential on compaction

Before looking at the advantages of combining CT and classic soil mechanical parameters to describe soil compaction, I shall briefly discuss the results found with respect to the effects of tillage treatment and matric potential on compaction, although this has been researched extensively before and is not the focus of this trial.

- Both tillage treatments initially displayed intact soil structures with BD values lower than a site-specific root-limiting density of 1.50 g cm^{-3} (Kaufmann et al., 2010), and K_s > 10 cm d^{-1} (Werner and Paul, 1999).

- The cultivator treatment showed a significantly higher initial BD than the plough treatment. Something similar was described by, for example, Amin et al. (2014), Nizami and Khan (1990) and Strudley et al. (2008).

- In this trial the plough treatment was associated with significantly higher K_s values compared to 'cultivator'. Previous studies have returned conflicting results with regard to the K_s value under different tillage systems. This was already discussed in section 5.1.1. and will be revisited in section 5.4.

- There was a positive correlation between mechanical precompression stress and BD. For that reason the samples from the cultivator treatment were less susceptible to compaction.

- As the load steps increased, regardless of matric potential, the plough treatment displayed a more pronounced progressive homogenisation of the soil structure than the cultivator treatment. This happened, because BD was initially lower in the plough treatment. Once BD reached the same value as in 'cultivator' the response to applied loads was the same.

- As in a variety of other studies (e.g. Imhoff et al., 2004; Saffih-Hdadi et al., 2009), I also found a negative correlation between mechanical precompression stress and matric potential (water content). This arises, because in unsaturated soils shear resisting forces are stronger, the more negative the matric potential is. In addition, they are higher, if soil density is higher (Cruse and Larson, 1977). Thus, the matric potential has a considerable impact on soil stability. This was confirmed again here by a disproportionately high increase in mechanical stability in the ploughed soil. This increase was found to a much lesser extent in the cultivator treatment.

- Aggregates have a much larger recompression range than the total soil. It is possible to determine the mechanical precompression stress using stress - AD curves. In our case the mechanical precompression stresses of the aggregates were not influenced by the different moisture regimes. Contrary to trial 1 a stress - AD curve could be derived now, because the applied stress was much higher (up to 2500 kPa compared to a maximum of 550 kPa in trial 2).

- Contrary to the the blabal in chapter x it is possible to determine the mechanical precompression stress using stress - AD curves, if stress was high enough.

- In our case the mechanical precompression stresses of the aggregates were not influenced by the different moisture regimes.

- Up to the 550 kPa load step the aggregates showed higher AD values at pF4.0 than at pF1.8 in both 'cultivator' and 'plough'. Given the higher level of interaggregate support at pF4.0, this would suggest a mechanically stabler soil structure which is accompanied by a higher aggregate stability.

5.2.2. Advantage of combining CT and classic soil mechanical parameters to describe soil compaction

The CT images of the pore structure revealed that the soils from the two tillage treatments reacted to mechanical loads in different ways. In the plough treatment the annual turning of the soil resulted in the creation of secondary pores (cracks, irregular voids > 60 µm) which, however, were unstable and therefore susceptible to compression, particularly under moist conditions. Also, the aggregates were more porous and therefore less dense. On the other hand, in the cultivator treatments the implement did not reach the sampling depth of 16-19 cm so that no secondary pores were created and fewer structural pores were available at that depth for compression compared to the plough treatment. If it was not for CT, one would not see these soil structures, but could only infer them from BD. Hence, CT provides a more definite picture of the situation.

Since the application of CT to soils is fairly new, there are no comparisons or classifications of the values of CT parameters in the literature, with the exception of macroporosity as previously pointed out in section 5.1.2. According to Pagliai (1988) the cultivator treatments here would be classified as highly compacted at the beginning of the load application, and the plough treatments as moderately porous.

BD is a widely used parameter to describe soil compaction. However, with BD or mechanical precompression stress alone there is no information on the arrangement, distribution or interconnection of pores. This is of great importance in the system 'soil' to

maintain aeration and the water balance. To illustrate this consider the following: Clay has a low BD and a large pore volume, but a low saturated hydraulic conductivity. Sandy soils on the other hand have a high BD and a small pore volume, but a high saturated hydraulic conductivity. This difference in K_s is due to a different pore size distribution. Now, when is a soil is loosened during tillage and then recompacted in the course of subsequent agronomic operations, the classic methods indicate an increase in dry bulk density, but provide no information about the change in pore size distribution. CT does.

Looking at the correlations between BD and the various CT parameters shown here for both tillage treatments and soil matric potentials it can be seen that for macroporosity and mean macropore diameter the correlation is not affected by these two variables. Load application reduced the higher macroporosity and the larger mean macropore diameter created by ploughing. At a certain load the values of these two parameters were reduced to those of the cultivator treatments where they were not altered by tillage in the first place. Thus, ploughing has only a temporary positive effect that persists as long as macroporosity and mean macropore diameter remain high.

For pore connectivity the correlation with BD is a bit more complicated. While the data for 'plough' at pF1.8 and the data for 'cultivator' at both matric potentials apparently fall on the same curve, the data for plough at pF4.0 take a different course, showing higher connectivities at a given BD. The correlation between BD and anisotropy is different again. Here the data for 'cultivator' and 'plough' show the same relationship, but it is different for the two matric potentials. At pF1.8 anisotropy is higher.

Hence, there is one value for the CT-parameters mean macropore diameter and macroporosity for a given BD_{xi}, but two different values for pore connectivity and anisotropy due to soil matric potential. This means that for the description of soil compaction BD alone is not sufficient, although it is very useful to assess parameters such as the mechanical precompression stress. This statement can be reinforced with obervations from trial 1 published already by Pöhlitz et al. (2018). For a given BD_{xi} they, too, reported different values of CT-parameters, in their case mean macropore diameter and macroporosity. In the trial here these two parameters were not dependent on tillage, even though a different behavior between 'cultivator' and 'plough' was expected.

For completeness it should be stated that for the correlation between BD_{xi} and pore connectivity and anisotropy, respectively, there was no dependence on tillage treatment in the study of Pöhlitz et al. (2018) either. Furthermore, the data for these two parameters from trial 1 and 2 fall on top of each other when pooled together. This topic shall be picked up again in the section 5.4.

At this point the controversial statements quoted above about the the effect of different tillage systems on K_s shall be picked up again. The data here may provide a possible explanation. Figure 4.2-1 and 2 show that dry bulk density is much lower right after ploughing than after applying a cultivator. As a consequence, macroporosity, mean macropore diameter and pore connectivity are higher (Fig. 4.2-1, 2 and 4). Since these three parameters ultimately determine K_s, ploughing results in higher values. However, with time this beneficial effect of ploughing on K_s disappears, because natural settlement and, more importantly, increasing traffic across the field in the process of various agronomic operations lead to compaction, i.e. an increase in BD (Fig. 4.2-1 and 2) and a concurrent decrease in macroporosity, mean macropore diameter and pore connectivity (Fig. 4.2-4) and, thus, K_s. Compaction occurs under a cultivator treatment, too, but to a much lesser extent (Fig. 4.2-1, 2 and 4).

If compaction in a ploughed field does not reach the BD values encountered under a cultivator treatment, then macroporosity, mean macropore diameter and pore connectivity remain higher under ploughing (Fig. 4.2-4), and therefore K_s. If, however, compaction does reach these values, then macroporosity, mean macropore diameter, pore connectivity and lastly K_s will be the same under both tillage treatments. However, there is a deviation from this. If compaction occurs while the soil is dry (here at a matric potential of -1000 kPa), it appears that pore connectivity (Fig. 4.2-4C) remains higher under ploughing, even if BD is reduced to the same values found with the use of a cultivator. This implies that K_s under ploughing would still be higher than under the use of a cultivator. Following the above, K_s under ploughing can be higher or the same as under the use of a cultivator, but never lower.

However, there is a lot of research which indicates a lower K_s under conventional tillage. This may have the following reasons: A cultivator loosens the soil only superficially. This entails that macroporosity, mean macropore diameter, pore connectivity and therefore K_s are hardly enhanced lower in the soil profile. However, it also means that the continuity of the pores is not disrupted very much. (I explicitly used the word continuity instead of connectivity to differentiate between the situation in a small soil core and in a soil profile.) In contrast, ploughing greatly loosens the soil down to a depth of around 20 to 30 cm. While this greatly increases macroporosity, mean macropore diameter, pore connectivity and therefore K_s in the plough layer, it severs the connection of pores from lower in the profile to the surface horizon. This in turn reduces the K_s-value of the soil as a whole, though not of the plough layer, below that of a cultivator treatment. Now, if K_s is determined on soil cores from the topsoil, then a ploughed soil will either have a higher or the same K_s as a soil treated with a cultivator. However, if K_s is determined using an in-situ infiltration test which penetrates beyond the surface layer, then K_s is lower under ploughing, due to the disruption of the pores.

The reasons for the contradictory results about the effect of different tillage systems on K_s just given appear logical and are consistent with the results from this trial and from other research. However, to back them up further a thorough analysis of data published in the literature on this topic should be carried out. In particular, attention should be given to the time after tillage when the K_s data were determined, the method used and the depth this method covered.

The CT-parameters were all closely and uniquely related to each other, i.e. the relationships were not affected by tillage treatment or matric potential. Macroporosity is best suited for correlations with the other parameters, because it is the parameter which is measured directly with CT.

Schlüter and Vogel (2016) observed a linear relationship when comparing macroporosity with mean macropore diameter. For the data presented here the relationship is non-linear, S-shaped to be precise. The difference probably arises, because the data of Schlüter and Vogel cover a smaller range. The relationship they found between macroporosity and pore connectivity is non-linear. Up to a certain macroporosity value (10-12 %) pore connectivity is virtually constant. This is followed by a sharp transition after which there is a large change in pore connectivity with just a small change in porosity. The data here show much the same behavior, except that the decrease in pore connectivity with macroporosity is less steep and starts later (at 15 % macoroporosity). The reason for that may be that they used sieved and reconstituted soil in a very regular packing (texture: silt loam). This resulted in a well-connected pore network with a large number of uniform pores.

The correlations between macroporosity and mean macropore diameter as well as between macorporosity and pore connectivity show an S-shaped course. The first correlation causes the second, i.e. compaction decreases the pore volume, predominantly by decreasing macroporosity, which in turn lowers the chance for pores to be connected.

The two remaining correlations, namely between macroporosity and anisotropy as well as between pore connectivity and anisotropy, show a threshold behaviour in which isotropy is preserved up to a certain value of macroporosity (0.025) or pore connectivity (0.10), and then decreases rapidly. In the cultivator treatments macroporosity and pore connectivity were low from the start. Hence, anisotropy decreased immediately with increasing load. In contrast, in the plough treatments the higher initial macroporosity and pore connectivity values effected that isotropy was sustained longer. A few large macropores withstood a compression stress up to 550 kPa and caused the connection probability to remain > 0.5 at a dry bulk density of < 1.6 g cm^{-3}.

5.3. Estimation of critical stress ranges to preserve soil functions at differently textured sites

5.3.1. General remarks

Before taking a look at the critical stress values and critical stress ranges resulting from soil compaction I shall briefly discuss the effects of compaction on the examined soil functions observed here.

- The initial BD's for the four sites were much lower than site-specific plant root limiting BD´s according to Kaufmann et al. (2010). Furthermore, the K_s values were much higher than the minimum rate recommended by Werner and Paul (1999). Hence, the soil structures were intact at all sites.

- With increasing load application a homogenization of the soil structure progressed at all sites. Some biopores, however, remained visible even at the highest load steps.

- Despite different initial densities, all stress - BD_{xi} curves showed a similar classic course. The individual curves were merely shifted somewhat along the ordinate. As a consequence the values for the mechanical precompression stress were similar.

- According to Pagliai (1988) the macroporosity at the beginning of the load application can be classified as follows for the sites: Buttelstedt, Rothenberga and Kranichborn were moderately porous and Quellendorf was dense. In general, the greater the macroporosity, the higher the chance for macropores to be connected (Luo et al., 2010). This was found here only for the Buttelstedt and Kranichborn site.

- Several individuals of *L. terrestris* shared biopores. This is in agreement with the studies of Jegou et al. (1998) and Joschko et al. (1989).

- The burrowing activity of *L. terrestris* varied with dry bulk density, following a parabolic curve. At low BD there was little burrowing activity, because there is less need to dig to obtain food and shelter. Up to a certain point (optimal BD) the number of burrows increased with increasing soil density. Beyond this point the burrowing activity decreased with BD, because *L. terrestris* was mechanically restricted, i.e. soil strength seemed to be a limiting factor at higher densities. A lower burrowing rate at higher densities was also found by Kemper et al. (1988) and Stovold et al. (2004). Schrader et al. (2007) and Kemper et al. (1988) observed that *L. terrestris* failed to penetrate a silt loam soil with a BD of 1.60-1.70 g cm^{-3}. Similarly, Horn (1999) named 1.67 g cm^{-3} as the BD limit for *L. terrestris.*

- At high soil densities *L. terrestris* tended to remain in a particular location. Such a behaviour was also reported by Perreault and Whalen (2006), if *L. terrestris* was

exposed to unfavorably cold and wet soil conditions. (Recall that in the trial here the soil was at 20°C and moist, i.e. the conditions were favorable.)

- The parabolic correlation between dry bulk density and burrowing activity of *L. terrestris* depends on the site. The optimal BD and the steepness of the curve differ.

- Very loose (bad soil root contact) as well as heavily compacted soil (high mechanical resistance to root penetration, reduced availability of oxygen, water and nutrients) leads to reduced yields, as found by Daddow and Warrington (1983), Håkansson (1989), Saqib et al. (2004) and Shah et al. (2017), too.

5.3.2. Stress ranges

Based on a multitude of tests concerning the compaction of soil due to loads, texture dependent maximum loads are quoted in the literature (Diserens, 2009). One key question to be addressed here is, how the critical stress values differ between textures and thus explain the differences between the critical stress ranges. In addition, the question arises, how well the mechanical precompression stress concurs with the value ranges of the other parameters determined here, because until recently the mechanical precompression stress was a common parameter for assessing the compaction sensitivity of soils due to mechanical loads. This is linked to the question of what is gained by considering the other parameters.

In chapter 4.3 stress values for various parameters were presented. Single values were taken from fitted curves. However, in some cases the curves were fairly flat and the data had a high standard deviation. As a consequence it is possible to pick a number of plausible critical stress values for a given parameter. For some the possible critical stress values have a rather big spread, for example the critical stress value for the number of biopores at Quellendorf. This is because the curve of the relationship between dry bulk density and number of biopores there was almost horizontal (see Fig. 4.3-8). Overall, the spread for grain and straw yield is widest.

The values for the mechanical precompression stress at the four sites are fairly similar. The spread is the lowest for all parameters. In general the mechanical precompression stress lies in the middle of the critical stress ranges for the other five investigated parameters and covers them reasonably well. Nevertheless, useful additional information is gained from considering the other parameters as well.

There is a tendency that the critical stress value for macroporosity is smaller than for pore connectivity. This can be seen clearly at three of the four sites, with Buttelstedt as the exception. However, if one considers the spread, than this is possible at this site, too. This tendency can be explained by the fact that with increasing load the pores are first reduced in

diameter, but can still be connected. Even if the mechanical precompression stress is exceeded, the macropores are still connected, as shown for Buttelstedt and Kranichborn in Fig. 4.8-8.

About the critical stress value for the number of biopores no general statement is possible. At the Quellendorf site it was highest and the spread was also highest. At Kranichborn it was lowest with the second lowest spread. The spread at these two as well as the other two sites overlap. For the Quellendorf site one can assume that the critical stress value is very low due to the high sand content, because the rough surface of the sand particles can impair burrowing activity. At higher bulk densities this effect may increase, because the particles move closer together, which further increases friction. However, with increasing dry bulk density no significant differences in the number of biopores could be determined. This could be attributed to the lack of aggregation (Beisecker et al., 1994) and the accompanying evenly distributed resistance. That may be why the earthworms were still able to burrow through the soil even after the mechanical precompression stress was exceeded. For the Kranichborn site the high content of organic matter qualifies the aforementioned effect of a high sand content, because it ensures a loose and thus easily penetrable packing. In general the bulk densities were low so that there was little burrowing resistance.

With the exception of Quellendorf, the critical stress value for grain yield is very close to the one for straw yield. If one considers the spread, this can also be the case at Quellendorf. Grain and straw yield tend to become critical before the mechanical precompression stress is reached. If one looks at the spread, grain and straw yield seem to be the most sensitive parameters and form the lower limit of the critical stress range. Iler and Stevenson (1991) report that sandy soils have high growth-limiting bulk densities of around 1.65-1.75 g cm^{-3}, but that plants already show a significant reduction in growth before those densities are reached. This implies, too, that soil conditions are limiting for plant growth before its mechanical precompression stress is reached. Ultimately grain and straw yield are the most important parameters for the farmer.

Grain and straw yield are more sensitive and have a wider spread than macroporosity and pore connectivity.

Following these explanations it is not surprising that at different sites the critical stress value for a given parameter may lie at the upper or lower end of the critical stress range for all parameters considered here, and that its value and spread may differ between sites. For example, the critical stress range is widest at Quellendorf and narrowest at Buttelstedt. However, if the medians of the critical stress ranges are looked at, it can be seen that they

are similar in value (50 - 100 kPa), and also similar to the values of the mechanical precompression stresses (45 - 71 kPa).

Since the soil textures are quite different at the four sites, it follows that it is not texture alone (or at least not primarily) which determines the compaction sensitivity of soils and the associated changes in soil functions. Therefore, based on the results presented here one should be careful to connect the compaction vulnerability of soils exclusively to texture. There is more to it.

5.4.   Comparison between BD_{xi} and CT parameters

In connection with trial 1 and 2 relationships between BD_{xi} and the CT parameters mean macropore diameter, macroporosity, pore connectivity and anisotropy were presented and discussed. In the course of trial 3 BD_{xi} and these CT parameters were determined as well, but not explicitly related to each other, because this did not fit in with the topic of this trial, namely critical stress values and ranges. Furthermore, the data for mean macropore diameter and anisotropy were not presented at all. In this section all relationships between BD_{xi} and the four CT parameters obtained in all three trials are combined, with the execption of the data for pF4.0 from trial 2. They are left out, because all other data were acquired at a soil moisture tension of pF1.8.

Table 5.4-1 summarizes the various treatments in the three trials. The first column gives the abbreviations assigned to the treatments in the respective chapters. For reasons which will become obvious in connection with the description of Figure 5.4-1 to 8 they are not ordered by trial. In some cases the abbreviations indicate a tillage system, in others a location. Therefore the trial sites and the manner of tillage carried out there are named explicitely in column 2, and in columns 4 and 5, respectively. Also listed are the soil texture (column 3) and the sampling depths (column 6). Note that the Buttelstedt site in trial 2 (C) is the same as in trial 3 (BS). The difference is the depth of tillage and the sampling depth.

Table 5.4-1: Summary of the treatments in the three trials.

treatment	site	texture	tillage implement	tillage depth	sampling depth
KB	Kranichborn	sandy loam	cultivator	30 cm	10-13 cm
QD	Quellendorf	loam	cultivator	25 cm	2-5 cm
RB	Rothenberga	silt loam	cultivator	25 cm	5-8 cm
MT	Bernburg	silt loam	disc harrow	25 cm	12-18 cm
STWS	Bernburg	silt loam	rotary tiller	25 cm	12-18 cm
NT	Bernburg	silt loam	–	–	12-18 cm
STBS	Bernburg	silt loam	–	–	12-18 cm
C	Buttelstedt	silty clay loam	cultivator	5 cm	16-19 cm
BS	Buttelstedt	silty clay loam	cultivator	15 cm	10-13 cm
P	Buttelstedt	silty clay loam	mouldboard plough	30 cm	16-19 cm

Recall that in trial 1 there were different courses for the relationship between mean macropore diameter and BD_{xi}, depending on the tillage treatment. The same was observed, though not as clearly, for the relationship between macroporosity and BD_{xi}. In contrast, in trial 2 there was no dependence on tillage, but on soil moisture tension in the relationship between pore connectivity and anisotropy and BD_{xi}.

Figure 5.4-1 shows the relationships between BD_{xi} and mean macropore diameter. In all treatments the mean macropore diameter decreases with increasing BD_{xi}. However, the data follow at least four different courses. The first is for KB and MT. The data seem to fall onto the same line, but they cover different ranges which do not overlap. Hence, it cannot be said for certain that they do follow the same line. Besides, the tillage systems used and the soil textures are different (Tab. 5.4-1).
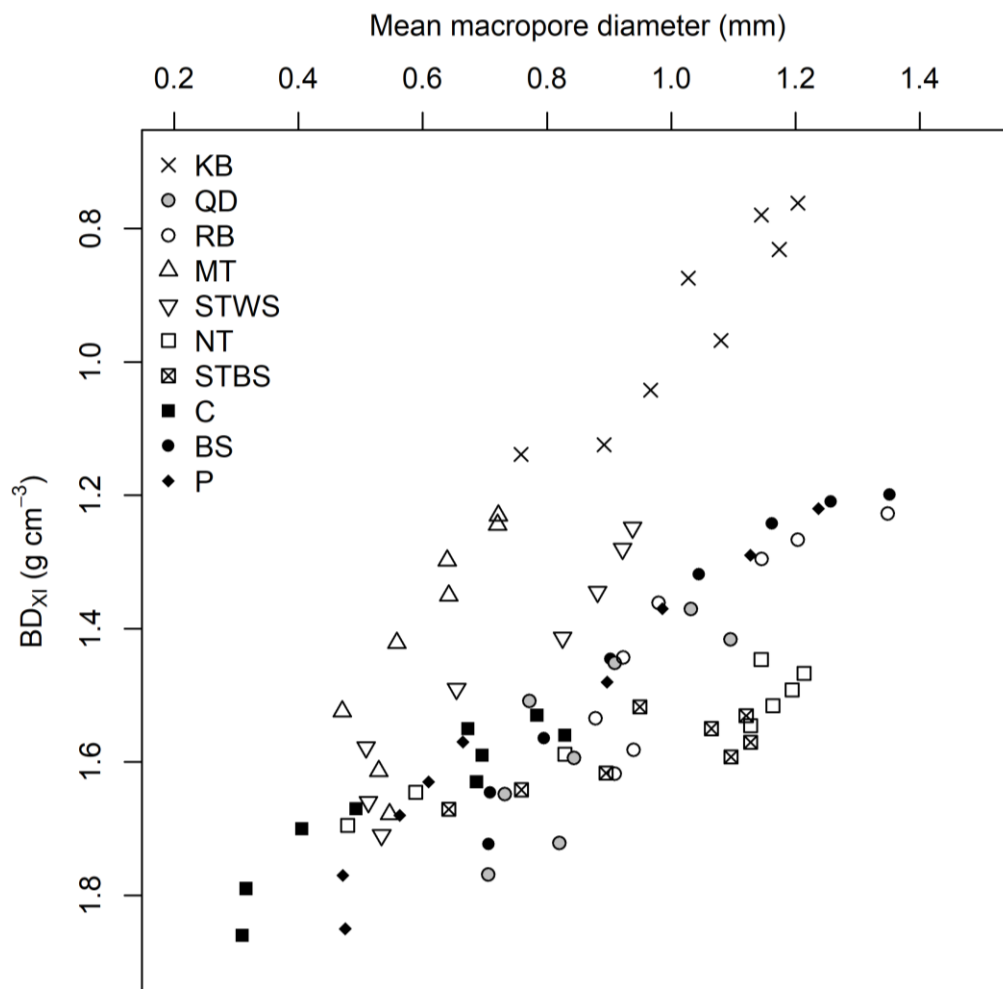
Figure 5.4-1: Correlation between dry bulk density (BD_{xi}) and mean macropore diameter for samples from all three trials. KB = Kranichborn, QD = Quellendorf, RB = Rothenberga, MT = mulch tillage, STWS = strip tillage within the seed row, NT = no tillage, STBS = strip tillage between seed rows, C = cultivator, BS = Buttelstedt, and P = plough.

The second course is for STWS only. It clearly differs from all others, even though texture and depth of tillage are similar to other treatments. The only real difference is the tillage implement (rotary tiller) which operates very differently to the others.

BS and RB form the third course. Both sites follow the same path for some distance, but not the entire way. So does QD, but with much more scatter. The tillage system was the same at all three sites (cultivator), but the soil textures were different.

The forth course is taken by NT, STBS and C. In NT and STBS there was no tillage. In C a cultivator was employed which, however, only worked the soil down to 5 cm depth, far above the sampled depth of 16-19 cm. Hence, C can be viewed as no tillage here, too. So, sites receiving the same tillage treament again follow a similar path, despite some differences in texture. This one is very different though from the course for three of the four cultivator treatments (course 3).

This leaves P. Up to BD = 1.5 g cm^{-3} P could be added to course 3, but at higher BD's it deviates clearly. This is not surprising, since tillage with a plough is something altogher different then applying one of the conservation (and no) tillage systems employed in the other treatments.

The above discussion reveals that the tillage system has an effect on the relationship between BD$_{xi}$ and mean macropore diameter. It also indicates that there may an effect of texture, too. To clarify this some of the data are replotted in Figure 5.4-2A to D.

In the five silt loam treatments the relationship is strongly affected by tillage (Fig. 5.4-2A). In the three silty clay loam ones (Fig. 5.4-2B) the course is similar at first, but then their courses diverge. Here the tillage effect is not as obvious, but definitely present. Figure 5.4-2C depicts the three no tillage treatments. The data are pretty close together, but nevertheless the points from the silty clay loam site at Buttelstedt (C) are always highest, those from the silt loam site at Bernburg (STBS) are always the lowest. This points to a certain dependence of texture, too. For the four cultivator sites (Fig. 5.4-2D) a similar observation can be made. The data for QD, RB and BS are close together, but not on top of each other. This again points to a slight texture dependence. The data for KB lie much higher, due to the high OM content mentioned before.
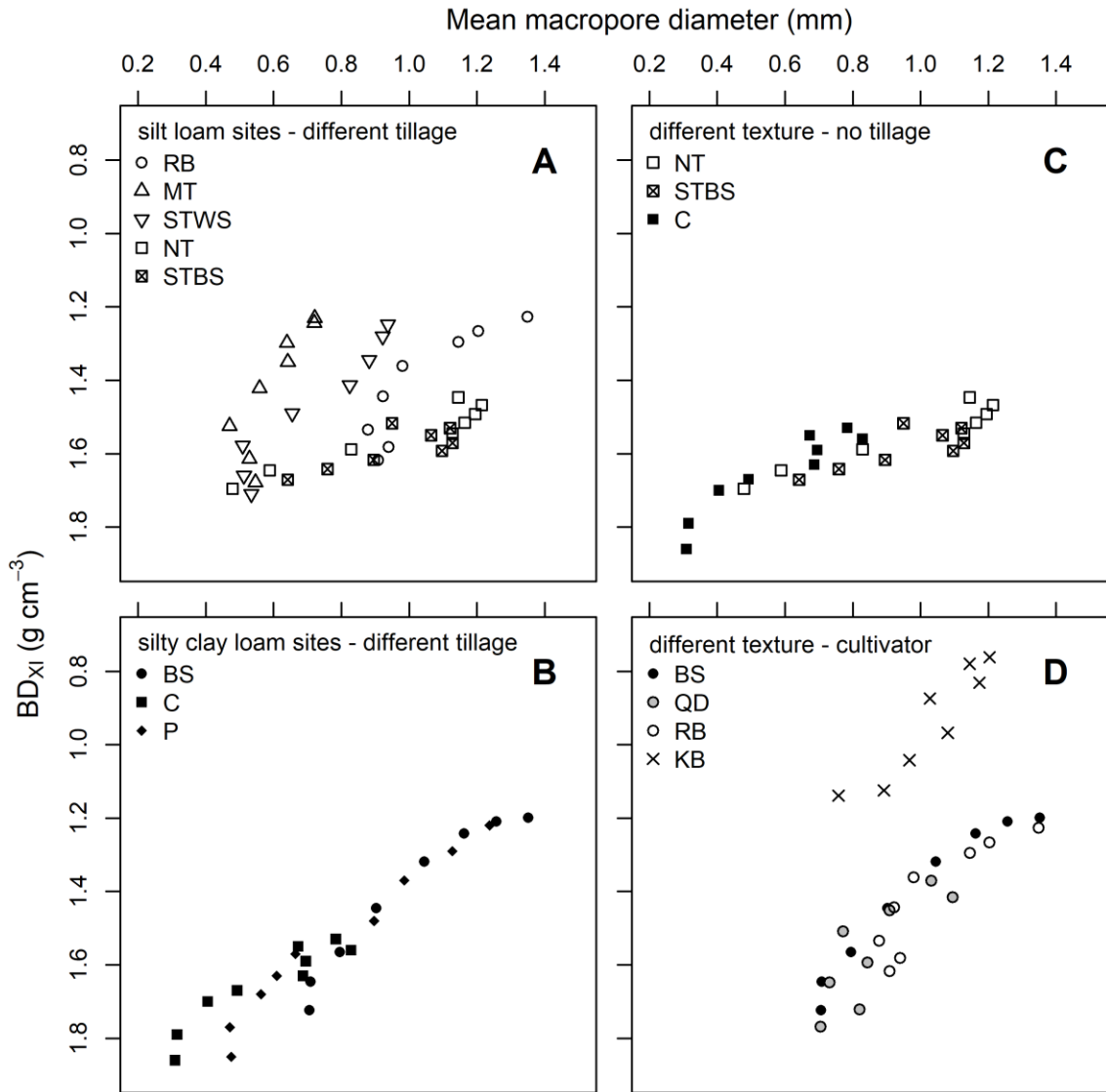
Figure 5.4-2: Correlation between dry bulk density (BD$_{xi}$) and mean macropore diameter for treatments with the same texture but a different tillage system (A, B), and for treatments with the same tillage system but different texture (C, D). The abbreviations are explained in Figure 5.4-1.

The relationship between BD_{xi} and macroporosity is depicted in Figure 5.4-3. Initially macroporosity decreases markedly for only a small change in BD_{xi}. Beyond a BD_{xi} of about 1.4 g cm^{-3} the reverse happens: There is only a small change in macroporosity for a substantial change in BD_{xi}. Most treatments follow virtually the same course, except KB and BS. The data for KB lie far above the other data points. Again, this is most likely due to the low bulk densities as a result of the high content of organic matter at this site. The data for BS fall below the others. If one shifts the data for BS up along the BD_{xi}-axis by about 0.15 g cm^{-3}, they merge with the other data. Similarly, if one shifts the data for KB downwards along the BD_{xi}-axis by about 0.4 g cm^{-3}, they merge with the other data, too. Interestingly, going back to Figure 5.4.-1, if one shifts the KB data there downwards along the BD_{xi}-axis by about 0.4 g cm^{-3}, they fall on course 3 for the treamtents tilled with a cultivator, just like KB was.
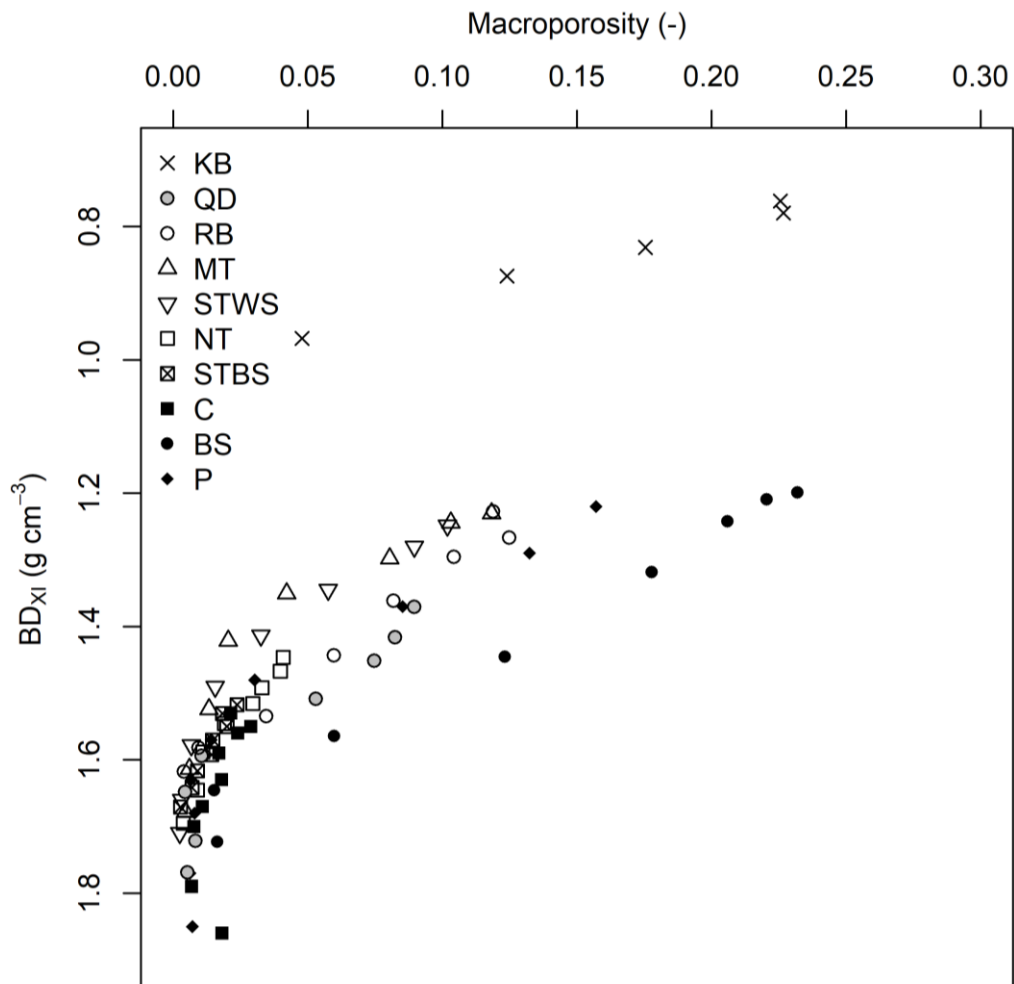
Figure 5.4-3: Correlation between dry bulk density (BD_{xi}) and macroporosity for samples from all three trials. The abbreviations are explained in Figure 5.4-1.

Again, some of the data are redrawn (Fig. 5.4-4A to D). Here the tillage dependence at the silt loam sites (Fig. 5.4-4A) is much smaller than for the parameter mean macropore diameter (Fig. 5.4-2A), but still discernable. Also, it is smaller than at the silty clay loam sites (Fig. 5.4-4B). For the latter three sites the data follow a different path at first, but come together at a BD_{xi} of about 1.6 g cm^{-3} (Fig. 5.4-4B). This is the reverse of the behavior observed for the mean macropore diameter (Fig. 5.4-2B). For the no tillage treatments there is no dependence on texture (Fig. 5.4-4C). For the cultivator treatments there is (Fig. 5.4-4D), and is about as evident as for the mean macropore diameter (Fig. 5.4-2D).
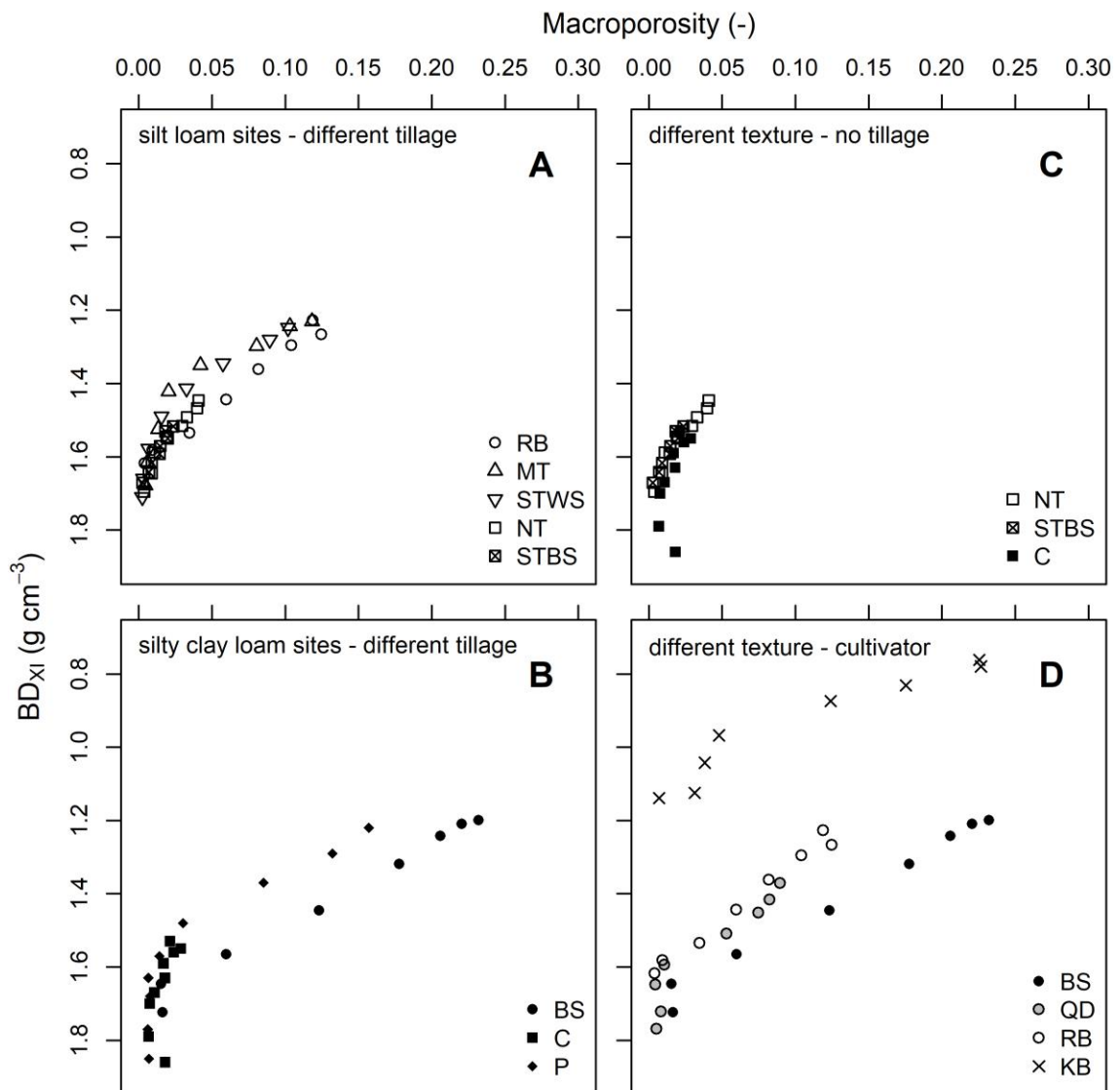

Figure 5.4-4: Correlation between dry bulk density (BD_{xi}) and macroporosity for treatments with the same texture but a different tillage system (A, B), and for treatments with the same tillage system but different texture (C, D). The abbreviations are explained in Figure 5.4-1.

The relationship between BD_{xi} and pore connectivity (Fig. 5.4-5) is similar for MT, STWS, and P. At first there is a big decline in connectivity with a small change in BD_{xi}. At $BD_{xi} > 1.4$ g cm^{-3} connectivity changes little with increasing BD_{xi}.
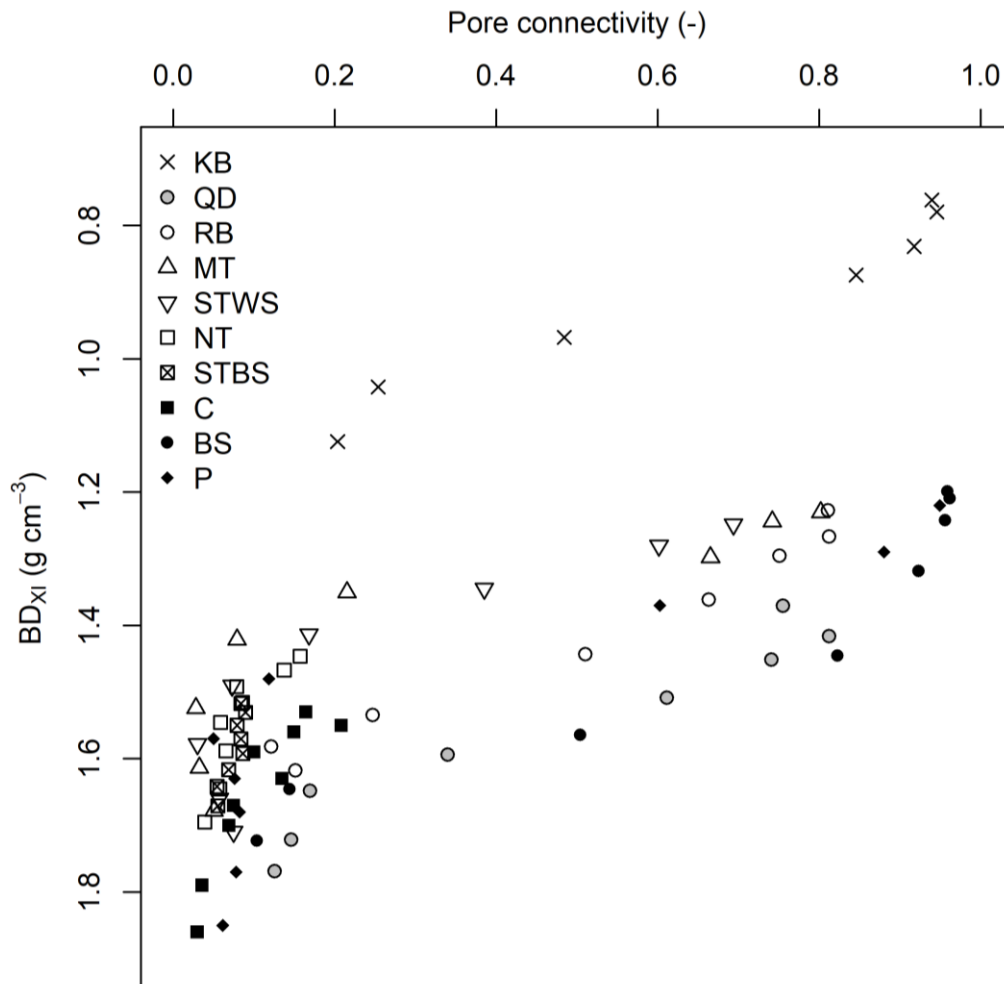

Figure 5.4-5: Correlation between dry bulk density (BD_{xi}) and pore connectivity for samples from all three trials. The abbreviations are explained in Figure 5.4-1.

The data for the no tillage variants NT, STBS, C only begin at $BD_{xi} > 1.4$ g cm^{-3}, but match the data for MT, STWS, and P. However, nothing can be said about their behaviour at lower BD values. Here, too, the data for KB lie above all the others, but their course is similar so that a downward shift merges them. The data for the other cultivator treatments (BS, QD and RB) fall below the bulk of the data. QD and BS are close together, while RB takes a somewhat different course.

Figure 5.4-6A to D depicts the data differentiated by texture and tillage system. The observations which can be made are essentially the same as for macroporosity, with two differences: The tillage dependence at the silt loam and the silty clay loam sites is equally

strong (Fig. 5.4-6A, B), and there is a small texture dependence in the no tillage treatments (Fig. 5.4-6C).

Figure 5.4-6: Correlation between dry bulk density (BD_{xi}) and pore connectivity for treatments with the same texture but a different tillage system (A, B), and for treatments with the same tillage system but different texture (C, D). The abbreviations are explained in Figure 5.4-1.

Notwithstanding a lot of scatter, for all treatments except KB the data for the last CT parameter, anisotropy (Fig. 5.4-7), follow the same course. Up to a BD_{xi} of 1.6 g cm^{-3} anisotropy remains practically constant. Thereafter it decreases as BD_{xi} increases. Shifting the data for KB downwards by 0.5 g cm^{-3} merges them with the rest.
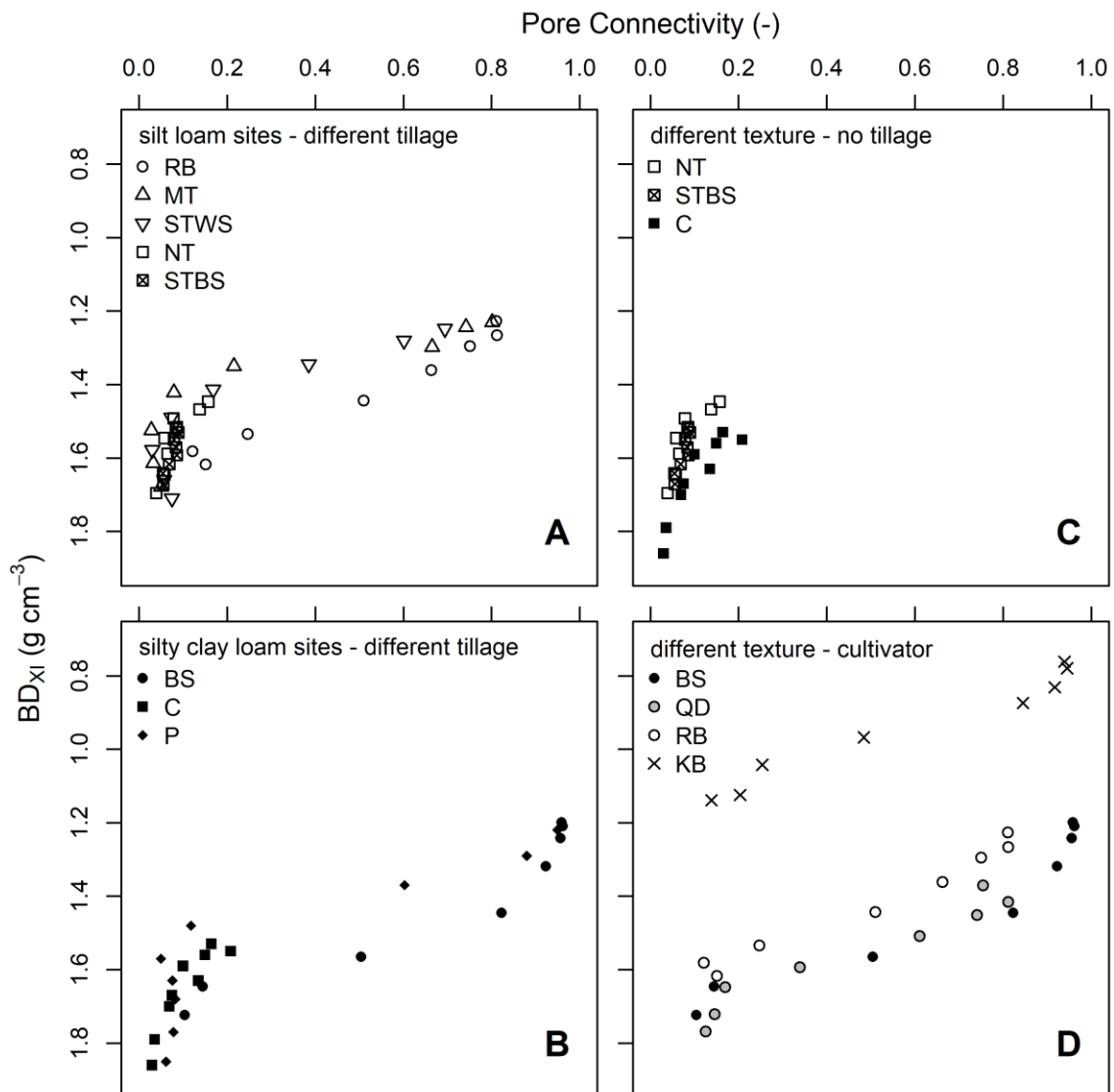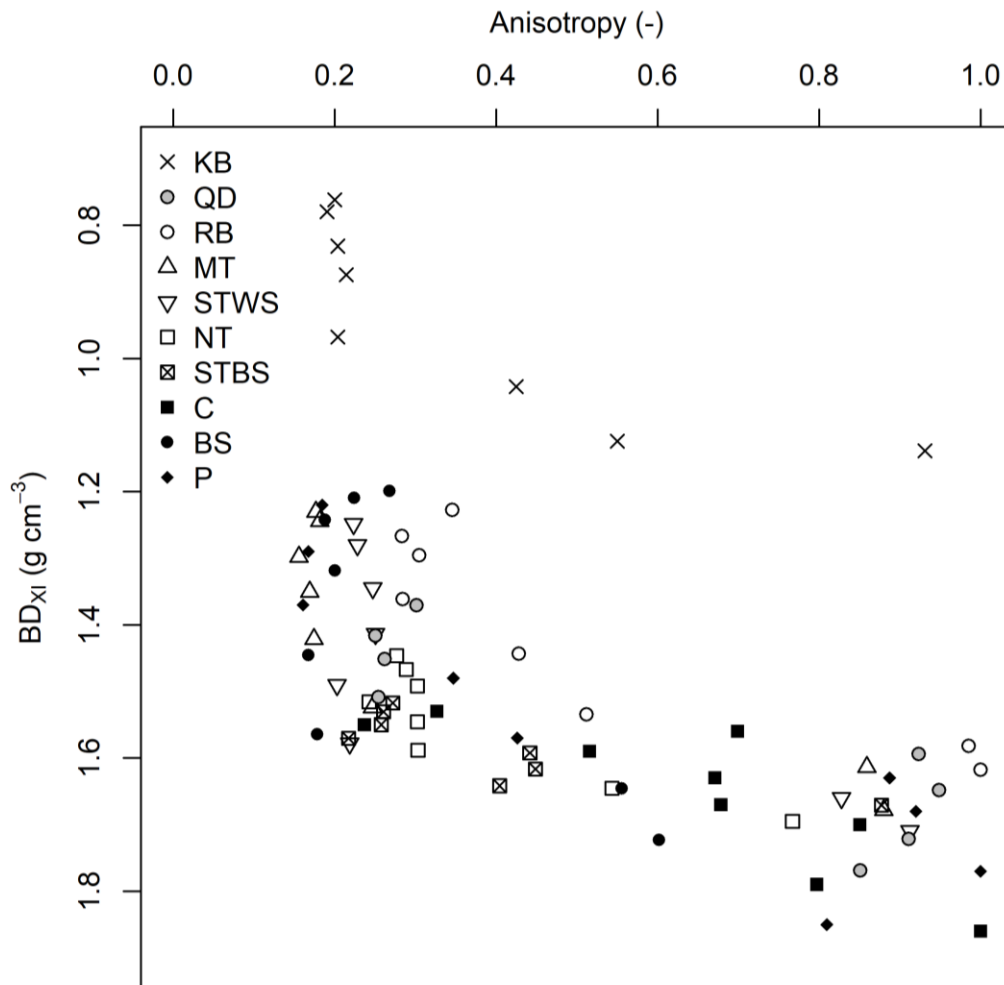
Figure 5.4-7: Correlation between dry bulk density (BD_{xi}) and anisotropy for samples from all three trials. The abbreviations are explained in Figure 5.4-1.

When separated by texture and tillage (Figure 5.4-8A to D) it becomes clearly visible that the relationship for the five silt loam treatments is strongly affected by tillage (Fig. 5.4-8A). The data from the three silty clay loam sites scatter (Fig. 5.4-8B). At no site do they follow a defined course. Hence, it cannot be said if there is a tillage dependence or not. The data from the no tillage sites follow the same course, albeit with some scatter, and do not exhibit an obvious texture dependence (Fig. 5.4-8C). In the cultivator treatments (Fig. 5.4-8D) the KB site falls, as usual, above the others. With respect to the other three sites, the situation is similar to the one in Figure 5.4-8B: The data from none of them delineate a describable course, they merely scatter. Consequently, it cannot be said if there is a texture dependence or not.

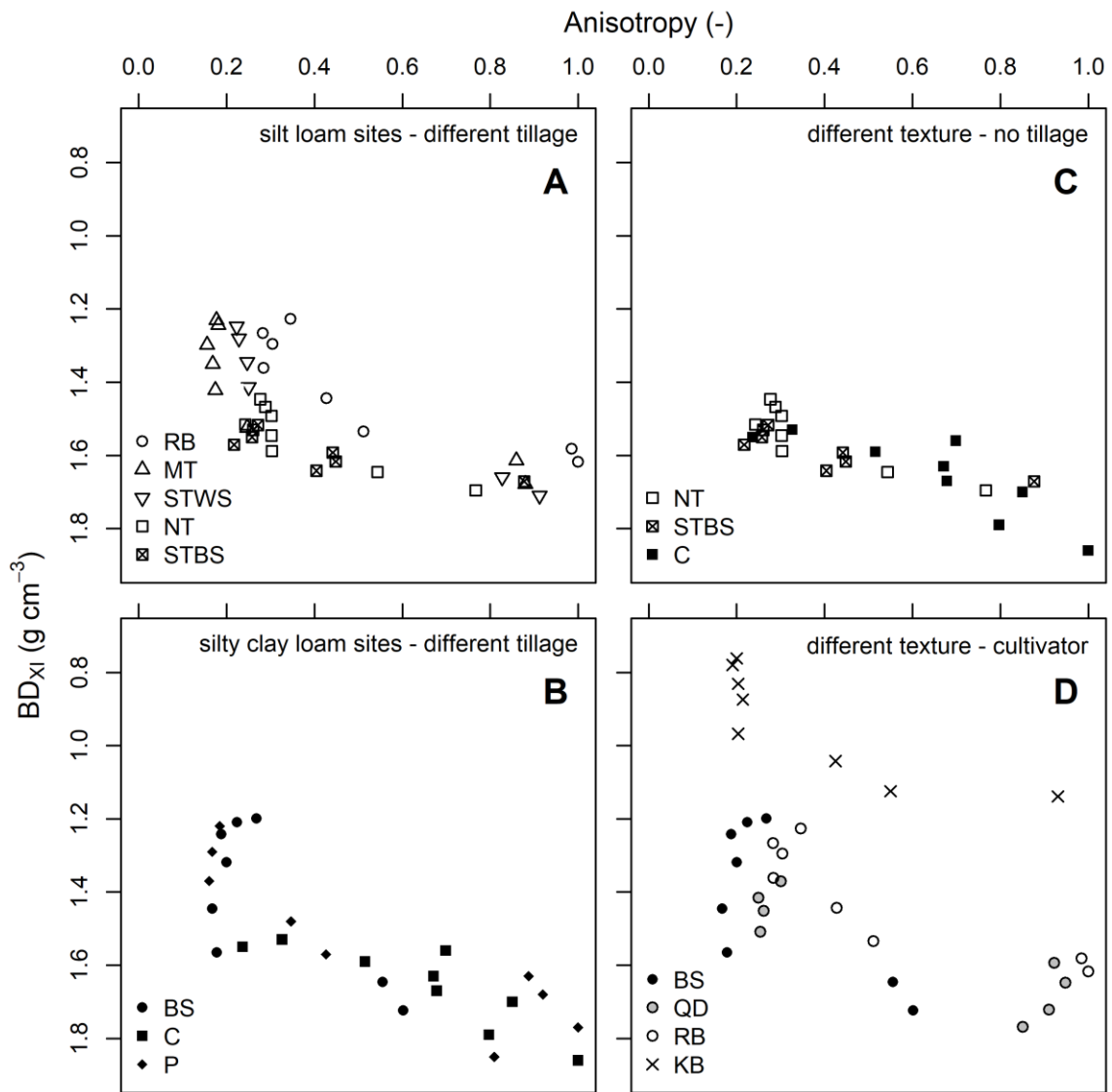**Figure 5.4-8:** Correlation between dry bulk density (BD_{xi}) and anisotropy for treatments with the same texture but a different tillage system (A, B), and for treatments with the same tillage system but different texture (C, D). The abbreviations are explained in Figure 5.4-1.

## 5.5. Comparison of the CT parameters with each other

To complete the data analysis the CT parameters are now cross-correlated with each other, as already done with some of the data in section 4.2.6. The result there was that all data points in most of the given correlations followed the same course. This will now be checked on the basis of the data from all three trials depicted in Figures 5.5-1 to 5.5-6. Note that here it was possible to display the data for all three trials (Fig. 5.5-1A to 5.5-6A) in the same size as the data differentiated by tillage and texture. In chapter 5.4 this was not possible, because the resulting figures would have been to confusing to read.

Decreasing mean macropore diameters results in a decrasing macroporosity until a macroporosity of around 0.05 is reached (Fig. 5.5-1A). Below this value the macroporosity hardly changes any more, even for a considerable further decline in the mean macropore diameter. In total two courses can be identified. The first one has data points in the area where the rapid changes of the mean macropore diameter occur and is followed by all treatments, except the no tillage ones NT, STBS and C. The latter form the second course where all macroporosites are below 0.05.

The data for the five silt loam sites (Fig. 5.5-1B) show a clear response to the different tillage treatments. The same holds for the silty clay loam sites (Fig. 5.5-1C), but the effect is much smaller. The data points for the no tillage sites are pretty close together (Fig. 5.5-1D), but nevertheless the points from the silty clay loam site at Buttelstedt (C) are always the highest, those from the silt loam site at Bernburg (STBS) always the lowest. This points to a certain dependence of texture. An even stronger texture dependence is visible in the cultivator treatments (Fig. 5.5-1E).

There is an S-shaped decline in pore connectivity as the mean macropore diameter decreases for all except the no tillage sites (Fig. 5.5-2A). At the latter sites the connectivites are always below 0.2 and do not become much less as mean macropore diameter decreases. The statements made in connection with Figure 5.5-1B to D apply to Figure 5.5-2B to D as well.

In Figure 5.5-3A anisotropy increases with decreasing mean macropore diameter. When the mean macropore diameter reaches ≤ 1 mm there is a rapid change in anisotropy for all treatments, except MT and STWS where the rapid change in anisotropy starts at diameters ≤ 0.6 mm. Despite the great scatter a tillage effect can be seen in the silt loam treatments (Fig. 5.5-3B). In the silty clay loam treatments (Fig. 5.5-3C) there is also scatter, but the course of the data points is more clearly defined (S-shaped). However, it is difficult to discern a tillage effect. The same holds true for Figure 5.5-3D and E with respect to a texture response. Here, though, the paths are not S-shaped.
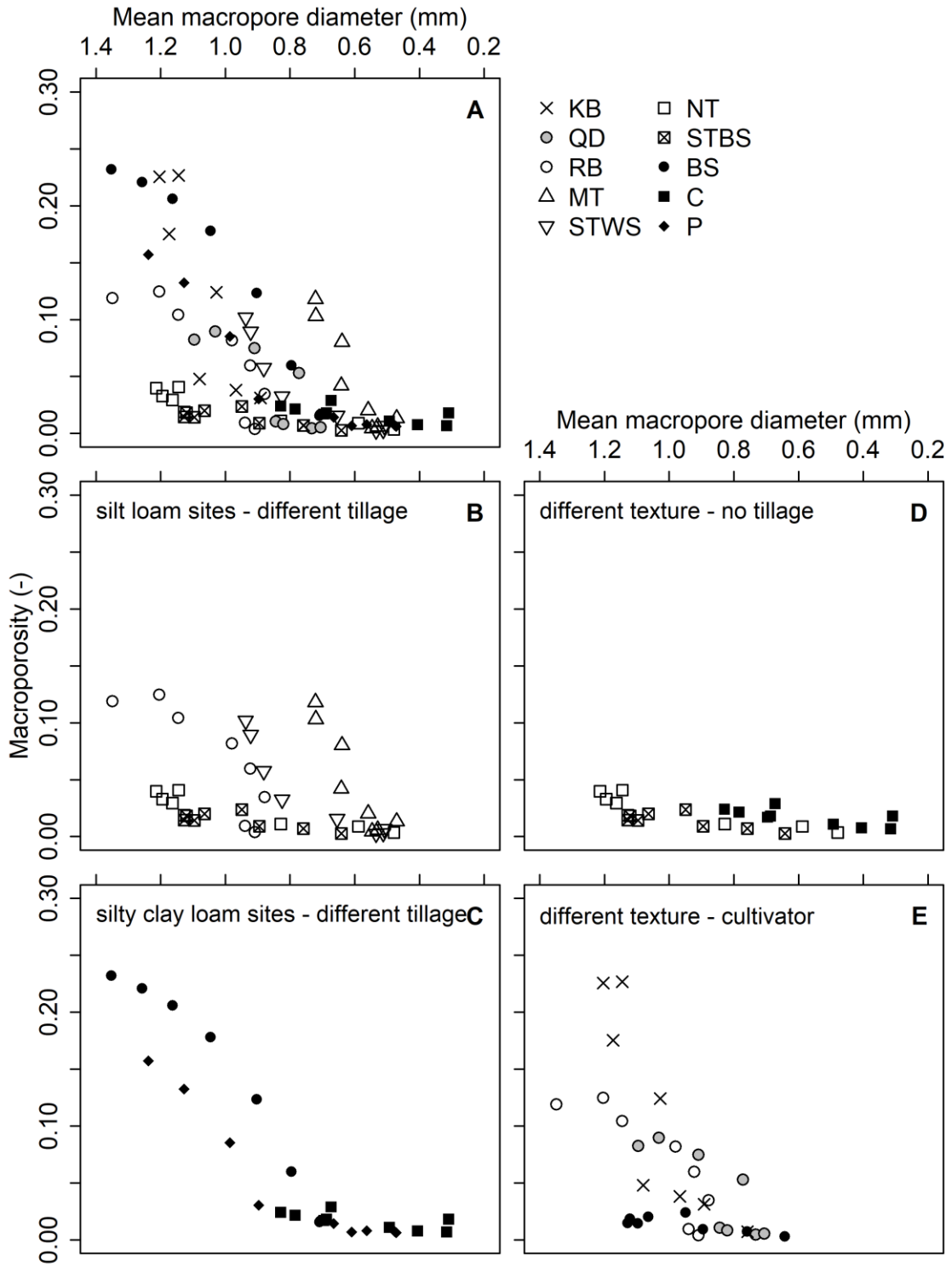
Figure 5.5-1: Cross-correlations between mean macropore diameter and macroporosity for samples from all three trials (A), for treatments with the same texture but a different tillage system (B, C), and for treatments with the same tillage system but different texture (D, E). The abbreviations are explained in Figure 5.4-1.
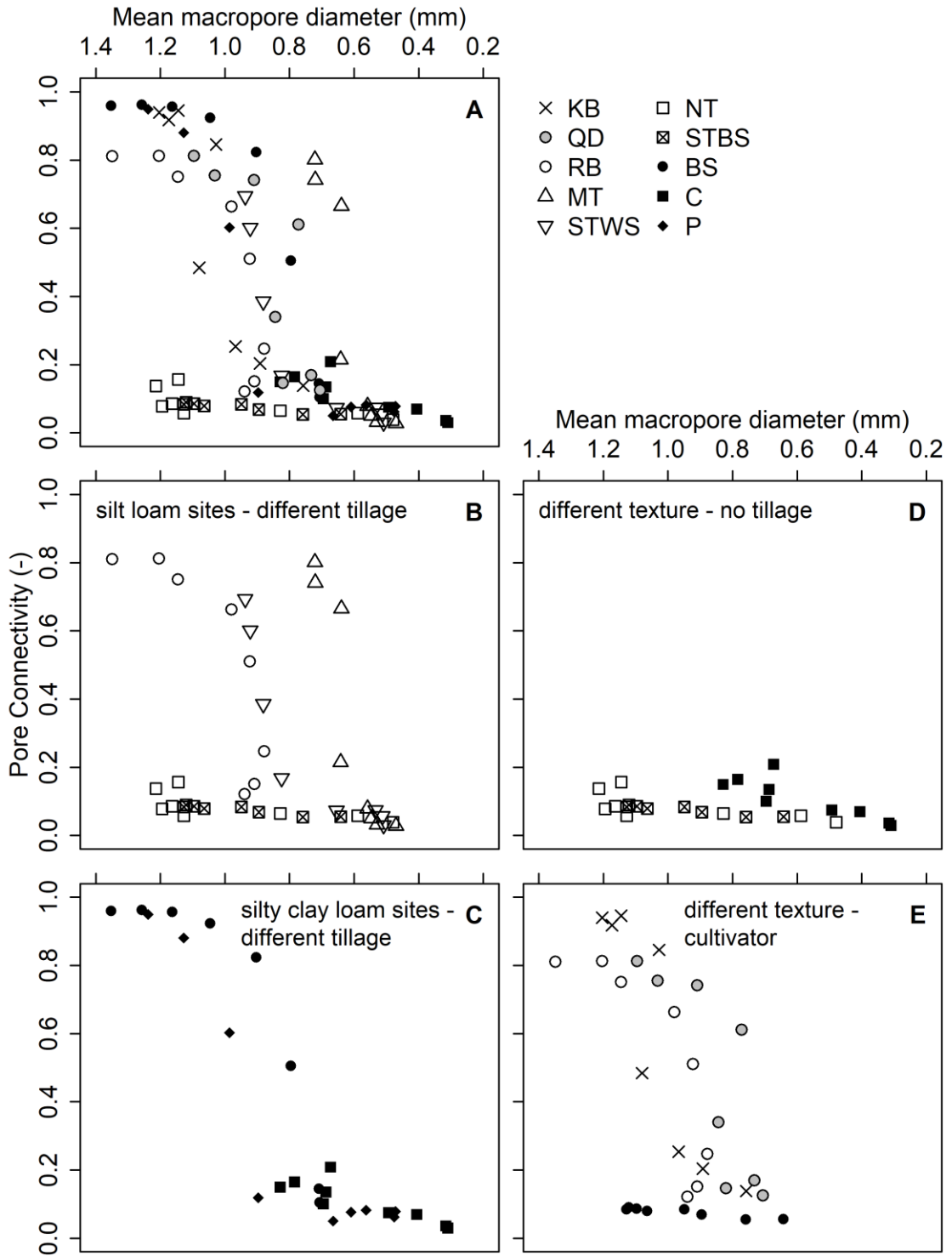
Figure 5.5-2: Cross-correlations between mean macropore diameter and pore connectivity for samples from all three trials (A), for treatments with the same texture but a different tillage system (B, C), and for treatments with the same tillage system but different texture (D, E). The abbreviations are explained in Figure 5.4-1.
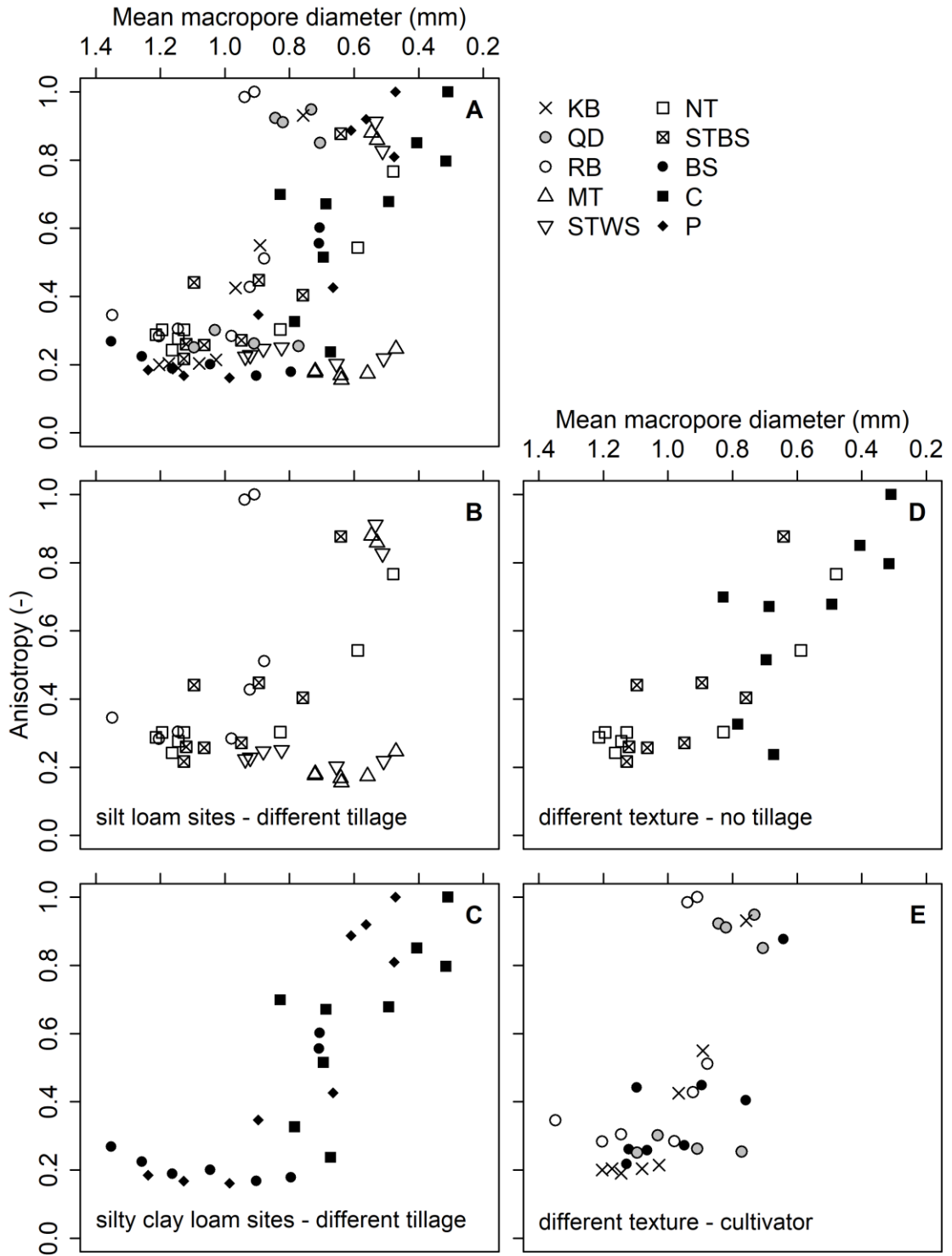
Figure 5.5-3: Cross-correlations between mean macropore diameter and anisotropy for samples from all three trials (A), for treatments with the same texture but a different tillage system (B, C), and for treatments with the same tillage system but different texture (D, E). The abbreviations are explained in Figure 5.4-1.

In summary, Figures 5.5-1 to 5.5-3 show many different courses and quite some scatter for the cross correlations involving mean macropore size.

The most striking relationship appears in Figure 5.5-4A. Here pore connectivity decreases with decreasing macroporosity in a treshold function. Almost all treatments follow the same course. The only one that differs slightly is QD. This is curious, because in the other data here it is usually KB which deviates, due to the high OM contents. The replotted Figures 5.5-4B to D reflect the same picture, which implies that this relationship seems to be influenced neither by tillage nor by texture.

This extraordinary connection means that for a given macroporosity value there is one corresponding pore connectivity and vice versa. Referring back to trial 3, there is no literature value for the critical stress values for pore connectivity, but there is one for macroporosity (8%). The above correlation could be used to derive one for pore connectivity based on the 8% macroporosity. This value would be around 0.65 and could be listed as a first literature value for pore connectivity at which restrictions may appear due to soil compaction.

Figure 5.5-5 and 5.5-6 look very similar. Therefore, the same statements can be made. At first anisotropy remains fairly constant as macroporosity or pore connectivity decrease, until a macroporosity of ~0.05 and a pore connectivity ~0.20 is reached. Thereafter follows a steep rise in anisotropy (Fig. 5.5-5A and 5.5-6A). The data show a pretty similar course, only RB and KB are responsible for some greater diversions. The treatments with the silt loam texture do not all show the same course. This is due to tillage (Fig. 5.5-5B and 5.5-6B). On the other hand, Figures 5.5-5C and 5.5-6C depict a single relationship with almost no scatter for the silty clay loam texture, i.e. no tillage dependence. In Figure 5.5-5D and 5.5-6D the data points are close to each other, which suggests that texture has only little or no effect in the no tillage treatments. In contrast, in Figure 5.5-5E and 5.5-6E the deviations for the different textures are larger and indicate a texture dependence.

Overall, it was possible to show that the differences between all shown relationships between the CT parameters are due to the tillage system and soil texture, with the former usually having a more pronounced influence than the latter.

Figure 5.5-4: Cross-correlations between macroporosity and pore connectivity for samples from all three trials (A), for treatments with the same texture but a different tillage system (B, C), and for treatments with the same tillage system but different texture (D, E). The abbreviations are explained in Figure 5.4-1.
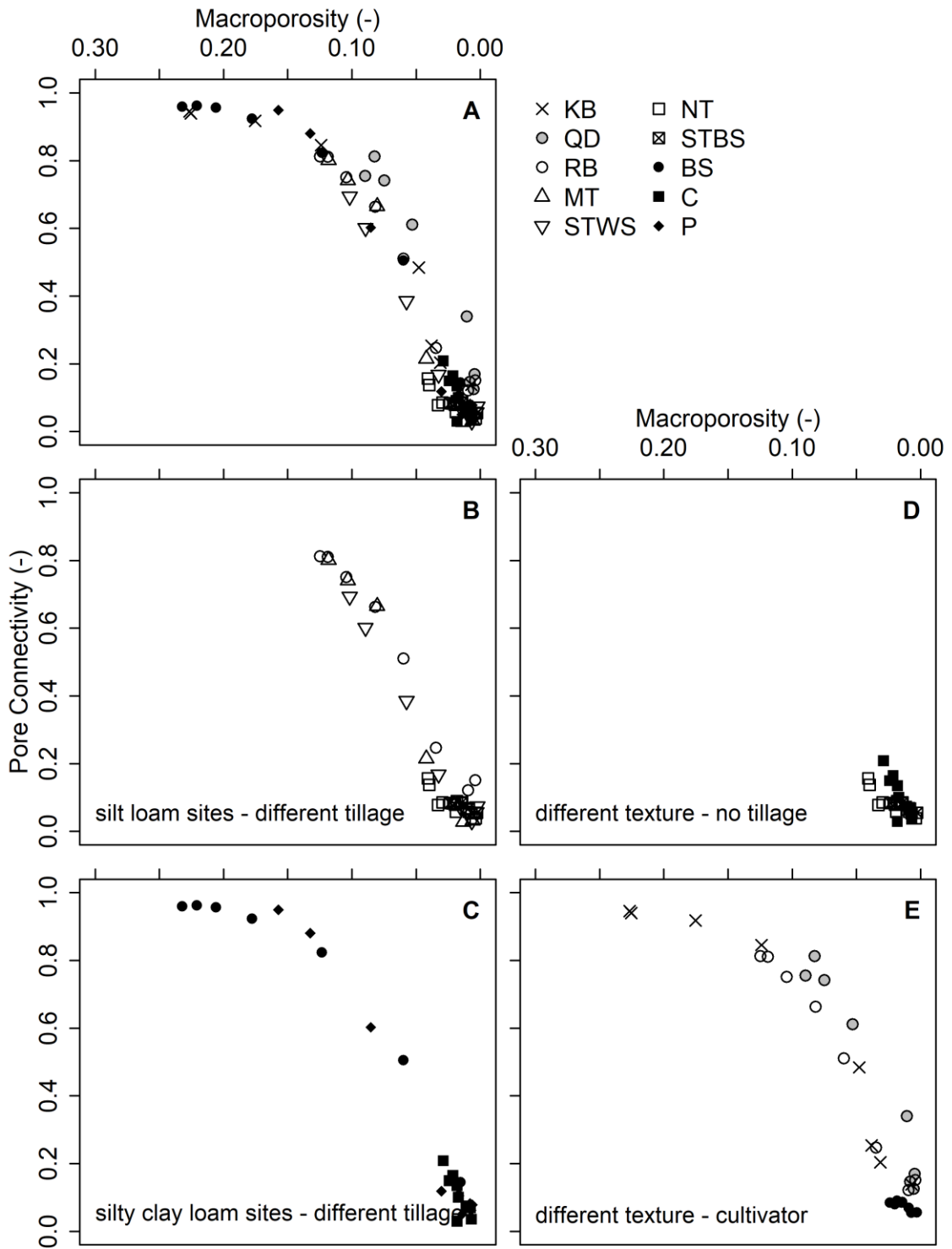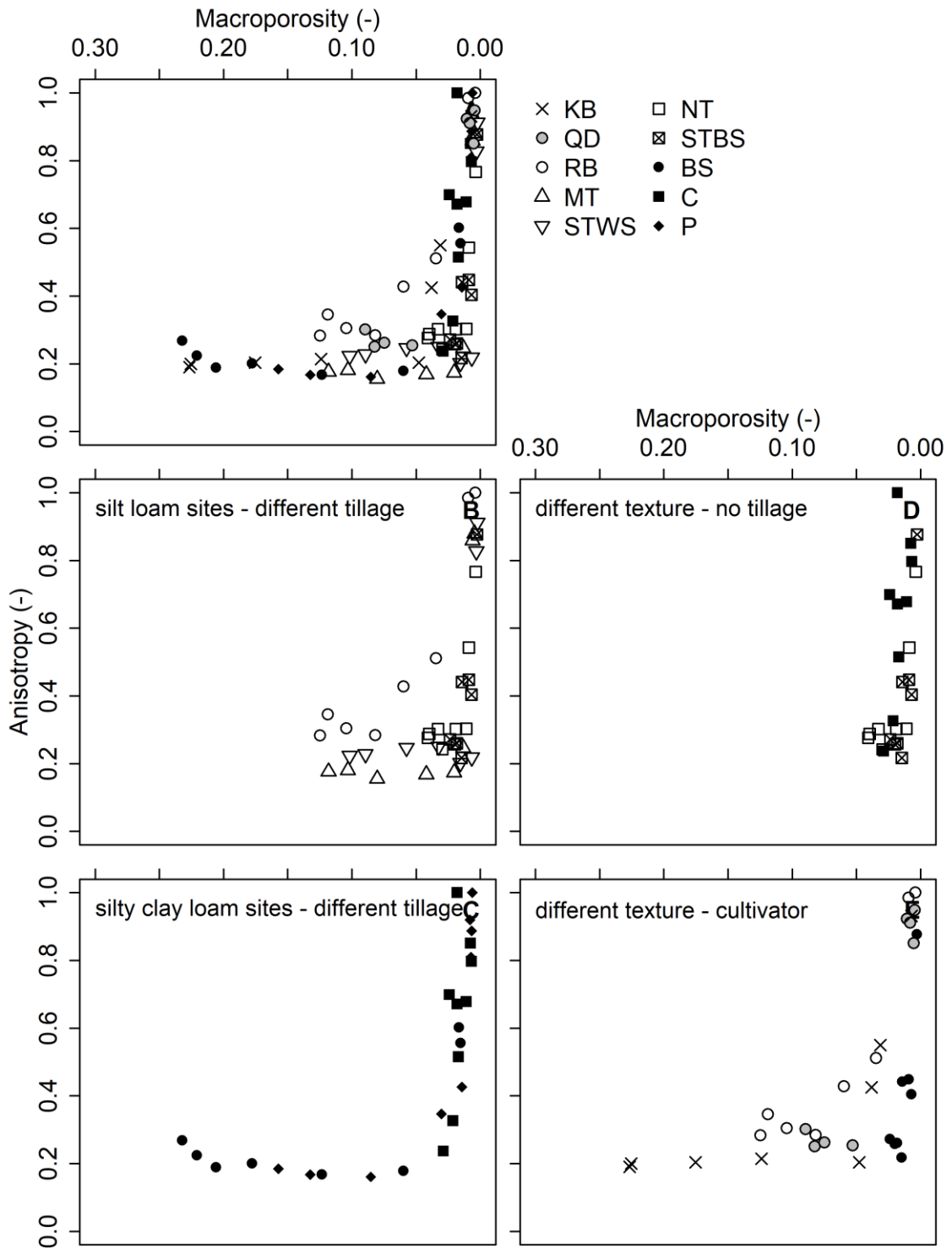
Figure 5.5-5: Cross-correlations between macroporosity and anisotropy for samples from all three trials (A), for treatments with the same texture but a different tillage system (B, C), and for treatments with the same tillage system but different texture (D, E). The abbreviations are explained in Figure 5.4-1.
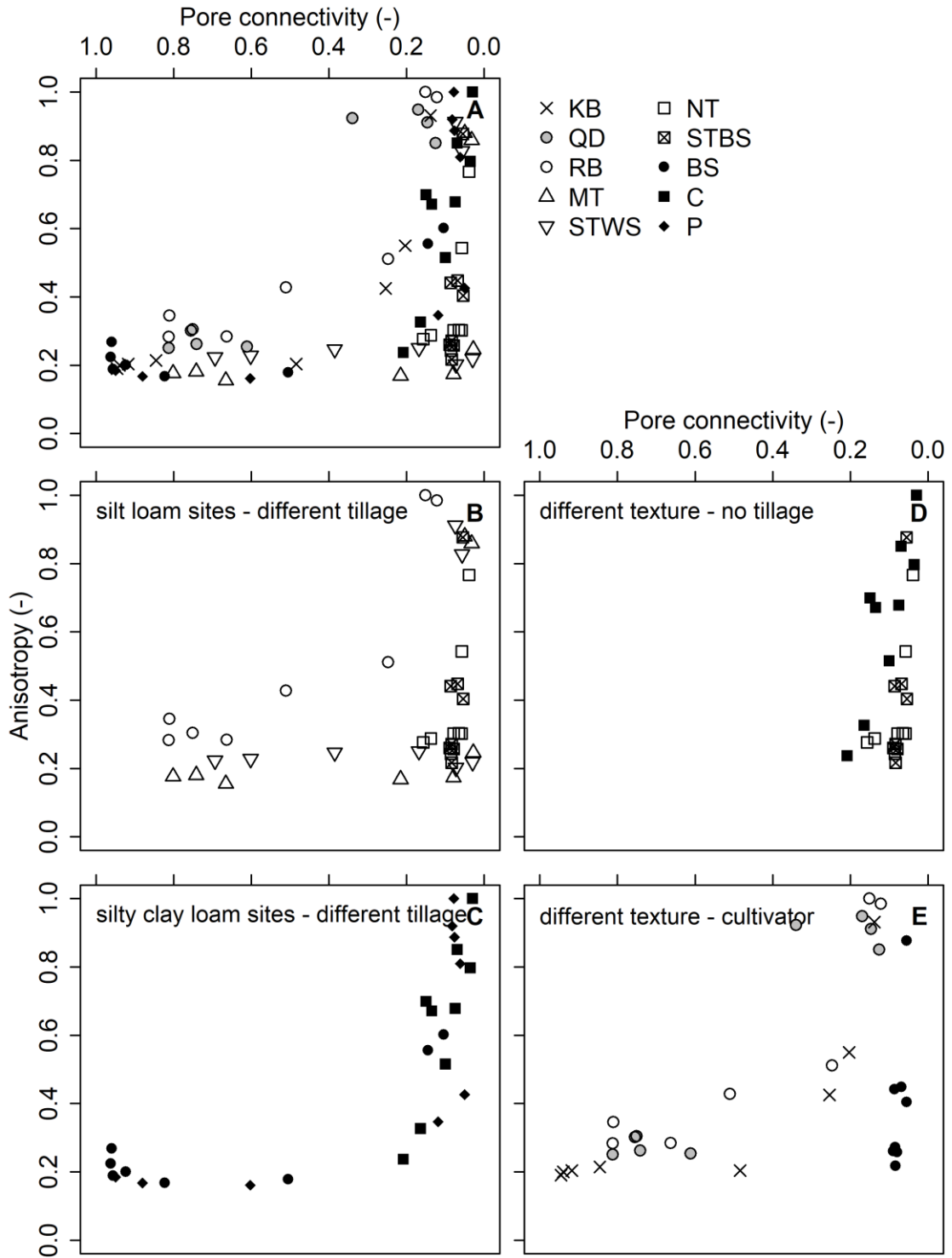
Figure 5.5-6: Cross-correlations between pore connectivity and anisotropy for samples from all three trials (A), for treatments with the same texture but a different tillage system (B, C), and for treatments with the same tillage system but different texture (D, E). The abbreviations are explained in Figure 5.4-1.

6. Conclusions

Trial 1 revealed that there can be clear differences in the initial structure and compaction behaviour due to different tillage treatments. In addition to higher mechanical precompression stress values strip tillage BS and no tillage also showed higher BD_{xi} and AD values than strip tillage WS and mulch tillage throughout almost the entire load range. The morphometric parameters obtained from CT scans also confirmed the mechanically more stable soil structure under strip tillage BS and no tillage. They revealed higher mean macropore diameters and lower macroporosity and pore connectivity values compared to strip tillage WS and mulch tillage. In all tillage treatments stress application resulted in a decrease in mean macropore diameter, macroporosity and pore connectivity, and an increase in anisotropy.

From an agronomic point of view the most important result from trial 1 is that it illustrated that strip tillage combines the advantages of no tillage with those of deeper non-turning primary tillage. Between the seed rows it is similar to no tillage and preserves an undisturbed and therefore stable soil structure. In addition, it leaves plant residues on the surface, which reduces evaporation and enhances soil tilth. Within the seed row the soil is loosend, which provides good conditions for crop establishment. Strip tillage thus offers farmers an advantageous soil structure which is capable of sufficiently withstanding mechanical stresses in the areas between seed rows which are driven over and, at the same time, allows optimal conditions for plant growth in the seed rows.

Trial 2 demonstrated that, if tillage was carried out with a plough, a more negative matric potential was clearly beneficial to the mechanical stability of a soil. In already dense soil structures, as in the cultivator treatment here, it was less effective. Furthermore, it was shown that ploughing has only a temporary positive effect on soil structure which persists merely as long as macroporosity and the mean macropore diameter remain high. Lastly, aggregates were found to have a much larger recompression range than the soil as a whole.

Trial 3 showed that macroporosity usually had a greater critical stress value than pore connectivity, because with increasing load the pores are first reduced in diameter, but can still be connected. The agronomic parameters grain and straw yield mostly occurred at the lower limit of the critical stress ranges and were therefore the most sensitive parameters. Nothing can be generalized about the number of biopores (earthworm activity). The critical stress ranges were different between the sites for all parameters, due to differences in the pore space. Although the soil textures at the four sites were quite different, the medians of the critical stress ranges were similar and concurred with the values of the mechanical precompression stresses which were similar at all four sites, too. Hence, the mechanical

precompression stress turns out to be well suited as a measure of the critical stress values and the critical stress ranges.

This trial did not find a dependence on texture of the critical stress value for various parameters, or the critical stress range defined by these critical stress values for a soil. This means that studies which recommend maximum values for mechanical loads to prevent harmful soil compaction solely on the basis of texture should be treated with caution.

All three trials proved that the morphometric parameters obtained with CT provide valuable additional information about the effect of mechanical stresses on the soil structure created by different tillage methods (or other external effects such as soil moisture tension). Classic soil physical methods and CT usefully complement each other. Hence, combining them greatly improves the understanding of the effects of different tillage methods on soil functions. With CT it is possible to make the structure in a soil sample visible, which can otherwise only be inferred from BD. Hence, the addition of CT parameters provides a more definite picture of compaction effects.

In addition, all three trials established that the classic soil mechanical parameters are closely related to the CT parameters. However, the course of the relationships is influenced by the tillage treatment, texture and soil moisture tension. On the whole the effect of tillage is greater than that of texture. Due to these two effects there are, for example, several different values for macroporosity for the same dry bulk density and vice versa. This implies that neither classic soil physical parameters alone, nor CT parameters alone provide a complete picture of soil compaction. To illustrate this consider the following: Mean macropore diameter, macroporosity, pore connectivity and anisotropy which are determined with CT control the hydraulic conductivity of a soil. Dry bulk density is a classic soil physical parameter which affects the shear stress faced by growing roots or burrowing earthworms. For a given BD there can be different values of the four CT parameters and vice versa. This means two soils with the same BD can have different hydraulic conductivities. Hence, based on BD alone nothing definite can be said about hydraulic conductivity. On the other hand, two soils with the same CT parameters can have different bulk densities so that based on CT parameters alone nothing definite can be said about shear stress. Consequently, a combination of classic and CT method allows a more complete analysis of the structural status of a soil.

Furthermore, the CT parameters were all related to each other, but the relationships were quite different in the various treatments, with one execption which will be discussed shortly. These differences were again due to the different tillage treatments and soil textures, with the former generally having the more pronounced effect.

In the relationship between macroporosity and pore connectivity there is no tillage or texture dependence. The data for all treatments follow the same course. Based on a macroporosity of 8 %, which is considered to be the minimum for an intact soil structure, this makes it possible to define a limiting value for pore connectivity of about 0.65, for which no threshold value was defined in the literature so far.

7. Outlook

More soils of different texture should be subjected to more tillage treatments to have more than just silt loam and silty clay loam soils with different tillage treatments, and more than just no tillage and cultivator applied to several soil textures.

The column experiments should be carried out with different crops to check, how the critical stress ranges change.

It would also be interesting to investigate, whether the unique correlation between macroporosity and pore connenctivity remains, if data for different soil moisture tensions are included. The few data from trial 2 for a different tension fall a bit outside of this course, but not a great deal.

It is necessary to determine the mechanical precompression stress of aggregates on more than one soil to assess, whether aggregates really have a virgin compression and a recompression line.

In all the studies proposed above the same classic and CT parameters as in this thesis should be determined. In addition, the CT parameters could be extended, for example by determining the tortuosity as an important criterion for the K_s value.

The K_s value itself should be measured repeatedly under different tillage systems and in connection with the CT parameters at different times of the year to find out, how the sampling time or tillage operations influence the values.

References

Alexandrou, A., Earl, R., 1998. The relationship among the pre-compaction stress, volumetric water content and initial dry bulk density of soil. J. Agric. Eng. Res. 71, 75-80.

Amin, M., Khan, M.J., Jan, M.T., Rehmann, M., Tariq, J.A., Hanif, M., Shah, Z., 2014. Effect of different tillage practices on soil physical properties under wheat in semi-arid environment. Soil Environ. 33, 33-37.

Anderson, S.H., Gantzer, C.J., Boone, J.M., Tully, R.J., 1988. Rapid nondestructive dry bulk density and soil-water content determination by computed tomography. Soil Sci. Soc. Am. J. 52, 35-40.

Beisecker, R., 1994. Einfluss langjährig unterschiedlicher Bodenbearbeitungssysteme auf das Bodengefüge, die Wasserinfiltration und die Stoffverlagerung eines Löß- und eines Sandbodens. Bodenökologie und Bodengenese 12.

Benjamin, J.G., 1993. Tillage effects on near-surface soil hydraulic properties. Soil Till. Res. 26, 277-288.

Berli, M., Kirby, J., Springman, S., Schulin, R.. 2003. Modelling compaction of agricultural subsoils by tracked heavy construction machinery under various moisture conditions in Switzerland. Soil Till. Res. 73, 57–66.

Blake, G.R., Hartge, K.H., 1986. Dry bulk density. In: Klute, A. (Ed.), Methods of soil analysis. Part 1: Physical and mineralogical methods, 2nd edition. American Society of Agronomy Monograph No. 28, Madison, Wisconsin, USA, pp. 363–382.

Bradford, J.M., Gupta, S.C., 1986. Compressibility. In: Klute, A. (Ed.), Methods of soil analysis. Part 1: Physical and mineralogical methods, 2nd edition. American Society of Agronomy Monograph No. 28, Madison, Wisconsin, USA, pp. 479–492.

Brown, J.M., Fonteno, W.C., Cassel, D.K., Johnson, G.A., 1987. Computed tomographic analyses of water distribution in three porous foam media. Soil Sci. Soc. Am. J. 51, 1121-1125.

Buades, A., Coll, B., Morel, J.M., 2005. A review of image denoising algorithms, with a new one. Multiscale Model. Simul. 4, 490-530.

Bullock, P., Newman, A.C.D., Thomasson, A.J., 1985. Porosity aspects of the regeneration of soil structure after compaction. Soil Till. Res. 5, 325-341.

Burmister, D., 1951. The application of controlled test methods in consolidation testing. ASTM Spec. Tec. Pub. 126, pp. 83-98.

Carter, M. R., 1986. Microbial biomass as an index for tillage-induced changes in soil biological properties. Soil Till. Res. 7, 29-40.

Carter, M. R., 1988. Penetration resistance to characterize the depth and persistence of soil loosening in tillage studies. Can. J. Soil Sci. 68, 657–668.

Carter, M.R., 2004. Researching structural complexity in agricultural soils. Soil Till. Res. 79, 1-6.

Carter, M.R., 2006. Quality: Critical limits and standardization. In: Lal, R. (Ed.), Encyclopedia of soil science, 2nd edition. Taylor and Francis, New York: Marcel Dekker pp. 1412–1415.

Casagrande, A. 1936. The determination of the pre-consolidation load and its practical significance. Proceedings of the International Conference on Soil Mechanics and Foundation Engineering, Vol. III, pp. 60–64. Harvard University, Cambridge, Massachussets, USA.

Cruse, R.M., Larson, W.E., 1977. Effect of soil shear strength on soil detachment due to raindrop impact. Soil Sci Soc Am J. 41, 777–781.

Culley, J.L.B., Larson, W.E., Randall, G.W., 1987. Physical properties of a typic haplaquoll under conventional and no-tillage. Soil Sci. Soc. Am. J. 51, 1587–1593.

Czyz, E. A., 2004. Effects of traffic on soil aeration, dry bulk density and growth of spring barley. Soil Till. Res. 79, 153–166.

Czyz, E. A., Tomaszewska, J., Dexter, A. R., 2001. Response of spring barley to changes of compaction and aeration of sandy soil under model conditions. Int. Agrophysics 15, 9–12.

Daddow, R.L., Warrington, G.E., 1983. Growth-limiting soil bulk densies as influenced by soil texture. WSDG Report TN-00005. USDA Forest Service, Watershed Systems Development Group, Fort Collins, Colorado, USA.

Dal Ferro, N., Sartori, L., Simonetti, G., Berti, A., Morari, F., 2014. Soil macro- and microstructure as affected by different tillage systems and their effects on maize root growth. Soil Till. Res. 140, 55–65.

Dewry, J.J., Cameron, K.C., Buchan, G.D., 2008. Pasture yield and soil physical property responses to soil compaction from treading and grazing – a review. Aust. J. Soil Res. 46, 237–256.

Dexter, A. R., 1988. Advances in characterization of soil structure. Soil Till. Res. 11, 199-238.

Dias Junior, F., Pierce, F.J., 1995. A simple procedure for estimating preconsolidation pressure from soil compression curves. Soil Tech. 8, 139–151.

Diserens, E., 2009. Calculating the contact area of trailer tyres in the field. Soil Till. Res. 103, 302–309.

Doube, M., Klosowski, M.M., Arganda-Carreras, I., Cordelieres, F., Dougherty, R.P., Jackson, J., Schmid, B., Hutchinson, J.R., Shefelbine, S.J., 2010. BoneJ: free and extensible bone image analysis in ImageJ. Bone 47, 1076–1079.

Drees, T., Karathanasis, A.D., Wilding, L.B., Belvins, R.L., 1994. Micromorphological characteristic of long-term no-tillage and conventionally tilled soils. Soil Sci. Soc. Am. J. 58, 508–517.

Dürr, H.-J., Petelkau, H., Sommer, C., 1995. Literaturstudie "Bodenverdichtung". Umweltbundesamt, Berlin.

DVWK, 1995. Gefügestabilität ackerbaulich genutzter Mineralböden, Teil 1: Mechanische Belastbarkeit. DVWK-Merkblatt 234.

DVWK, 1997. Bodenphysikalische Untersuchung über Ursachen und Auswirkungen von Bodenverdichtungen. DVWK-Materialien 1.

DVWK, 1997. Gefügestabilität ackerbaulich genutzter Mineralböden, Teil 2: Auflastabhängige Veränderung von bodenphysikalischen Kennwerten. DVWK Merkblatt 235.

Estler, M., Knittel, H., 1996. Praktische Bodenbearbeitung: Grundlagen, Gerätetechnik, Verfahren, Bewertung, 2. Auflage. DLG, Frankfurt.

FAO, 1993. Soil tillage in Africa: needs and challenges. FAO Soils Bulletin No. 69. FAO, Rome, Italy.

FAO, 1998. World Reference Base for Soil Resources. ISSS–ISRIC–FAO. World Soil Resources Report No. 84, Rome, Italy.

Fazekas, O., Horn, R., 2005. Zusammenhang zwischen hydraulischer und mechanischer Bodenstabilität in Abhängigkeit von der Belastungsdauer. J. Plant Nutr. Soil Sci. 168, 60-67.

Ferreira, T., Rasband, W.S., 2010-2012. "ImageJ user guide - IJ 1.46", im-agej.nih.gov/ij/docs/guide/

Gantzer, C.J., Anderson, S.H., 2002. Computed tomographic measurement of macroporosity in chisel-disk and no-tillage seedbeds. Soil Till. Res. 64, 101–111.

Gardner, W.H., 1986. Water content. In: Klute, A. (Ed.), Methods of soil analysis. Part 1: Physical and mineralogical methods, 2nd edition. American Society of Agronomy Monograph No. 28, Madison, Wisconsin, USA, pp. 493-544.

Gee, G.W., J.W. Bauder. 1986. Particle-size analysis. In: Klute, A. (Ed.), Methods of soil analysis. Part 1: Physical and mineralogical methods, 2nd edition. American Society of Agronomy Monograph No. 28, Madison, Wisconsin, USA, pp. 383–411.

Glinski, J., Lipiec, J., 1990. Soil physical conditions and plant roots. CRC Press, Boca Raton.

Greenland, D.J., 1981. Soil management and soil degradation. J. Soil Sci. 32, 301–322.

Håkansson, I., 1988. A method for characterizing the state of compactness of an arable soil. Catena Suppl. 11, 101–105.

Håkansson, I., 1989. Compaction of the plough layer-which degree of compactness is the best? Swedisch Univ. Agric. Sci., Uppsala. Fakta/mark-växter 1, 4.

Håkansson, 1990. A method for characterizing the state of compactness of the plough layer. Soil Till. Res. 16, 105–120.

Håkansson, I., Lipiec, J., 2000. A Review of the usefulness of relative dry bulk density values in studies of soil structure and compaction. Soil Till. Res., 53, 71–85.

Hamza, M. A., Anderson, W. K., 2005. Soil compaction in cropping systems: A review of the nature, causes, and possible solutions. Soil Till. Res. 82, 12-145.

Hartge, K.H., Bohne, H., 1983. Der Einfluss der Gefügegeometrie auf die Verdichtbarkeit des Bodens und auf die Keimung von Roggen. Z. f. Kulturtechnik und Flurbereinigung 24, 5-10.

Hartge, K.H., Horn, R., 1991. Einführung in die Bodenphysik, 2. Auflage. Enke, Stuttgart.

Horn, R., 1981. Die Bedeutung der Aggregierung von Böden für die mechanische Belastbarkeit in dem für Tritt relevanten Auflastbereich und deren Auswirkungen auf physikalische Bodenkenngrößen. Schriftenreihe des Fachbereichs 14 der TU Berlin.

Horn, R., 1999. Verdichtung von Böden – Überlegungen zum Prozess und zur Prognose der mechanischen Belastbarkeit. Wasser und Boden 51, 9–13.

Horn, R., Peth, S., 2011. Stress - strain relationships: A possibility to quantify soil strength defined as the precompression stress. In: Gliński, J., Horabik, J., and J. Lipiec, J. (Eds.), Encyclopedia of agrophysics. Springer, New York.

Horn, R., Grade, W., Kühner, S., 1996. Einige theoretische Überlegungen zur Spannungs- und Deformationsmessung in Boden und ihre meßtechnische Realisierung. Z. Pflanzenernähr. Bodenk. 159, 137-142.

Hubbard, R.K., Hargrove, W.L., Lowrande, R.R., Williams, R.G., Mullinix, B.G., 1994. Physical properties of a clayey coastal plain soil as affected by tillage. J. Soil Water Conserv. 49, 276–283.

Iler G.S., Stevenson C.K., 1991. The effects of soil compaction on the production of processing vegetables and field crops. A review. Ridgetown College of Agricultural Technology, Ontario.

Imhoff, S., Da Saliva, A.P., Fallow, D., 2004. Succeptibility to compaction, load support capacity and soil compressibility of a hapludox. Soil Sci. Soc. Am. J. 68, 17-24.

Ishaq., M., Hassan, A., Saeed, M., Ibrahim, M., Lal, R., 2001a. Subsoil compaction on crops in Punjab, Pakistan. I. Soil physical properties and crop yield. Soil Till. Res. 59, 57–65.

Ishaq, M., Ibrahim, M., Hassan, A., Saeed, M., Lal, R., 2001b. Subsoil compaction effects on crops in Punjab, Pakistan: II. Root growth and nutrient uptake of wheat and sorghum. Soil Till. Res. 60, 153–161.

Jarvis, N., Larsbo, M., Koetsel, J., 2017. Connectivity and percolation of structural pore networks in a cultivated silt loam soil quantified by X-ray tomography. Geoderma 287, 71–79.

Jegou, D., Cluzeau, D., Wolf, H. J., Gandon, Y., Trehen, P., 1998. Assessment of the burrow system of *Lumbricus terrestris*, *Aporrectodea giardi*, and *Aporrectodea caliginosa* using X-ray computed tomography. Biol. Fertil. Soils 26, 116–121.

Joschko, M., Diestel, H., Larink, O., 1989. Assessment of earthworm burrowing efficiency in compacted soil with a combination of morphological and soil physical measurements. Biol. Fert. Soils 8, 191–196.

Jose, B.T., Sridharan, A., Abraham, B.M., 1989. Log-log method for determination of preconsolidation pressure. Geotech. Testing J. 12, 230–237.

Kaufmann, M., Tobias, S., Schulin, R., 2010. Comparison of critical limits for crop plant growth based on different indicators for the state of soil compaction. J. Plant Nutr. Soil Sci. 173, 573–583.

Kay, B.D., Angers, D.A., 1999. Structure. In: Sumner, M.E. (Ed.), Handbook of soil science, pp. A229-A276.

Kay, B.D., VandenBygaart, A.J., 2002. Conservation tillage and depth stratification of porosity and soil organic matter. Soil Till. Res., 66, 107–118.

Keller, T., Lamand, M., Peth, S., Berli, M., Delenne, J.-Y., Baumgarten, W., Rabbel, W., Radja, F., Rajchenbach, J., Selvadurai, A., Or, D., 2013. An interdisciplinary approach towards improved understanding of soil deformation during compaction. Soil Till. Res. 128, 61–80.

Kemper, W.D., Jolley, P., Roseneau, R.C., 1988. Soil management to prevent earthworms from riddling irrigation ditch banks. Irrig. Sci. 9, 79–87.

Ketcham, R.A., Carlson, W.D., 2001. Acquisition, optimization and interpretation of X-ray computed tomographic imagery: Applications to the geosciences. Comput. Geosci. 27, 381-400.

Kezdi, A., 1969. Handbuch der Bodenmechanik. Band I: Bodenphysik. Verlag für Bauwesen, Berlin.

Khan, F.-U.-H., Tahir, A.R., Yule, I.J., 1999. Impact of different tillage practices and temporal factors on soil moisture content and soil dry bulk density. Int. J. Agric. Biol. 3, 163-166.

Klute, A., 1986. Water Retention: Laboratory Methods. In: Klute, A. (Ed.), Methods of soil analysis. Part 1: Physical and mineralogical methods, 2nd edition. American Society of Agronomy Monograph No. 28, Madison, Wisconsin, USA, pp. 635–662.

Klute, A., Dirksen, C., 1986. Hydraulic Conductivity and Diffusivity: Laboratory Methods. In: Klute, A. (Ed.), Methods of soil analysis. Part 1: Physical and mineralogical methods, 2nd edition. American Society of Agronomy Monograph No. 28, Madison, Wisconsin, USA, pp. 687–734.

Koblenz, B., Umann, M., Wensch-Dorendorf, M., Rücknagel, J., Christen, O., 2016. Impact of different tillage systems on root growth and earthworm population in maize. Proceedings of the 14th European Society of Agronomy Conference, Edinburgh, Scotland, pp. 49–50.

Koch, H.J., Heuer, H., Tomanova, O., Märländer, B., 2008. Cumulative effect of annually repeated passes of heavy agricultural machinery on soil structural properties and sugar beet yield under two tillage systems. Soil Till. Res. 101, 69–77.

Koenigs, F.F.R., 1981. Bestimmung des Aggregatvolumens nach Vorsättigung mit Petroleum mittels der Reaktionskraft des Auftriebs in Petroleum. Mitteilgn. Dtsch. Bodenkundl. Gesellsch. 32, 39-42.

Koolen, A.J., Kuipers, H., 1983. Agricultural soil mechanics. Springer, New York.

Krümmelbein, J., Peth, S., Horn, R., 2008. Determination of pre-compression stress of a variously grazed steppe soil under static and cyclic loading. Soil Till. Res. 99, 139-148.

KTBL, 1993. Definition und Einordnung von Verfahren der Bodenbearbeitung und Bestellung. KTBL Arbeitsblatt 236. KTBL.

Kühner, S., 1997. Simultane Messung von Spannungen und Bodenbewegungen bei statischen und dynamischen Belastungen zur Abschätzung der dadurch induzierten Bodenbeanspruchung. Schriftenreihe des Instituts für Pflanzenernährung und Bodenkunde der Universität Kiel, Nr. 39.

Lal, R., 1983. No-tillage farming: Soil and water conservation and management in the humid and sub-humid tropics. IITA Monograph No. 2, Ibadan, Nigeria.

Larson, W.E., Allmaras, R.R., 1971. Management factors and natural forces as related to compaction. In: Barnes, K.K., Carleton, W.M. (Eds.), Compaction of agricultural soils. Am. Soc. Agric. Eng., St. Joseph, Michigan, USA, pp. 368–427.

Lebert, M., 1989. Beurteilung und Vorhersage der mechanischen Belastbarkeit von Ackerböden. Bayreuther bodenkundliche Berichte 12.

Lebert, M., Horn, R., 1991. A method to predict the mechanical strength of agricultural soils. Soil Till. Res. 19, 275–286.

Lehfeldt, J., 1988. Auswirkungen von Krumenbasisverdichtungen auf die Durchwurzelbarkeit sandiger und lehmiger Bodensubstrate bei Anbau verschiedener. Arch. Acker-Pflanzenb. Bodenk. 32, 533–539.

Lemitri, A., Gilles, C., Alabi, T., Cluzeau, D., Zirbes, I., Haubruge, E., Franics, F., 2014. Impacts of earthworms on soil components and dynamics. A review. Biotechnol. Agron. Soc. Environ. 18, 121–133.

Licht, M.A., Al-Kaisi, M., 2005. Strip-tillage effect on seedbed soil temperature and other soil physical properties. Soil Till. Res. 80, 233–249.

Lindstrom, M.J., Onstad, C.A., 1984. Influence of tillage systems on soil physical parameters and infiltration after planting. J. Soil Water Conserv. 39, 149-152.

Lipiec, J., Simota, C., 1994. Role of soil and climate factors in influencing crop responses to soil compaction in central and eastern Europe. Developm.Agric. Eng. 11, 365–390.

Lipiec, J., Hatano, R., 2003. Quantification of compaction effects on soil physical properties and crop growth. Geoderma 116, 107–136.

Lipiec, J., Tarkiewicz, S., Kossowski, J., Håkansson, I., 1991. Soil physical properties and growth of spring barley related to the degree of compactness of two soils. Soil Till. Res. 19, 307–317.

Luo, L., Lin, H., Li, S., 2010. Quantification of 3-D soil macropore networks in different soil types and land uses using computed tomography. J. Hydrol. 393, 53–64.

Mackie-Dawson, L.A., Mullins, C.E., Goss, M.J., Court, M.N., Fritzpatrick, E.A., 1989. Seasonal changes in the structure of clay soils in relation to soil management and crop type. 11. Effects of cultivation and cropping at Compton Beauchamp. J. Soil Sci. 40,283-292.

Marshall, T.J ., Holmes, J.W., 1979. Soil physics. Cambridge University Press, Cambridge.

Mosaddeghi, M.R., Hemmat, A., Hajabbasi, M.A., Alexandrou, A., 2003. Pre-compression stress and its relation with the physical and mechanical properties of a structurally unstable soil in central Iran. Soil Till. Res. 70, 53-64.

Nichols, T.A., A.C. Bailey, C.E. Johnson, and R.D. Grisso. 1987. A stress state transducer for soil. Trans. ASAE 30, 1237-1241.

Nizami, M.I., Khan, M.I., 1990. Effects of tillage practices on soil physical characteristics and crop yield on three selected soil families. Pakistan J. Agric. Res. 11, 21-29.

Nowatzki, J., Endres, G., DeJong-Hughes, J., Aakre, D., 2009. Strip tillage for field crop production: Equipment, production, economics. North Dakota State University Extension Service. AE-1370, 1-8.

O´Connell, D.J., 1975. The measurement of apparent specific gravity of soils and its relationship to mechanical composition and plant root growth. In: Soil physical conditions and crop production. Ministry of Agriculture, Fisheries, and Food, Technical Bulletin 29. H.M. Stat. Off., London, pp. 298–313.

Otsu, N., 1979. A treshold selection method from gray-level histograms. IEEE Trans. Syst. Man, Cybern. B, Cybern. Vol. SMC-9, No. 1, 62-66.

Pagliai, M., 1988. Soil porosity aspects. Intern. Agrophysics, 4: 215-232.

Pagliai, M., Jones, R., 2002. Sustainable land management – environmental protection – a soil physical approach. Advances in Geo Ecology, 35, Catena, Reiskirchen.

Pagliai, M., Pellegrini, S., Vignozzi, N., Rousseva, S., Grasselli, O., 2000. The quantification of the effect of subsoil compaction on soil property and related physical properties under conventional to reduced management practices. Adv. Geoecol. 32, 305–313.

Perreault, J.M., Whalen, J.K., 2006. Earthworm burrowing in laboratory microcosms as influenced by soil temperature and moisture. Pedobiologia 50, 397–403.

Peth, S., Horn, R., 2011. Stress - strain relations. In: Gliński, J., Horabik, J., Lipiec, J. (Eds.), Encyclopedia of Agrophysics. Springer Science and Business Media, Dordrecht, pp. 862–67.

Peth, S., Nellesen, J., Fischer, G., Horn, R., 2010. Non-invasive 3D analysis of local soil deformation under mechanical and hydraulic stresses by µCT and digital image correlation. Soil Till. Res. 111, 3-18.

Pires, L.F., Borges, J.A.R., Bacchi, O.O.S., Reichardt, K., 2010. Twenty-five years of computed tomography in soil physics: A literature review. Soil Till. Res. 110, 197-210.

Pöhlitz, J., Rücknagel, J., Koblenz, B., Schlüter, S., Vogel, H.-J., Christen, O., 2018. Computed tomography and soil physical measurements of compaction behaviour under strip tillage, mulch tillage and no tillage. Soil Till. Res. 175, 205-216.

Rabot, E., Wiesmeier, M., Schlüter, S., Vogel, H.J., 2018. Soil structure as an indicator of soil functions: A review. Geoderma 314, 122-137.

Raghavan, G.S.V., Ohu, J.O., 1985. Prediction of equivalent pressure of Proctor compaction blows. Trans. ASAE 28, 1398–1400.

Rasband W.S., 1997 - 2015. ImageJ. U.S. National Institute of Health, Bethesda, Maryland, USA. http://imagej.nih.gov/ij/

Rashid, S., Sheikh, K.H., 1977. Response of wheat to different levels of soil compaction. Phyton 18, 43–56.

Renard, P., Allard, D., 2013. Connectivity metrics for subsurface flow and transport. Adv. Water Res. 51, 168-196.

Reynolds, W.D., Drury, C.F., Tan, C.S., Fox, C.A., Yang, X.M., 2009. Use of indicators and pore volume-function characteristics to quantify soil physical quality. Geoderma 152, 252–263.

Rücknagel, J., Hofmann, B., Paul, R., Christen, O., Hülsbergen, K., 2007. Estimating precompression stress of structured soils on the basis of aggregate density and dry bulk density. Soil Till. Res. 92, 213–220.

Rücknagel, J., Brandhuber, R., Hofmann, B., Lebert, M., Marschall, K., Paul, R., Stock, O., Christen, O., 2010. Variance of mechanical precompression stress in graphic estimations using the Casagrande method and derived mathematical models. Soil Till. Res. 106, 165–170.

Rücknagel, J., Rücknagel, S., Christen, O., 2012a. Impact on soil compaction of driving agricultural machinery over ground frozen near the surface. Cold Reg. Sci. Technol. 70, 113–116.

Rücknagel., J., Christen, O., Hofmann, B., Ulrich, S., 2012b. A simple model to estimate change in precompression stress as a function of water content on the basis of precompression stress at field capacity. Geoderma 177-178, 1-7.

Rücknagel, J., Götze, P., Hofmann, B., Christen, O., Marschall., K., 2013. The influence of soil gravel content on compaction behaviour and pre-compression stress. Geoderma 209-210, 226-232.

Rücknagel, J., Dumbeck, G., Harrach, T., Höhne, E., Christen, O., 2013. Visual structure assessment and mechanical soil properties of recultivated soils made up of loess. Soil Use Manag. 29, 271–278.

Rücknagel, J., Rademacher, A., Götze, P., Hofmann, B., Christen, O., 2017. Uniaxial compression behaviour and soil physical quality of topsoils under conventional and conservation tillage. Geoderma 286, 1–7.

Rütemann, B., 1996. Einfluß verschiedener Verfahrenstechniken auf die Bodenbelastung und Bodenverdichtung im Freilandgemüsebau. Gartenbautechnische Informationen 39, Universität Hannover, Institut für Technik in Gartenbau und Landwirtschaft.

Saffih-Hdadi, K., Defossez, P., Richard, G., Cui, Y.J., Tang, A.-M., Chaplain, V., 2009. A method for predicting soil susceptibility to the compaction of surface layers as a function of water content and dry bulk density. Soil Till. Res. 105, 96-103.

Saqib, M., Akhtar, J., Qureshi, R. H., 2004. Pot study on wheat growth in saline and waterlogged compacted soil. I. Grain yield and yield components. Soil Till. Res. 77, 169–177.

Schjonning, P., van den Akker, J.J.H., Keller, T., Greve, M.H., Lamande, M., Simojoki, A., Stettler, M., Arvidsson, J., Breuning-Madsen, H., 2015. Drive-Pressure-State-Impact-Response (DPSIR) analysis and risk assessment for soil compaction – a European perspective. Adv. Agr. 133, 183–237.

Schlüter, S., Vogel, H.-J., 2016a. Analysis of soil structure turnover with garnet particles and X-ray microtomography. PLOS ONE 17, 1-17.

Schlüter, S., Weller, U., Vogel, H.-J., 2011. Soil structure development including seasonal dynamics in a long-term fertilization experiment. J. Plant Nutr. Soil Sci. 174, 395–403.

Schlüter, S., Sheppard, A., Brown, K., Wildenschild, D., 2014. Image processing of multiphase images obtained via X-ray microtomography: A review. Water Resour. Res. 50, 3615-3639.

Schlüter, S., Leuther, F, Vogler, S., Vogel, H.-J., 2016b. X-ray microtomography analysis of soil structure deformation caused by centrifugation. Solid Earth 7, 129–140.

Schmertmann, J.H., 1955. The undisturbed consolidation behavior of clay. Trans. ASCE, 120, 1201–1233.

Schrader, S., Rogasik, H., Onasch, I., Jegou, D., 2007. Assessment of soil structural differentiation around earthworm burrows by means of X-ray computed tomography and scanning electron microscopy. Geoderma 137, 378–387.

Semmel, H., Horn, R., 1995. Möglichkeiten zur Bestimmung der mechanischen Belastung und der Druckfortpflanzung im Boden im Hinblick auf die Ableitung von bodentyp- und maschinenspezifischen Grenzwerten. In: Bodenverdichtung. KTBL Schrift 362, 41-59. KTBL-Schriften-Vertrieb: Münster-Hiltrup (Westfalen).

Shafiq, M., Hassan, A., Ahmad, S., 1994. Soil physical properties as influenced by induced compaction under laboratory and field conditions. Soil Till Res. 29, 13–22.

Shah, A. N., Tanveer, M., Shahzad, B., Yang, G., Fahad, S., Ali, S., Bukhari, M. A., Tung, S. A., Hafeez, A., Souliyanonh, B., 2017. Soil compaction effects on soil health and crop productivity: An overview. Environ. Sci. Pollut. Res. 24, 10056–10067.

Soil Science Society of America, 1996. Glossary of soil science terms. Madison, Wisconsin, USA, 134 pp.

Soil Survey Staff, 1997. Keys to soil taxonomy by the Soil Survey Staff, 7th edition. Soil Conservation Service, U.S. Department of Agriculture (USDA). Pocahontas Press, Blacksburg, Virginia.

Stovold, R. J., Whally, W. R., Harris, P. J., White, P. W., 2004. Spatial variation in soil compaction, and the burrowing activity of the earthworm *Aporrectodea caliginosa*. Biol. Fertil. Soil 39, 360-365.

Strudley, M.W., Green, T.R., Ascough, J.C., 2008. Tillage effects on soil hydraulic properties in space and time: State of the science. Soil Till. Res. 99, 4-48.

Sällfors, G., 1975. Preconsolidation pressure of soft high plastic clays. Ph.D. thesis, Department of Geotechnical Engineering, Gothenburg, Sweden.

Taina, I.A., Heck, R.J., Elliot, T.R., 2008. Application of X-ray computed tomography to soil science: A literature review. Can. J. Soil Sci. 88, 1-19.

Thomasson, A.J., 1978. Towards an objective classification of soil structure. J. Soil Sci. 29, 38-46.

Tollner, E., Hargrove, W., Langdale, G., 1984. Influence of conventional and no-tillage practices on soil physical properties in the southern Piedmont. J. Soil Water Conserv. 39, 73-76.

Tursic, I., 1982. The effect of soil compaction and mineral fertilization on the yield of spring barley. Polj. Znan. Smotra-Agr. Consp. 58, 39-48 (in Croatian with an English summary).

Vogel, H.J., Roth, K., 1998. A new approach for determining effective soil hydraulic functions. Europ. J. Soil Sci. 49, 547–556.

Voorhees, W.B., 1986. The effect of compaction on crop yield. Proc. Earthmoving Industry Conf., Paper No. 860729, Peoria, Illinois, USA, 7 pp.

Vorderbrügge, T., Brunotte, J., 2011. Vulnerability to compaction of agricultural subsoils – validation of pedotransfer function for identification of risk areas in Europe and a practicable solution for good farming practice that avoids subsoil compaction. Part I: Validation of pedotransfer function. Agric. For. Res. 61, 1–22.

Werner, D., 1993. Ergebnisse röntgenmorphologischer Untersuchungen verdichteter und gelockerter Bodengefüge. Mitteilgn. Dtsch. Bodenkundl. Gesellsch. 72, 281-284.

Werner, D., Paul, R., 1999. Kennzeichnung der Verdichtungsgefährdung landwirtschaftlich genutzter Böden. Wasser und Boden 51, 10-14.

Wiermann, C., 1998. Auswirkungen differenzierter Bodenbearbeitung auf die Bodenstabilität und das Regenerationsvermögen lößbürtiger Ackerstandorte. Dissertation, Schriftenreihe des Instituts für Pflanzenernährung und Bodenkunde der Universität Kiel, Nr. 45.

Wiermann, C., Way, T.R., Horn, R., Bailey, A.C., Burt, E.C., 1999. Effect of various dynamic loads on stress and strain behavior of a Norfolk sandy loam. Soil Till. Res. 50, 127-135.

Wildenschild, D., Hopmans, J.W., Vaz, C.M.P., Rivers, M.L., Rikard, D., Christensen, B.S.B., 2002. Using X-ray computed tomography in hydrology: Systems, resolutions, and limitations. J. Hydrol. 267, 285-297.

Witzenberger, A., Hack, H., van den Boom, T., 1989. Erläuterungen zum BBCH-Dezimal-Code für die Entwicklungsstadien des Getreides - mit Abbildungen. Gesunde Pflanzen 41, 384-388.

Erklärung / Declaration under oath

Ich erkläre an Eides statt, dass ich, Julia Pöhlitz, die Arbeit selbstständig und ohne fremde Hilfe verfasst, keine anderen als die von mir angegebenen Quellen und Hilfsmittel benutzt und die den benutzten Werken wörtlich oder inhaltlich entnommenen Stellen als solche kenntlich gemacht habe.

I, Julia Pöhlitz declare under penalty of perjury that this thesis is my own work entirely and has been written without any help from other people. I used only the sources mentioned and included all the citations correctly, both in word and content.

_____   _____

Datum / Date   Unterschrift / Signature

**Erklärung über bestehende Vorstrafen und anhängige Ermittlungsverfahren /
Declaration concerning the criminal record and pending Investigations**

Hiermit erkläre ich, Julia Pöhlitz, dass ich weder vorbestraft bin noch dass gegen mich Ermittlungsverfahren anhängig sind.

I, Julia Pöhlitz, hereby declare that I have no criminal record and that no preliminary investigations are pending against me.

_____   _____

Datum / Date   Unterschrift / Signature

Tabellarischer Lebenslauf / Curriculum vitae

Name: Julia Pöhlitz

Geburtsdatum / Date of birth: 10.02.1992

Geburtsort / Place of birth: Weißenfels

Beruflicher Werdegang / Professional career

01/2018 - aktuell

wissenschaftliche Mitarbeiterin, Martin-Luther-Universität Halle-Wittenberg, Institut für Agrar- und Ernährungswissenschaften, Allgemeiner Pflanzenbau/Ökologischer Landbau
Research scientist, Martin-Luther-University Halle-Wittenberg, Institute of Agricultural and Nutritional Sciences, Agronomy and Organic Farming Group

10/2015 - 12/2017

Doktorandin, Martin-Luther-Universität Halle-Wittenberg, Institut für Agrar- und Ernährungswissenschaften, Allgemeiner Pflanzenbau/Ökologischer Landbau
Ph.D. student, graduate scholarship, Martin-Luther-University Halle-Wittenberg, Institute of Agricultural and Nutritional Sciences, Agronomy and Organic Farming Group

04/2015 - 09/2015

wissenschaftliche Mitarbeiterin, Johannes Gutenberg Universität Mainz, Geographisches Institut, Abteilung Bodenkunde
Research scientist, Johannes Gutenberg University Mainz, Institute of Geography, Soil Science Section

Studium / Academic education

10/2013 - 03/2015
M. Sc. Bodenwissenschaften, Universität Hohenheim
M. Sc. Soil Science, University of Hohenheim

10/2010 - 09/2013:
B. Sc. Geographie, Martin-Luther-Universität Halle-Wittenberg
B. Sc. Geography, Martin-Luther-University Halle-Wittenberg

Publikationsliste

2018

Pöhlitz, J., Rücknagel, J., Koblenz, B., Schlüter, S., Vogel, H.-J., Christen, O., 2018. Computed tomography and soil physical measurements of compaction behaviour under strip tillage, mulch tillage and no tillage. Soil Till. Res. 175, 205-2016.

Pöhlitz, J., Rücknagel, J., Schlüter, S., Vogel, H.-J., Christen, O., 2018. Soil physical and X-ray computed tomographic measurements with different tillage and matric potential. BONARES Conference 2018, Berlin, Germany.

Pöhlitz, J., Rücknagel, J., Schlüter, S., Vogel, H.-J., Christen, O., 2018. Soil physical and morphometric measurements to investigate small-scale structural differences under strip tillage compared to mulch till and no-till. IV European Society for Agronomy Congress (ESA) 2018, Genf, Switzerland.

Pöhlitz, J., Rücknagel, J., Schlüter, S., Vogel, H.-J., Christen, O., 2018. Abschätzung kritischer Spannungsbereiche zur Erhaltung der Bodenfunktionen verschieden strukturierter Standorte. 61. Jahrestagung der Gesellschaft für Pflanzenbauwissenschaften 2018, Kiel, Deutschland.

Pöhlitz, J., Rücknagel, J., Schlüter, S., Vogel, H.-J., Christen, O., 2018. Linking stress-strain test with X-ray CT analysis to examine the effects of soil moisture and soil tillage on soil structure. 21st International Soil and Tillage Research Organization (ISTRO) Conference, Paris, France.

2017

Pöhlitz, J., Rücknagel J., Schlüter, S., Vogel, H.-J., 2017. Soil physical and X-ray computed tomographic measurements to investigate small-scale structural differences under strip tillage compared to mulch till and no tillage. Geophysical Research Abstracts, Vol. 19, EUG2017-6422. EUG General Assembly 2017, Vienna, Austria.

Pöhlitz, J. Rücknagel, J., Schlüter, S., Vogel, H.-J., 2017. Suitability of computed tomography to map the compaction process using the example of cultivator and plough for two matric potentials. Proceedings of the 15th International Symposium of Soil and Plant Analysis (ISSPA), Nanjing, China.

Pöhlitz, J., Rücknagel, J., Schlüter, S., Vogel, H.-J., Christen, O., 2017. Bodenphysikalische und computertomographische Messungen zur Untersuchung verdichtungsabhängiger Gefügeveränderung bei Strip-Till im Vergleich zu Mulchsaat und Direktsaat. Jahrestagung der Deutschen Bodenkundlichen Gesellschaft, Göttingen, Deutschland.